UNIVERSITY OF OKLAHOMA

GRADUATE COLLEGE

# MIDDLE EAR BIOMECHANICS

# IN CHINCHILLA MODEL OF ACUTE OTITIS MEDIA

A DISSERTATION

SUBMITTED TO THE GRADUATE FACULTY

in partial fulfillment of the requirements for the

Degree of

DOCTOR OF PHILOSOPHY

By

XIYING GUAN
Norman, Oklahoma
2014

MIDDLE EAR BIOMECHANICS
IN CHINCHILLA MODEL OF ACUTE OTITIS MEDIA

A DISSERTATION APPROVED FOR THE
DEPARTMENT OF BIOENGINEERING

BY

_____
Dr. Rong Z. Gan, Chair

_____
Dr. Vassilios I. Sikavitsas

_____
Dr. Lei Ding

_____
Dr. Edgar A. O'Rear

_____
Dr. Harold L. Stalford

I dedicate my dissertation work to my family for their company and support during my PhD study at University of Oklahoma.

**ACKNOWLEDGEMENTS**

First, I would like to express my appreciation and gratitude to my advisor, Professor Rong Z. Gan, for her patient guidance and mentorship she provided to me, from the first day I enrolled in Bioengineering PhD program at University of Oklahoma, through to completion of my degree. Dr. Gan not only gave me opportunities to learn skills through research projects, but also taught me to think as a research scientist. She spent countless hours on helping me to improve my writing. Her enthusiasm for research and mentoring has impacted me deeply. I am very fortunate to have been working with her in the past six years.

I would also like to thank Dr. Thomas Seale in Department of Pediatrics at University of Oklahoma Health Science Center for his friendly guidance and suggestions on my research projects. It has been a great honor and pleasure to work with him.

Thank my committee members, Drs. Lei Ding, Vassilios Sikavitsas, Edgar O'Rear, and Harold Stalford, for agreeing to serve on my committee.

Many thanks go to my team members in Biomedical Engineering lab at OU. Don Nakmali provided assistance to setup of the experiments. Xiangming Zhang, who had graduated in 2013, helped me in both experiments and theoretical analysis. Shangyuan Jiang, a new PhD student in our lab, assisted me in the histologic study. Chenkai Dai, Fan Yang, and Wei Li were former lab members and they shared research experience with me during my early years in the lab. Dr. Xiao Ji and Dr. Xuelin Wang are senior scientists and we had a lot of discussions on the experiments. Zachary Yokell, who joined us two years ago, always provided help on my writing.

Sincere thanks go to Dr. Mark Wood at Hough Ear Institute for being so friendly and spending time on editing my manuscripts. Thanks to Dr. Xiaopin Du and his wife at Hough Ear Institute for sharing their experience of histologic study with me. I also thank Brett Cole at University of Oklahoma Health Science Center and Shih-Feng Lan at OU for their assistance on cell culture. Many thanks go to Mario Pineda and Vikrant Palan from Polytec Inc. for providing technical support on usage of scanning laser vibrometry.

Thank Dr. Matthias Nollert who is the graduate liaison for providing suggestions and convenience during my study at OU. Thank staffs at AME, OUBC, and SRTC, they are Billy Mays, Greg Williams, Vicki Pollock, Debbie Mattax, Donna King, Pamela Roberts, Dora Rapp, and Meghan Thomas, for providing assistance and convenience during my study at OU. Thanks Scott Zerger and Keith Curlee at OU animal facility for taking care of the guinea pigs and chinchillas. Thank Professor Tyrrell Conway, Professor Jizhong Zhou, and their students for sharing cell culture facilities.

I also thank Professor Hongbin Lu, Dr. Zhenxin Hu, and Dr. Huiyang Luo, and William Young at Unversity of Texas at Dallas for cooperating with my research projects.

Finally, I appreciate the unconditional support from my family. I would like to thank my parents, father-in-law, and mother-in-law for their support. I am grateful for the joy and love from my wife, Jing Che and my lovely daughter, Lia Guan.

**TABLE OF CONTENTS**

**LIST OF TABLES**

**LIST OF FIGURES**

**ABSTRACT**

Acute otitis media (AOM) is a rapid onset of infection in the middle ear and the most frequently diagnosed disease in pediatric population. Conductive hearing loss is the most prevalent outcome of AOM because pathological changes in the infected middle reduce mobility of the tympanic membrane (TM). Mechanisms of TM mobility loss associated with AOM are not well understood. We hypothesize that middle ear pressure (MEP), middle ear effusion (MEE), and structural changes of ossicular adhesions and ear soft tissues are the main factors contributing to the loss of TM mobility in AOM ears and their effects vary during the course of the disease.

In this dissertation, a chinchilla AOM model was produced by transbullar injection of *Haemophilus influenzae*. Changes of MEP, MEE, and ossicular adhesions were characterized at day 4 (4D) and day 8 (8D) post inoculation. These time points represent relatively early and later phases of AOM. Microstructural changes of the TM, round window membrane (RWM), and stapedial annular ligament (SAL) in the early and later phases of AOM were investigated by histology. Hearing loss in both AOM phases was evaluated by auditory brainstem response (ABR). TM mobility at the umbo and middle ear energy absorbance (EA) were measured in 4D and 8D AOM ears. In each group, the vibration of the umbo and EA was measured at three experimental stages: unopened, pressure-released, and effusion-removed ears. The effects of MEP and MEE and middle ear structural changes were quantified in each group by comparing the TM mobility or EA at one stage with that of the previous stage.

Our findings show that the factors affecting TM mobility change with the disease time course. The MEP was the dominant contributor to reduction of TM

mobility in 4D AOM ears, but showed little effect in 8D ears when MEE filled the tympanic cavity. MEE was the primary factor affecting TM mobility loss in 8D ears, but affected the 4D ears only at high frequencies. After the release of MEP and removal of MEE, residual loss of TM mobility was seen mainly at low frequencies in both 4D and 8D ears, and was associated with ossicular adhesions. The effects of MEP and MEE on EA were similar to those on TM mobility. Residual loss of EA seems was more likely associated with mechanical property changes of TM.

Our findings demonstrate that MEP, MEE, together with middle ear structural changes, contribute to TM mobility loss in the chinchilla AOM ears. Their effects on TM movement at early and later phases of the disease were quantified. This study provides useful experimental data for understanding the mechanism of conductive hearing loss in AOM.

# CHAPTER 1: INTRODUCTION

## 1.1 Structure and function of middle ear

The human ear has outer, middle, and inner ear portions. Figure 1.1 shows a schematic diagram of human ear. The middle ear consists of the eardrum, the ossicular chain, and the middle ear cavity. The eardrum, or tympanic membrane (TM), is a cone-shaped membrane. The ossicular chain consists of three ossicles: malleus, incus, and stapes. The long process of the malleus, or manubrium, is attached to the eardrum and pulls the membrane medially to form its conical shape. The point of maximum concavity is the umbo, which is the far end of the manubrium of the malleus. The malleus is connected to the incus via a joint. In some species, such as guinea pig or chinchilla, the malleus and the incus fuse together without a joint in between (Goksu et al. 1992; Wysocki et al. 2005; Hanamure et al. 1987; Vrettakos et al. 1988). The incus is connected with the stapes via the incudo-stapedial joint (IS joint), which is relatively soft compared with the malleus-incus joint. The stapes sits in the oval window. The stapedial annular ligament (SAL) connects the stapes footplate to the oval window of the inner ear. The middle ear cavity is a hollow space surrounding the ossicles. The eustachian tube connects the middle ear cavity with the nasal cavity, allowing pressure to equalize between the middle ear and throat.

The primary function of the middle ear is to transform the acoustic vibration from the ear canal to the fluid motion within the cochlea. Sound waves propagate through the ear canal and cause vibration of the TM. The vibration is transmitted to the cochlea via the three ossicles. The piston-like motion of the stapes sets the cochlear fluid into vibration, which stimulates the mechano-sensitive hair cells (Møller 1983).

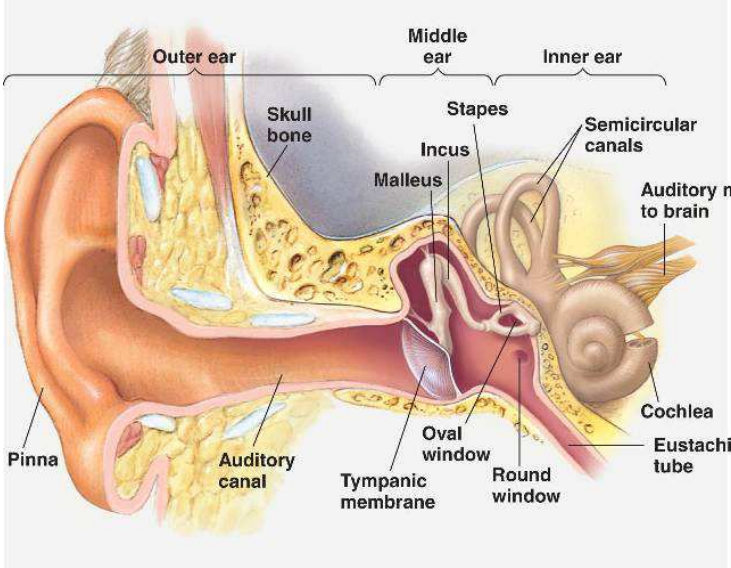


**Figure 1.1** Schematic diagram of human ear. (http://bio1903.nicerweb.com/Locked/media/ch50/50_08aOverviewEarStruc-L.jpg)

### 1.2 History of experimental studies on middle ear biomechanics

Multiple techniques and devices have been used to study biomechanics of the middle ear. In the current literature, the experimental research have focused on four categories: (1) the vibration of the TM or ossicles in response to sound; (2) the acoustic impedance of the ear; (3) the sound energy absorbed or reflected by the middle ear; and (4) the mechanical properties of a specific soft tissue in the middle ear, such as TM, IS joint, or SAL. An overview of the published work for each category is given in this section.

Vibration of the eardrum or ossicles represents the mechanical response of the middle ear to the sound. The amplitude of the vibration indicates the mobility of the middle ear. Since von Békésy first examined the middle ear vibration by using capacitive probes or strobe lights (von Békésy 1960), the vibrations of the TM at the umbo or ossicles were studied in human temporal bones and animals with different

measurement techniques (Dankbaar 1970; Goode 1993; Gyo et al. 1987; Gyo et al. 1986; Heiland et al. 1999; Gan et al. 2004; Chien et al. 2006; Ruggero et al. 1990; Manley and Johnstone 1974). The vibration amplitude of the umbo or ossicles in normal human ears is smaller than 1 μm in response to sound at normal voice level (70-80 dB SPL). The displacement of vibration under acoustic stimulus is frequency-dependent and has been characterized in various species. In the last decade, single point laser Doppler vibrometer (LDV), which enables nanometer-sized vibration measurements, was widely used to determine the velocity/displacement of the umbo or stapes in human cadaveric bones (Voss 2000 et al.; Ravicz et al. 2004; Gan et al. 2006), guinea pigs (Guan et al. 2011; Guan et al. 2013; Turcanu et al. 2009), mice (Qin et al .2010), and chinchillas (Thornton et al. 2013). Recently, sound-induced motion of the entire surface of human TM was measured by using stroboscopic holography (Cheng et al. 2010; Cheng et al. 2013) and scanning LDV (Zhang et al. under review).

Acoustic impedance (AI) is defined as the ratio of the acoustic pressure to the volume velocity generated by the pressure. Ear's impedance measures the response of the whole TM to sound stimulus in the ear canal (Zwislocki 1962; 1963). After the early investigations of human ear impedance by Zwislocki (1957) and Feldman (1963), AI as a function of frequency has been determined in live human (Allen 1986; Merchant et al. 1997; Merchant et al. 1998; Møller 1965; Rabinowitz 1981; Rosowski 1990), cats (Guinan and Peake 1967), lion (Huang et al. 1997), gerbils (Ravicz et al. 1992), and chinchillas (Margolis et al. 2001). AI is usually measured by using a sound source and a microphone at certain location in the ear canal. AI is affected not only by the impedance

at the TM (middle ear AI) but also by the impedance of the air space between the measurement location and the TM (Rabinowitz 1981; Zwislocki 1962).

Middle ear energy absorbance (EA) is another measure of the response of the entire TM to sound stimulation in the ear canal. EA describes the sound power absorbed by the TM. Two decades ago, Keefe et al. (1993) and Voss and Allen (1994) described a technique to measure the power transfer into the middle ear over the range of auditory frequency. In their studies, EA was mathematically related to the AI measured in the ear canal and the cross-sectional area of the ear canal. The instruments for the measurement of EA were similar to those used for the measurement of AI. The advantage of using EA is that the absorbance is relatively insensitive to the air in the ear canal between the measurement point and the TM compared with impedance (Keefe et al. 1993; Rosowski et al. 2013). Normative EA or energy reflectance (ER = 1-EA) of normal human ears over the auditory frequencies has been reported in several studies (Voss et al. 2000; Feeney et al. 2003; Voss et al. 2008; Beers et al. 2010; Prieve et al. 2013). There are only few studies of EA measurement made in animals. Margolis et al. (2001) and Hsu et al. (2001) reported ER in the chinchilla ears. Their findings show that the pattern of the ER in chinchilla ears is similar to that of human ears.

Middle ear soft tissues, such as TM, IS-joint, and SAL, together with ossicles, transfer vibrations from ear canal to inner ear. Mechanical properties of the soft tissues affect the sound transmission in the middle ear. Young's modulus of the human TM was first reported by von Békésy (1960). Since then, numerous studies have been done to determine the mechanical properties of the human TM with various techniques (Kirkae 1960; Decraemer et al. 1980; Fay et al. 2005; Cheng et al. 2007; Luo et al.

2009; Huang et al. 2008; Daphalapurkara et al. 2009; Zhang et al. 2010). Due to experimental challenges, numbers of studies on other middle ear soft tissues are far less compared to TM. Recently mechanical properties of the human IS-joint and SAL were reported by Zhang and Gan (2011) and Gan et al. (2011), respectively.

### 1.3 Acute otitis media

Otitis media (OM) is an inflammation of the middle ear and is the second most prevalent disease in pediatric population after the common cold (Hendley 2002). Otitis media with effusion (OME) and acute otitis media (AOM) are two main types of OM. OME describes the symptoms of middle ear effusion (MEE) without signs of active infection (Stool 1994). AOM is an acute infection of the middle ear and caused by bacteria in about 70% of cases (Gould and Matz 2010).

AOM is the most frequently diagnosed illness in children in the United States and the leading indication for antibiotics therapy in children (Hoberman et al. 2011). Approximately 9 million children were diagnosed with AOM per year in the United States. As a result, the costs associated with AOM are greater than 3 billion annually (Ahmed et al. 2014).

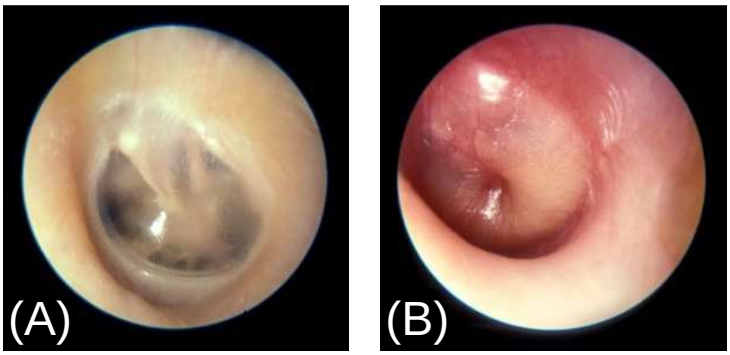


**Figure 1.2** Tympanic membrane of (A) normal ear and (B) AOM ear. (me.hawkelibrary.com).

Figure 1.2 shows the comparison between a normal ear and an AOM ear. As can be seen in the figure, the signs and symptoms of AOM usually include a hyperemic tympanic membrane and purulent effusion in the middle ear (Bluestone and Klein 1983A; Shaikh et al. 2011). AOM is commonly associated with reduction of TM mobility as a result of middle ear pressure and middle ear effusion (Bluestone and Klein 1983B). As a consequence of poorly mobile TM, conductive hearing loss is the most prevalent outcome of AOM (Bluestone and Klein 1983B).

## 1.4 Current stage of research on middle ear biomechanics in AOM

Efficiency of the sound transmission in the middle ear is sensitive to middle ear disorders. The pathological changes in the middle ear associated with AOM include abnormal pressure in the middle ear, effusion accumulated in the cavity (Bluestone and Klein 1983;), ossicular adhesions (Caye-Thomasen et al. 1996; 2000), and morphological changes of the soft tissues such as TM (von Unge et al. 1997; Larsson et al. 2003) and round window membrane (Gan et al. 2013). Those factors each would contribute to decrease of middle ear mobility. Among those changes associated with AOM, middle ear pressure and effusion have been simulated in human temporal bones or animal ears by injection of air pressure and saline into the cavity, respectively. The influence of middle ear pressure or effusion on sound transmission has been well studied. However, effects of the structural changes including ossicular adhesions and changes of middle ear tissues on the mechanical response of the middle ear are not well understood.

### 1.4.1 Effect of middle ear pressure

Middle ear pressure is regulated by eustachian tube, which links the nasopharynx to the middle ear cavity. Temporary opening of the eustachian tube enables ventilation of the middle ear to equilibrate air pressure in the middle ear with atmospheric pressure (Bluestone and Klein 1983A). Inflammation or infection in the middle ear leads to blockage of the eustachian tube. Thus, abnormal pressure commonly occurred in the middle ear cavity of AOM ears.

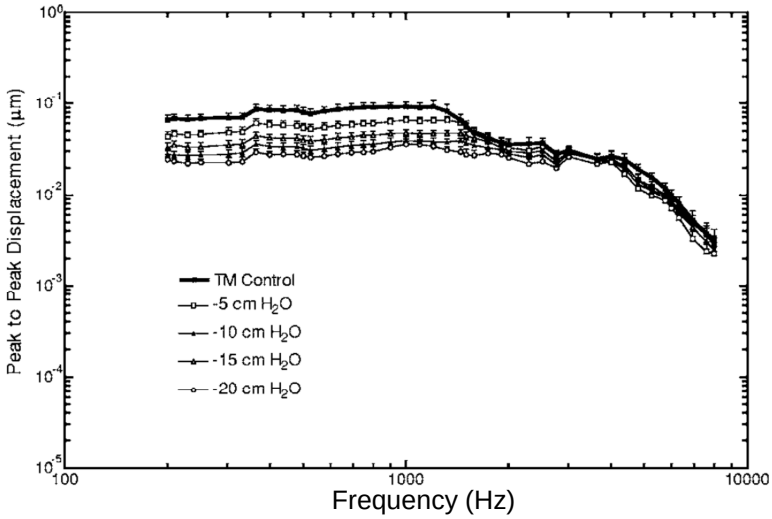


**Figure 1.3** Peak to peak displacement of the TM at umbo when the middle ear pressure varied from 0 to -20 cm $H_2O$ (Gan et al. 2006).

Several studies have investigated the effect of positive or negative middle ear pressure on middle ear mobility (Dai et al. 2008; Gan et al. 2006; Lee and Rosowski 2001; Murakami et al. 1997; Petrova et al. 2006; Rosowski and Lee 2002). In human temporal bone studies, Gan et al. (2006) introduced air pressure in the middle ear and investigated the vibration displacement of the TM. Figure 1.3 displays the effect of negative middle ear pressure on TM displacement at the umbo measured by Gan et al. (2006). The results showed that the negative pressure reduced the TM movement mainly at low frequencies. Same pattern of the reduction of TM displacement was observed when positive pressure was present in the middle ear (Gan et al. 2006). The

results observed in human ears by Murakami et al agreed with the findings by Gan et al. In a guinea pig OME model, Dai and Gan (2008) reported that the middle ear pressure caused reduction of TM vibration mainly at frequencies less than 2 kHz. It is generally accepted that pressure in the middle ear increases the stiffness of the TM and thus decreases the TM movement at low frequencies.

To study the middle ear pressure's effect on energy or power absorbed by the middle ear, Voss et al. (2012) introduced static pressure in the middle ear cavity of the cadaveric temporal bones. Their results showed that increasing positive or negative MEP caused decrease of EA below 2 kHz.

### 1.4.2 Effect of middle ear effusion

The effect of middle ear effusion on vibration of the TM have been studied in human temporal bones (Ravicz et al., 2004; Gan et al., 2006; Dai et al., 2007;) and animal models (Turcanu et al., 2009; Qin et al., 2010; Guan and Gan, 2011). In those studies, saline was injected into the middle ear cavity to simulate the effusion. Figure 1.4 shows the changes of the TM displacement when fluid level was increased in the guinea pig middle ears (Guan and Gan 2011). As can be seen, the displacement was reduced mainly at high frequencies as a small amount of fluid was injected, and the reduction was greater and extended to low frequency range when more fluid was present in the middle ear. Ravicz et al. (2004) also measured the TM vibration as saline was injected incrementally into the middle ear of human temporal bones. They concluded that the primary mechanism of TM mobility loss at high frequencies was the increased mass on the TM by the middle ear fluid. The reduction of TM movement at low frequencies was due to the reduced middle ear air space.

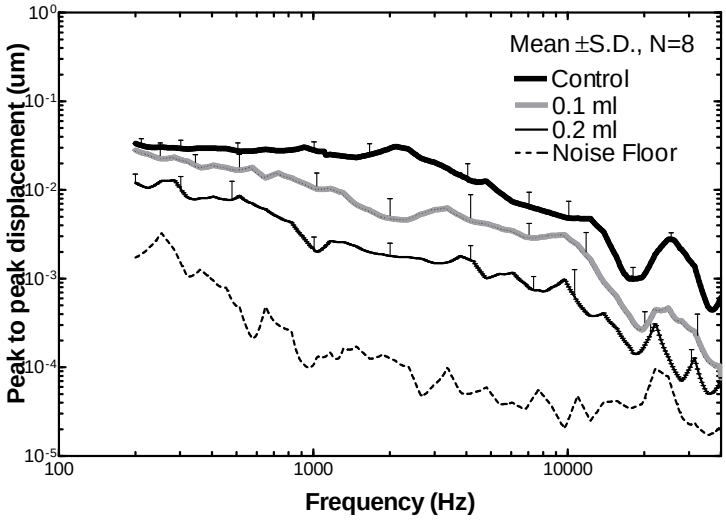


**Figure 1.4** Peak to peak displacement of the TM at umbo in response to 80 dB SPL sound input in the ear canal when the middle ear effusion varied from 0 to 0.2 ml (Guan and Gan 2011).

Several studies showed the changes of EA in patients with OME (Feeney 2003; Allen et al. 2005; Beers et al. 2010). Because OME usually leads to effusion and pressure in the middle ear, EA was affected by the fluid and pressure together in those clinical studies. In the study of human temporal bones, Voss et al. (2012) showed that the middle ear fluid alone decreased EA over 0.2-6 kHz.

### 1.4.3 Effect of structural changes

In addition to the pressure and effusion, the infection of AOM frequently results in structural changes of the ossicles and the soft tissues in the middle ear. Bacteria can form surface-attached communities on the mucosal layer of the middle ear cavity during the infectious process of AOM (Ehrlich et al. 2002; Hoa et al. 2009; Reid et al. 2009), which promotes formation of purulent adhesions in narrow spaces of the cavity such as the round window niche (Caye-Thomasen et al. 1996). The adhesions can form between the ossicles and surrounding bony wall and cause the fibrous fixation of the TM or

ossicular chain (Caye-Thomasen et al. 1996; Caye-Thomasen and Tos 2000; von Unge et al. 1997).

Moreover, the infectious process can induce morphological changes of the TM (Bluestone and Klein 1983A). It has been reported that the structures and elastic properties of the TM in the AOM ears of gerbils are different from that in normal gerbil ears (Larsson et al. 2003; von Unge et al. 1993; 1997). Changes of TM property would also impact its mechanical response to the input sound.

The previous studies have revealed mechanisms of the loss of TM mobility and EA associated with fluid or pressure in the middle ear cavity. However, little is known about the effects of ossicular adhesions and tissue changes on acoustic response of the middle ear. The sound transmission in the ear of AOM would be influenced by a combination of the middle ear pressure, effusion, ossicular adhesions, and tissue changes. How these different factors contribute to the changes of middle ear biomechanics in AOM? What are the mechanisms of conductive hearing loss in the infected ears?

### 1.4.4 The guinea pig AOM model

To answer those questions, we produced an AOM model in guinea pigs by transbullar injection of *Streptococcus Pneumoniae*, one of the most common bacteria found in AOM effusion (Guan and Gan 2013). Three days post inoculation, typical signs of AOM, such as purulent effusion, hyperemic TM, and ossicular adhesions, were observed in the inoculated ears. A comparison of the TM and ossicles between control ear (i.e. healthy ear) and AOM ear can be seen in Figure 1.5.

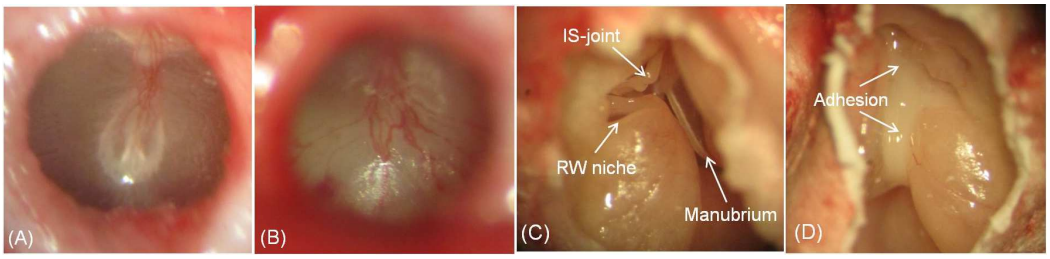


**Figure 1.5** Photographs of (A) control eardrum, (B) AOM eardrum, (C) middle ear cavity and ossicles in control ear (right ear), and (D) middle ear cavity in ear of AOM (left ear). IS-joint represents incudo-stapedial joint and RW represents round window.

On day 3 after inoculation, vibrations of the TM at umbo in response to input sound in the ear canal was measured at three experimental stages: (1) OM-1: the intact or original AOM ear with middle ear pressure and effusion, (2) OM-2: pressure released, and (3) OM-3: effusion drained ear.

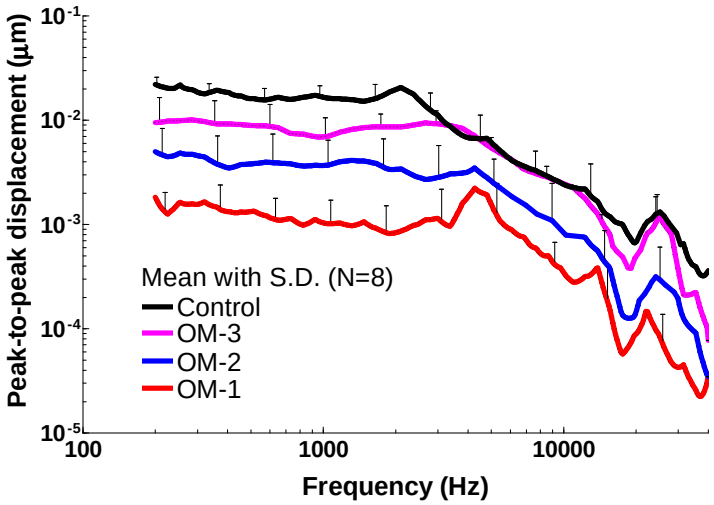


**Figure 1.6** Peak to peak displacement of the TM at umbo in response to 80 dB SPL sound input at the ear canal in OM-1 (red line), OM-2 (blue line), OM-3 (purple line), and control ears (black line).

Figure 1.6 displays the TM displacement curves of the control and three experimental stages over the range of 0.2-40 kHz. The TM displacement of OM-1 was smaller than that of the control or the other OM stages. When the pressure in the middle ear was released (OM-2), the displacement increased significantly at low frequencies

(0.2-3 kHz). As the effusion was drained from the cavity (OM-3), the TM displacement showed significant increase compared to OM-2 ears over all tested frequencies except 32 kHz.

Comparing OM-3 with control, there was residual loss of TM mobility at low frequencies (f < 3 kHz). There were two major structural differences between the normal and the AOM ears at stage OM-3: (1) purulent adhesions on the ossicles were undisturbed during the aspiration of fluid and remained in the AOM ears at this stage (see Figure 1.5D); (2) morphology of the TM changed in the infected ears (see Figure 1.5B). The residual loss of TM displacement demonstrates that those middle ear structural changes contributed to the total loss of TM mobility in the AOM ears.

This study unequivocally showed that middle ear pressure, effusion, together with infection-induced structural changes each affected the middle ear mobility. It was the first time that the contributions of each AOM factor to the reduction of sound transmission were quantified in the early phase of the disease.

However, because such data are lacking in other animal species used as models of human AOM, it remained unclear whether our findings are species specific (i.e. unique to the guinea pig) or occur generally among the various animal models of AOM. An important additional issue not addressed in our guinea pig study is whether time course-specific changes in the processes altering middle ear mobility occur during the course of AOM. It is known that the level of middle ear pressure, production of middle ear effusion, and the degree of inflammation change during the AOM course (Suzuki and Bakaletz 1994; von Unge et al., 1993; von Unge et al., 1997). How these factors contribute to the loss of TM mobility at different phases of middle ear disease is not

well understood. The influence of these factors on sound energy absorption of the TM is also unclear.

### 1.5 The chinchilla AOM model

Nontypeable *Haemophilus influenzae* is another bacteria considered as an important pathogen for AOM (Bluestone and Klein, 1983; Bluestone et al., 1992; Giebink, 1999). *H. influenzae* has been used to produce AOM models in different species including chinchilla (Jurcisek et al. 2005; Bakaletz 2009), mouse (Melhus and Ryan, 2003), rat (Melhus and Ryan 2000), guinea pig (Sato et al. 1999), and gerbil (Fulghum et al. 1982; Soriano et al. 2000).

The chinchilla (*Chinchilla laniger*) is a frequently employed animal model in auditory research. The size of a chinchilla's TM is close to that of humans (Browning and Granich 1978; Hanamure and Lim 1987; Vrettakos et al., 1988). Nontypeable (acapsular) *H. Influenzae* strain 86-028NP, a clinical isolate from a patient with otitis media, frequently has been used in studies investigating host-pathogen interactions during AOM development and resolution in the chinchilla middle ear (Bakaletz et al., 1999; Mason et al., 2003; Morton et al., 2004; Morton et al., 2012; Suzuki and Bakaletz, 1994).

Pathologic findings associated with the chinchilla AOM model induced by *H. Influenzae* 86-028NP were first characterized by Suzuki and Bakaletz (1994). Otoscopic examination indicated that the middle ear of chinchillas exhibited inflammation as early as one day following transbullar challenge. Thereafter, the degree of inflammation increased and peaked approximately 7-10 days post inoculation (Suzuki and Bakaletz,

1994). This well established and widely used animal model provides an opportunity to investigate the factors decreasing middle ear mobility in ears affected by AOM and their variation at different stages of the disease process. It also allows comparison of AOM outcomes between species and the opportunity to assess whether the bacteria species causing AOM influences the type and severity of the acute biomechanical changes occurring in the middle ear.

### 1.6 Objectives

AOM is the most prevalent disease in young children and frequently leads to conductive hearing loss in patients. Hearing loss can delay or impair development of language and speech. Mechanism and development of conductive hearing loss associated with AOM are not completely understood. Studying biomechanics of the middle ear in AOM would help understanding the fundamental causes of sound transmission loss in the infected ears.

Our previous study in guinea pigs quantified the effects of middle ear pressure, middle ear effusion, ossicular adhesions, and ear tissue morphologic changes on loss of TM mobility in early phase of AOM. However, it is not clear how those factors vary along the course of the disease and whether those effects are reproducible in different species.

To characterize development of the middle ear pathologic changes and their roles on sound transmission during the course of AOM, we carried out detailed experiments in the chinchilla AOM model initiated by transbullar injection of strain *H. Influenzae* 86-028NP. As outlined in the following objectives, we employed

measurement of auditory brainstem response threshold to evaluate the conductive hearing loss in two treatment groups: 4 days and 8 days post inoculation. These time points represent relatively early and later phases of AOM. Meanwhile, we investigated the development of middle ear pressure, effusion, ossicular adhesion, and soft tissue microstructural changes from the early phase to the later phase of infection and determined their effects on TM vibration in response to sound stimulation and EA of the middle ear. The results of this study elucidate the fundamental mechanism of conductive hearing loss in ears with AOM.

Objective 1: Investigate levels of middle ear pressure, production of middle ear effusion and adhesion, and microstructures of middle ear soft tissues in early and later phases of AOM.

Objective 2: Evaluate conductive hearing loss at the two AOM phases by measuring thresholds of auditory brainstem response.

Objective 3: Determine effects of middle ear pressure, effusion, and structural changes on TM vibration at umbo in early and late AOM phases in chinchilla and compare their effects with those in guinea pig AOM model.

Objective 4: Determine effects of middle ear pressure, effusion, and structural changes on sound energy absorbed by the middle ear in early and late AOM.

### 1.7 Outline

Chapter 2 presents detailed method to produce AOM in the chinchillas, procedures of histological preparation of the temporal bones, and histopathologic

changes of the TM, SAL, and round window membrane (RWM) in early and the later phases of infection.

Chapter 3 presents method of auditory brainstem response measurement and quantitative results of conductive hearing loss at two AOM phases in chinchilla.

Chapter 4 presents method of TM vibration measurement at umbo, mechanisms of umbo mobility loss at two infection phases in chinchillas, and comparison between the chinchilla AOM model and the guinea pig AOM model.

Chapter 5 presents results of middle ear EA measurement in two phases of AOM in chinchillas and mechanisms of EA reduction in AOM.

Chapter 6 presents summary of this study and future works.

# CHAPTER 2: MIDDLE EAR HISTOPATHOLOGIC CHANGES IN CHINCHILLA AOM MODEL

## 2.1 Introduction

Loss of middle ear mobility depends on degree of the pathologic changes in the middle ear. As infection progresses in the cavity, level of middle ear pressure, production of middle ear effusion and adhesion, and microstructure of middle ear soft tissues would vary from early to later phases of the disease. Variation of each factor would affect middle ear mechanical response to sound. Before studying the loss of hearing or TM mobility, a quantitative description of these middle ear changes in the AOM ears needs to be established. In the current literature, the middle ear changes in this chinchilla model have not been quantified. Development of the middle ear pressure, effusion, and adhesion in the AOM ears is described in Chapter 4. In the current chapter, we focus on studying the microstructural changes of the TM, RWM, and SAL during the course of AOM by histology.

Mechanical properties of the middle ear soft tissues are crucial for sound transmission. Changes of the elastic property of the ear tissues can directly affect the middle ear function. For example, a stiffened TM would reduce the amplitude of its vibration. Increase of the stiffness in SAL would increase the overall stiffness of the ossicular chain and subsequently decrease the middle ear mobility. Round window is one of the two openings into the inner ear from the middle ear. RWM is an elastic membrane facilitating motion of the fluid in the cochlea. A stiffened RWM results in an increase of the cochlear load and reduces the middle ear vibration. Studying structural

changes of the TM, RWM, and SAL would help understanding their mechanical property changes associated with AOM.

Cross-sectional images of those tissues not only provide morphology of the internal structure, but also yield thickness of the membrane or ligament. Recently, our lab established a new method to measure dynamic properties of ear membrane tissues by coupling the experimental results with the finite-element modeling derived results. Mechanical properties of the human TM (Zhang and Gan 2010) and RWM (Zhang and Gan 2013), and the guinea pig RWM (Gan et al. 2013) were determined via this method. Thickness of the TM or RWM is a key parameter during the process of modeling. Characterizing thickness changes of the soft tissues in the AOM model would provide a data base for deriving their mechanical properties through the experiment-modeling couple method.

In this chapter, the procedures to induce AOM in chinchillas are described. Microstructures of the TM, RWM, and SAL were investigated at 4 days (4D) and 8 days (8D) post inoculation by histology and compared with those in control (untreated) ears. Thickness at multiple locations of the TM and RWM in control, 4D, and 8D AOM ears were measured from the histologic sections. This study was undertaken to characterize the histopathologic changes of those ear tissues in the chinchilla AOM model and provide fundamental structural evidence to aid in understanding their mechanical properties.

## 2.2 Methods

### 2.2.1 Production of AOM in chinchilla

Ten chinchillas (*chinchilla lanigera*) weighing between 600-800 g were included in histologic study. The study protocol was approved by the Institutional Animal Care and Use Committee of the University of Oklahoma and met the guideline of the National Institutes of Health. All animals were free from middle ear disease (as evaluated by otoscopic examination) at the beginning of the study.

The animals were divided into control, 4D AOM, and 8D AOM groups. The control group included three animals, and the two AOM groups each included two animals. AOM was produced by transbullar injection of HI 86-028NP suspension in both ears following the procedure described by Morton et al. (2012). Under general anesthesia [ketamine (10 mg/kg) and xylazine (2 mg/kg)], 0.3 ml bacterial suspension containing 3000 CFU was injected into the superior bulla bilaterally using a 1 cc syringe with a 26 gauge needle. After the challenge dose was administrated, otoscopic examination was performed daily. The animals of control group were untreated.

**2.2.2 Histologic preparation**

At the 4th or 8th day post-inoculation, animals were deeply anesthetized by overdose of ketamine (100 mg/kg) and xylazine (20 mg/kg) and intracardially perfused with fixative (4.0% paraformaldehyde in 0.1 M phosphate buffer solution, pH 7.2) (Dai and Gan 2008). The temporal bones or bullas were then harvested. To facilitate perfusion of fixative into the middle and inner ear, the bulla was widely opened at superior and inferior side and the bony wall of the cochlea at apex was removed. Then the temporal bone was immersed in the same fixative overnight at room temperature. The next day, the bulla was removed from the fixative, serially washed in phosphate buffered saline (PBS) and distilled water, and decalcified with 10% ethylene diamine

tetraacetic acid (EDTA). The acid was then changed daily for 8 days. After decalcification, the ossicular chain was disrupted at IS-joint by using a #11 surgical blade, and the bulla was cut and separated into two parts: TM with malleus-incus complex and cochlea with stapes. Thereafter, both parts were washed in distilled water and dehydrated in a graded series of alcohols from 50% to absolute alcohol.

Upon completion of dehydration, the specimen with the TM was embedded in paraffin in such an orientation that the handle of malleus was approximately perpendicular to the plane of sectioning. For studying RWM, the specimen with the cochlea was oriented in paraffin so the short axis of RWM was normal to the cutting plane. For study of SAL, the cochlea specimen was oriented in such a way that the short axis of stapes footplate was perpendicular to the sectioning plane.

After hardening of paraffin, the specimen was cut into 8-µm thickness sections, serially mounted on glass slides, stained with Hematoxin-Eosin, and cover slipped.

To date, two TMs, two RWMs, and two SALs in each experimental group were prepared from specimen to finished slide for examination.

### 2.2.3 Histopathologic analysis

The histologic slides were examined and photographed under a calibrated Omano light microscope (Omano, China). Particular attention was given to thickness of the TM and RWM, which was measured directly from the photographs with the aid of image analysis software ImageJ.

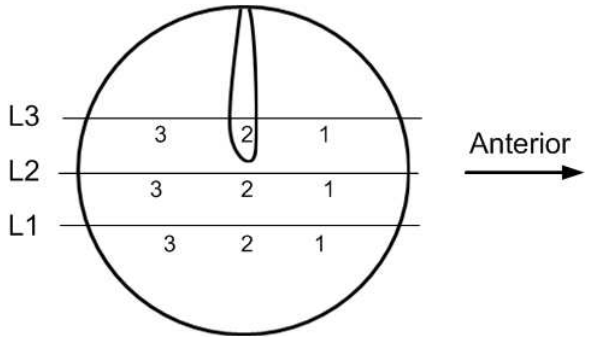


**Figure 2.1** Schematic of histologic sectioning of TM. TM thickness was measured at locations #1-3 for each section.

Measurements of the TM thickness was made directly in three histologic sections from inferior to superior side as shown in Figure 2.1. Sections of L1, L2, and L3 was approximately 2.5 mm below, 0.5 mm below, and 2 mm above the low edge of the umbo, respectively. In each level the thickness was measured at three locations evenly spaced from anterior to posterior side and those locations are indicated in Figure 2.1. The only exception is that location #2 of the L3 section was 0.5 mm anterior to the manubrium.

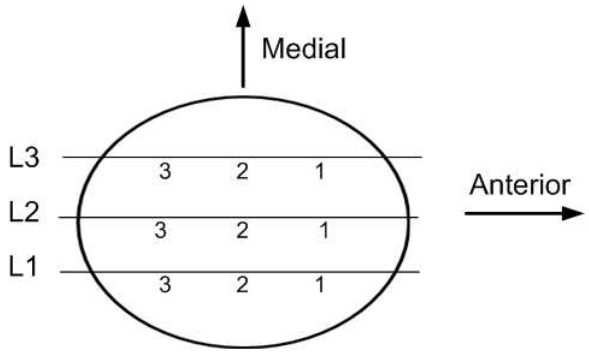


**Figure 2.2** Schematic of histologic sectioning of RWM. RWM thickness was measured at locations #1-3 for each section.

RWM thickness was measured in three sections from lateral to medial side as displayed in Figure 2.2. The middle level, L2, was at the long axis of the membrane.

Sections of L1 and L3 were 250 µm lateral and 250 µm medial to the middle section, respectively. As shown in Figure 2.2, the thickness was measured at three locations evenly spaced from anterior to posterior side in each section.

## 2.3 Results

### 2.3.1 TM

Figure 2.3 displays histologic structure of a control TM. The image was taken near the center of superior-posterior quadrant of the membrane. The TM consists of three distinct layers: outer layer facing the ear canal is composed of a single layer of squamous epithelium; middle layer consists of fibrous tissue; inner layer is the mucosal layer composed of a single layer of flat epithelial cells.

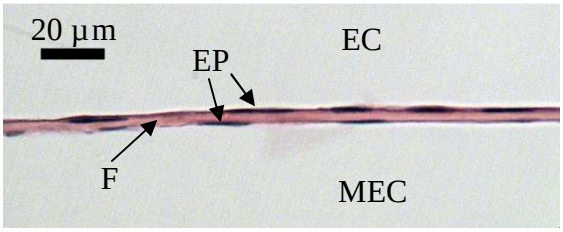


**Figure 2.3** Light micrographs of TM in control ear near center of superior-posterior quadrant. EC, ear canal; MEC, middle ear cavity; EP, epithelium; F, fibrous layer.

Figure 2.4 shows cross sections of control TM near the annulus and the manubrium. The TM is thick in the region of the annulus, thins out in the midway, and thickens again near the manubrium. TM thickness of the middle portion is generally uniform and can vary from 6 to 10 µm.

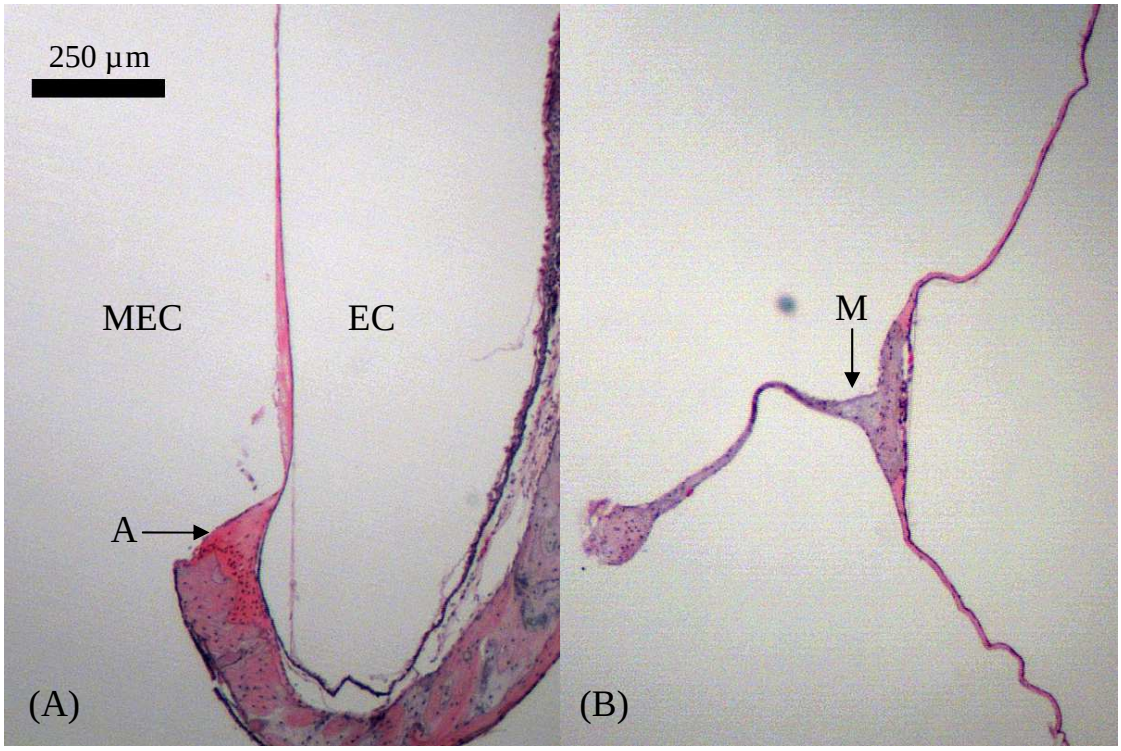


**Figure 2.4** Light micrographs of TM in control ear near (A) annulus and (B) manubrium. EC, ear canal; MEC, middle ear cavity; A, annulus; M, manubrium.

Figure 2.5 shows TM structure at two locations of a 4D AOM ear. The 4D TM underwent substantial changes compared with control. The epithelial cells in the outer layer proliferated and stratified. The outer most epithelium of the TM seems to be keratinized. The outer layer was usually two to three cell layers thick as shown in Fig. 2.5A, but occasionally four to five layers thick as shown in Fig 2.5B. Dilated capillary and infiltration of neutrophils were observed in the subepithelial area. Thickness of the fibrous layer in 4D was not much different from that of control ear. The cells in mucosal layer proliferated, became round in shape, but maintained a single layer. The thickness of mucosa was slightly increased. Neutrophil infiltration occurred also in mucosal layer. It should be emphasized that in 4D TM, the epithelial and subepithelial layers displayed more thickening than the other two layers of the TM.

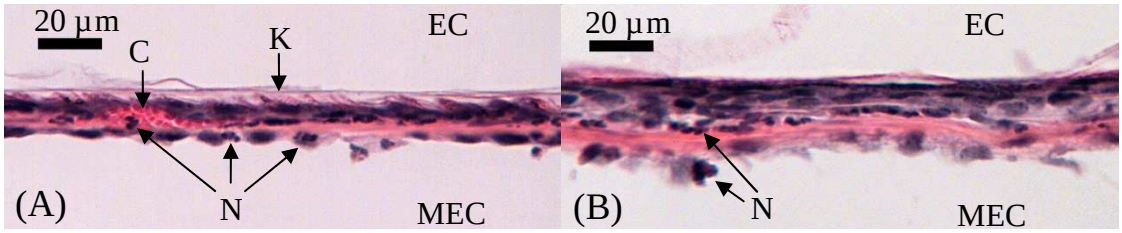


**Figure 2.5** Light micrographs of TM in 4D AOM ear with (A) two to three cell layers thick epithelial layer and (B) four to five cell layers thick epithelial layer. EC, ear canal; MEC, middle ear cavity; C, capillary; N, neutrophil; K, keratin.

Figure 2.6 displays TM structure at two locations of an 8D AOM ear. As inflammation persisted in the middle ear, the TM of 8D was thicker than that of 4D. The outer layer was in general three to five cell layers thick due to proliferation of the epithelium. Keratin filaments were frequently observed on surface of the TM. The subepithelial area was swollen because of edema. A greater number of inflammatory cells infiltrated into the subepithelial area compared with 4D. The middle fibrous layer seems unchanged. The epithelial cells of the mucosal layer proliferated and stratified. Edema and neutrophils were also observed in the mucosal layer. Thickness of the outer and inner layers were substantially increased in the 8D TM.

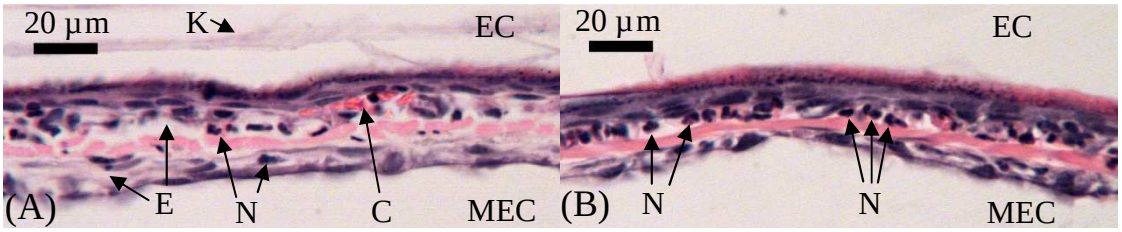


**Figure 2.6** Light micrographs of TM in 8D AOM ear. (A) Proliferation of epithelium, dilated capillary, edema, and infiltration of neutrophils occurred. (B) a great number of neutrophils infiltrated in subepithelial area. EC, ear canal; MEC, middle ear cavity; C, capillary; N, neutrophil; K, keratin; E, edema.

Table 2.1 lists the TM thickness at various locations of control, 4D, and 8D AOM ears. To date, TM thickness was measured in two specimens for each group.

**Table 2.1** TM thickness at nine locations of control, 4 days, and 8 days AOM ears. Each experimental group contains results of two specimens. Unit in μm.

| | | L1 – Inferior level | | | L2 – Intermediate level | | | L3 – Superior level | | |
|---|---|---|---|---|---|---|---|---|---|---|
| | | #1 | #2 | #3 | #1 | #2 | #3 | #1 | #2 | #3 |
| Control | 2-1R | 6 | 7 | 6 | 7 | 8 | 7 | 8 | 10 | 7 |
| | 2-2L | 9 | 8 | 9 | 8 | 7 | 9 | 8 | 11 | 10 |
| 4D AOM | 2-3L | 11 | 12 | 16 | 17 | 16 | 12 | 15 | 24 | 13 |
| | 2-3R | 15 | 12 | 15 | 12 | 19 | 11 | 14 | 25 | 11 |
| 8D AOM | 2-6R | 22 | 31 | 24 | 24 | 22 | 29 | 17 | 45 | 26 |
| | 2-6L | 20 | 24 | 23 | 25 | 31 | 28 | 35 | 52 | 39 |

As can be seen in Table 2.1, the TMs of both AOM groups were thicker than those of controls at all nine locations. TM thickness of 8D ears was greater than that of 4D ears at all measured locations. In each group, TM near the manubrium (location #2 in superior level) was thicker than other locations. If we exclude the thickness result obtained near the manubrium, based on a total of sixteen measurements on two TM samples for each group the average TM thickness of control, 4D, and 8D AOM was 7.8 ± 1.1, 13.8 ± 2.4, and 26.3 ± 5.5 µm, respectively.

### 2.3.2 RWM

Figure 2.7 shows histologic structure at the center of a control RWM. The chinchilla RWM consists of three layers: outer layer facing middle ear cavity is composed of squamous epithelium one to two cell layers thick; middle layer is connective tissue composed of collagen fibers; inner layer facing scala tympani is composed of a single layer of flat cells.

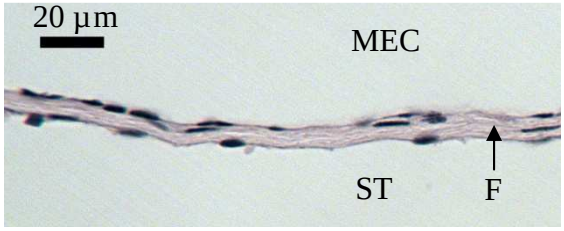


**Figure 2.7** Light micrographs of RWM in control ear. MEC, middle ear cavity; ST, scala tympani; F, fibrous layer.

Figure 2.8 displays low magnification images of control RWM. The image in Fig. 2.8A shows the cross section of the RWM lateral to its long axis. Fig. 2.8B shows the section medial to its long axis. As can be seen, the membrane is thick in the region of the bony rim and thin out in the central portion. At lateral side of the RWM, the thickness was uniform from end to end as shown in Fig. 2.8A. At medial side, the

RWM in the region posterior to the center was up to twice thicker than the rest part of the membrane due to thickening of the fibrous layer as shown in Fig. 2.8B. This local increase of thickness was observed in all the RWM specimens. Our histologic results demonstrate that in chinchillas posterior-medial quadrant of the RWM is thicker than other quadrants.

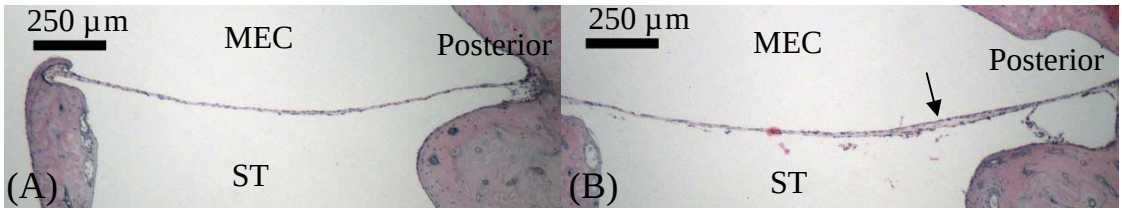


**Figure 2.8** Light micrographs of control RWM at (A) lateral side and (B) medial side of the membrane. MEC, middle ear cavity; ST, scala tympani. Arrow indicates local increase of thickness in posterior region of RWM.

Figure 2.9 shows the RWM of a 4D AOM ear. Substantial thickening occurred at the periphery of the membrane as shown in Fig. 2.9A. The higher magnification image of the RWM near the rim indicates that the thickening was caused mainly by edema and infiltration of neutrophils (Fig. 2.9B).

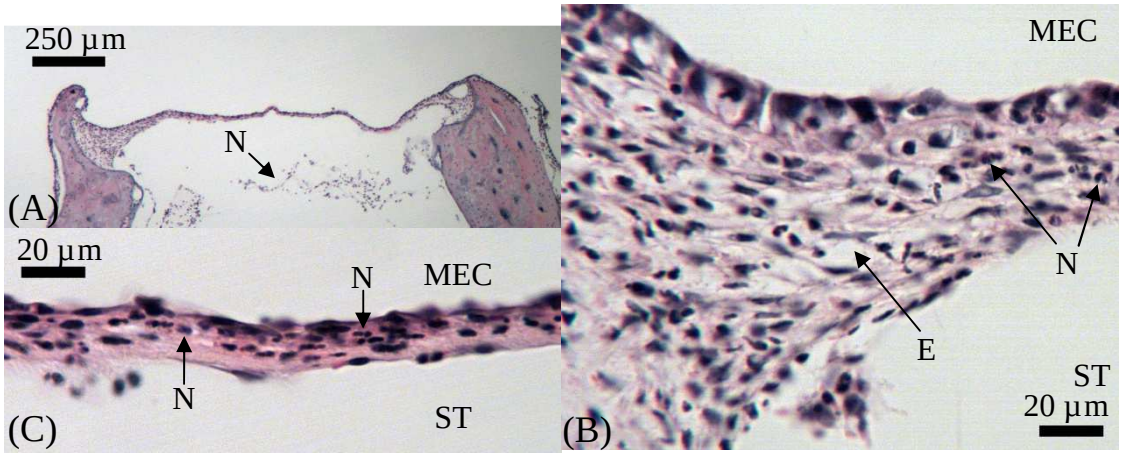


**Figure 2.9** Light micrographs of 4D RWM at (A) low magnification and (B) high magnification near the rim and (C) the center of the membrane. MEC, middle ear cavity; ST, scala tympani; N, neutrophil; E, edema.

Figure 2.9C displays the 4D RWM structure near the center of the membrane. Infiltration of inflammatory cells was observed in the middle fibrous layer. The middle layer was thickened due to the infiltration. The outer epithelial layer and inner layer were not much different from those of control samples. The thickness in the central portion of the membrane increased compared with that of control. It is noticed that inflammatory cells were present in the scala tympani of the 4D ear.

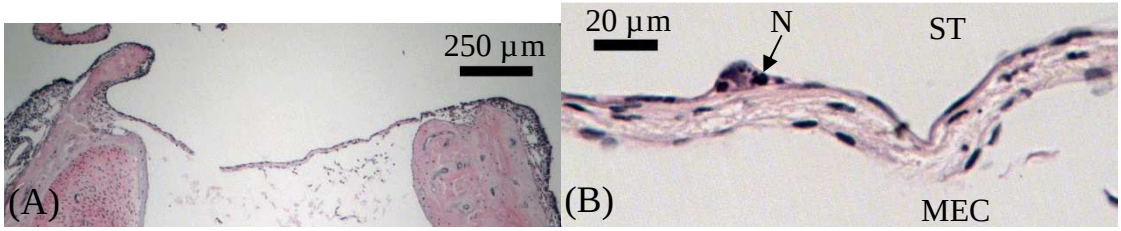


**Figure 2.10** Light micrographs of 8D RWM at (A) low magnification and (B) high magnification near the center of the membrane. MEC, middle ear cavity; ST, scala tympani; N, neutrophil.

Figure 2.10 displays the RWM structure of an 8D AOM ear. Compared with 4D RWM, the swelling at the boundary of the membrane decreased in 8D as shown in Fig. 2.10A. The structure at the center of the membrane is shown in Fig. 2.10B. The outer and inner layers were single layer thick. Less inflammatory cells were observed in the middle fibrous layer compared with 4D ear. The most dramatic changes of the 8D RWM was that the connective tissue of the middle layer was loose, which might have resulted from edema. The whole membrane was thicker than that of control ear.

Table 2.2 lists the thickness at nine locations of control, 4D, and 8D RWMs. To date, the thickness was measured in two specimens for each group. As shown in the table, the RWMs of 4D and 8D ears were thicker than those of control ears at all the locations. The RWM thickness of 8D was not much different from that of 4D. In each specimen, the thickness in posterior-medial quadrant of the membrane (#2 and #3 in L3)

was in general greater than that at other measured locations. The mean RWM thickness cross the nine locations of control, 4D, and 8D ears was 11.2 ± 2.5, 16.7 ± 2.4, and 16.1 ± 2.8 µm, respectively.

**Table 2.2** RWM thickness at nine locations of control, 4 days, and 8 days AOM ears. Each experimental group contains results of two specimens. Unit in μm.

| | | L1 – Lateral side | | | L2 – Intermediate section | | | L3 – Medial side | | |
|---|---|---|---|---|---|---|---|---|---|---|
| | | #1 | #2 | #3 | #1 | #2 | #3 | #1 | #2 | #3 |
| Control | 2-1L | 9 | 10 | 10 | 9 | 10 | 9 | 9 | 14 | 16 |
| | 2-2L | 10 | 12 | 9 | 11 | 12 | 9 | 10 | 16 | 16 |
| 4D AOM | 2-3L | 17 | 16 | 17 | 16 | 12 | 15 | 14 | 22 | 21 |
| | 2-4L | 15 | 16 | 16 | 15 | 17 | 16 | 16 | 20 | 19 |
| 8D AOM | 2-5L | 15 | 16 | 14 | 12 | 16 | 16 | 16 | 24 | 18 |
| | 2-6L | 16 | 16 | 11 | 14 | 15 | 16 | 15 | 20 | 19 |

### 2.3.3 SAL

Figure 2.11 shows structure of a control SAL. The stapes footplate is attached to the margin of the oval window via the SAL (Fig. 2.11A). Structure of the chinchilla SAL containing articular cartilage, articular capsule, and cavity between two cartilage layers (Fig. 2.11B). The surface of the oval window and the rim of the footplate are covered by a layer of hyaline cartilage. In control specimen, the SAL capsule at vestibular side frequently ruptured in the histologic process, but its structure still can be identified. As shown in Fig. 2.11B, the capsule facing the middle ear cavity or scala vestibuli is composed of squamous cells one or occasionally two layers thick. No fibrous tissue was observed in the SAL cavity.

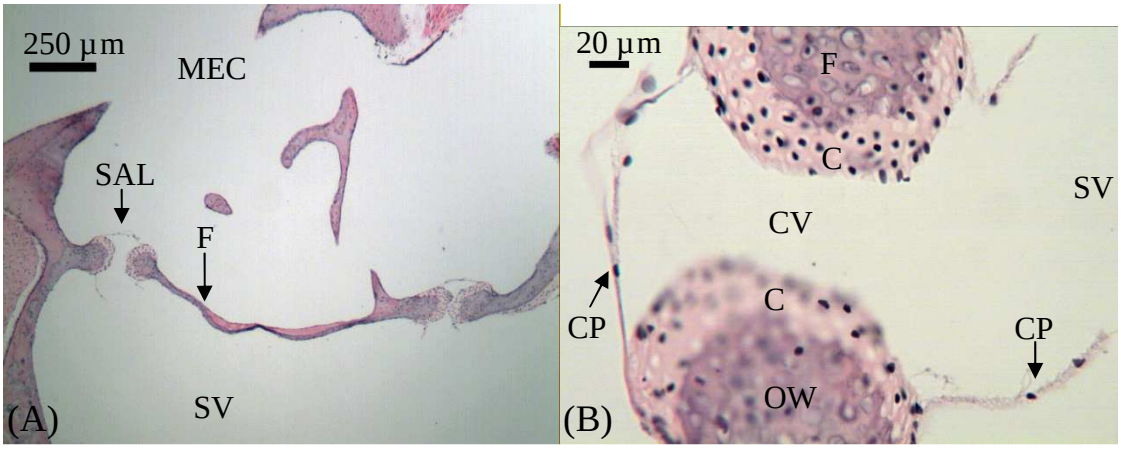


**Figure 2.11** Light micrographs of control SAL at (A) low magnification and (B) high magnification. MEC, middle ear cavity; SV, scala vestibuli; F, footplate; SAL, stapediovestibular joint; OW, oval window; CP, capsule; C, cartilage; CV, cavity.

Figure 2.12 displays SAL of a 4D AOM ear. Neutrophils were present in the middle ear near the footplate. No inflammatory cells were observed in scala vestibuli (Fig. 2.12A). Dramatic changes occurred in the capsule facing the middle ear. Thickness of the outer capsule was substantially increased due to infiltration of inflammatory cells (Fig. 2.12B). The capsule at inner ear side was not different from

that of control SAL (Fig. 2.12C). The cartilage layers and cavity in the SAL also appeared normal.

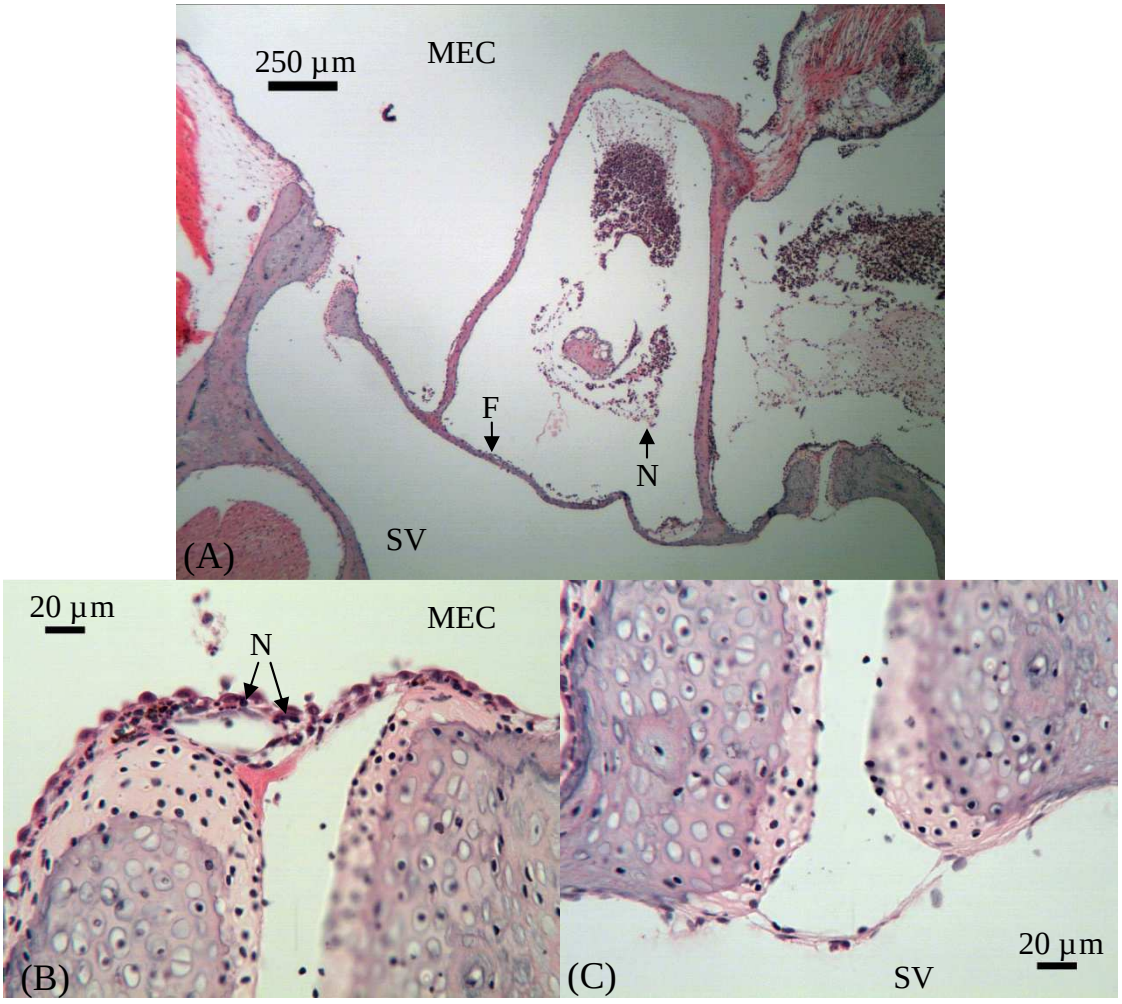


**Figure 2.12** Light micrographs of 4D SAL showing (A) inflammatory cells were within middle ear side of the footplate, (B) infiltration of neutrophils into the joint capsule facing the middle ear, and (C) normal appearance of the capsule at inner ear side. MEC, middle ear cavity; SV, scala vestibuli; F, footplate; N, neutrophil.

Figure 2.13 shows SAL of an 8D AOM ear. Inflammatory cells were observed in the middle ear side of the footplate, but were not found in the scala vestibule (Fig. 2.13A). Edema and inflammatory cells were observed in the SAL capsule at middle ear side (Fig. 2.13B). This outer capsule thickened further compared with 4D ear. The capsule at inner ear side appeared normal in 8D ear (Fig. 2.13C). The articular cartilage

and the cavity were not much different from those of control ear. In summary, the SAL cartilage, cavity, and inner capsule were not affected by the middle ear infection in both 4D and 8D ears. The SAL's outer capsule thickened in the early AOM and the thickening was more prominent in the later phase of the disease.

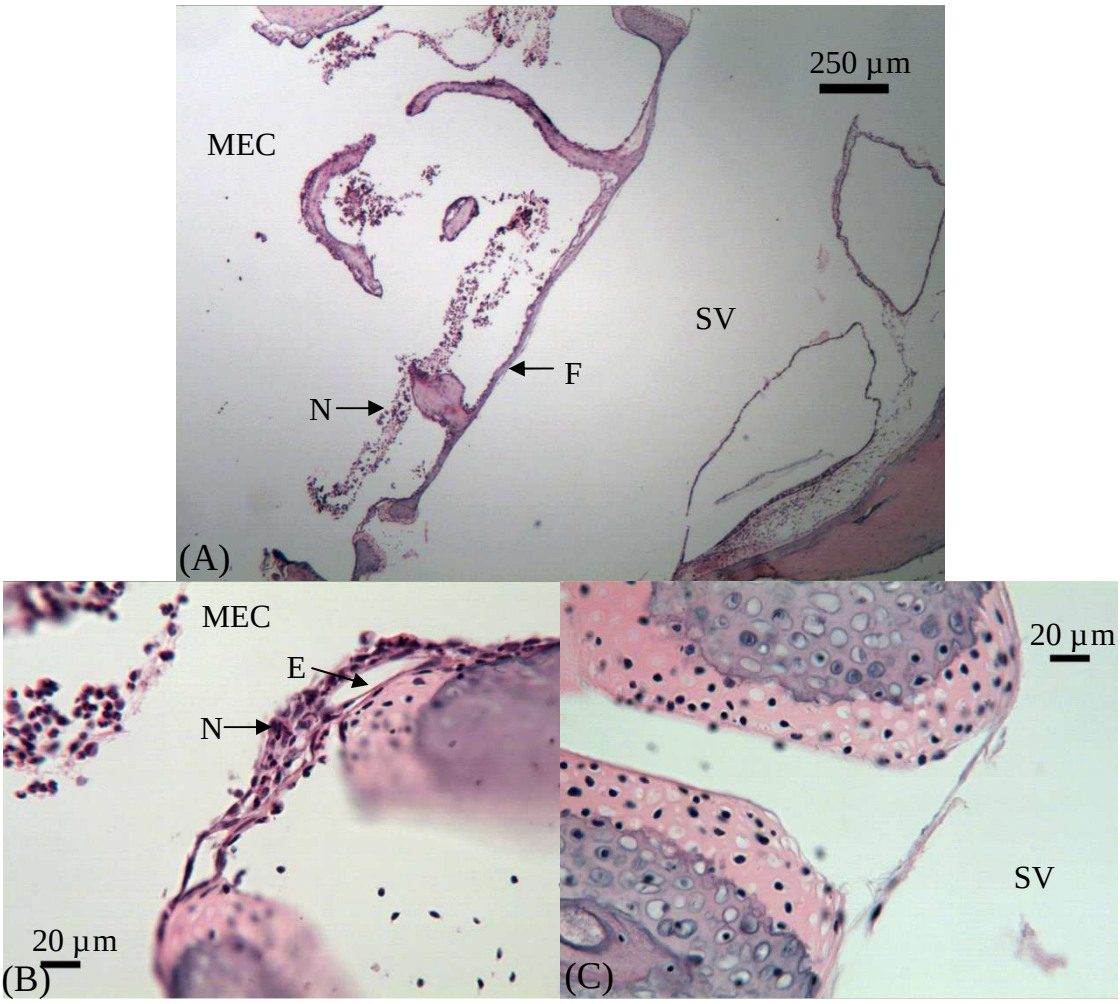


**Figure 2.13** Light micrographs of 8D SAL showing (A) inflammatory cells were within middle ear side of the footplate, (B) edema and neutrophils in the joint capsule facing the middle ear, and (C) normal appearance of the capsule at inner ear side. MEC, middle ear cavity; SV, scala vestibuli; F, footplate; N, neutrophil; E, edema.

## 2.3 Discussion

### 2.3.1 Compared with published data

Like many other species, the chinchilla TM consists of outer epithelial layer, middle fibrous layer, and inner mucosal layer. The number of studies on TM thickness of normal chinchilla was limited and there is noticeable discrepancy between the published data. Hsu et al. (2000) reported the thickness at seven locations across four quadrants of the chinchilla TMs in five age groups. In the 14 days-old chinchillas (oldest group in their study), the TM thickness varied from 18 to 31 µm over the measured locations (Table III in Hsu et al. 2000). Another study by Hsu et al. (2001) showed that TM thickness of adult chinchilla was 24 µm. Parekh et al. (2009) reported the morphology of normal chinchilla TM (Fig. 7 in their paper). Based on their histologic sections the TM thickness was between 6 to 10 µm, which was significantly smaller than the data reported by Hsu et al. In our current study, TM thickness of normal chinchilla ear is consistent with the results reported by Parekh et al. (2009).

The chinchilla RWM is also a three-layered membrane consisting of the outer epithelium, the middle connective layer, and the inner epithelium. Structure and thickness of normal chinchilla RWM has been reported in a few studies. Schachern et al. (1982) reported that the central portion of the normal chinchilla RWM had a mean thickness of 13.7 µm. Goycoolea and Lundman (1997) mentioned that the RWM thickness was 10 to 14 µm in chinchilla. Our thickness results of normal chinchilla RWM generally agree with those published data.

Our histologic study demonstrated that the chinchilla SAL contains articular capsule, cartilage, and cavity. To date, my literature review of structural assessment on chinchilla SAL identify only one relevant study. Bolz and Lim (1972) examined the SALs of different species including chinchilla. Their results also showed that the

chinchilla SAL had structure of a synovial joint, which is similar to our observation. The rim of the footplate was attached to the oval window via thin capsules. There was no fibrous connection between the two cartilage layers in the joint. The structure of chinchilla SAL differs significantly from that of other lab animals and human. There are ligament fibers transversely crossing in the space between the two cartilage layers in the SALs of human (Bolz and Lim 1972; Takanashi et al. 2013), rat (Ohashi et al. 2006), dog, cat, and sheep (Bolz and Lim 1972).

### 2.3.2 Histopathlogic changes of TM, RWM, and SAL in AOM

The chinchilla TM underwent substantial changes in early phase of AOM and the changes were more prominent in later phase of the disease. At day 4 post inoculation, the outer epithelium of the TM proliferated and became two to three cells in thickness. Inflammatory cells infiltrated into the subepithelial area. The change in inner mucosal layer was relatively small. The middle fibrous layer remained unchanged. Thickening of the TM in 4D AOM ears was primarily contributed by the outer layer changes. At day 8 of the infection, thickness of the outer epithelium further increased. The subepithelial area was edematous and infiltrated with more neutrophils. The fibrous layer was not much different from that of control or 4D TM. Cells in the mucosal layer proliferated and stratified. Edema and neutrophil infiltration also occurred in the mucosal layer. Changes of outer and inner layer were the primary contributors to the thickening of the 8D TM. Edema and neutrophils in those two layers were likely to be a result of dilated capillaries, allowing fluid and inflammatory cells to escape from the capillaries. Berger et al. (1996) histologically examined the human temporal bones with AOM. They reported that the epithelial layer of the TM was thicker in patients with

AOM and identified that swelling, infiltration with inflammatory cells, and distended capillaries affected mostly the subepithelial and submucosal layers, whereas the fibrous layers remained intact. Our findings on TM changes in the chinchilla AOM model are similar to their results.

Thickness of the chinchilla RWM was increased in 4D AOM. The thickening was resulted from infiltration of inflammatory cells into the middle fibrous layer of the membrane. Those inflammatory cells are believed to escape from the capillaries in the middle layer and migrate towards the middle ear cavity and inner ear scala tympani. Under light microscope examination, the outer and inner epithelial layers of 4D RWM were not different from those of control. As AOM persisted to 8D, in middle layer of the RWM the fibrous tissue was loose and swollen and the number of inflammatory cells decreased. No substantial changes were observed in the outer and inner layers. The thickness of 8D RWM was similar to that of 4D RWM. Schachern et al. (1981) produced OM in chinchillas by intrabullar injection of staphylococcal exotoxin and examined the RWMs by electron microscope. They also observed inflammatory cell infiltration of the fibrous layer and basal portion of the scala tympani. Furthermore, they identified intercellular edema, cellular and nuclear swelling of the epithelium in both surface layers. In our study, such changes in RWM epithelium were not observed under light microscope.

Changes of the SAL in both 4D and 8D AOM ears were limited in the capsule facing the middle ear. Inflammatory cells infiltrated into the capsule and subsequently increased the capsule thickness in the early phase of AOM. Thickening of the SAL outer capsule was more prominent at day 8 due to cell infiltration and swelling. The

epitheliums of the outer capsule line with the middle ear mucosa. The inflammatory cells and fluid in the capsule might migrate from the middle ear mucosa adjacent to the joint. The inner capsule facing the cochlear cavity was unchanged and no inflammatory cells were observed in the scala vestibuli near the footplate. The inflammation did not cross the oval window. It suggests that the SAL is less susceptible to middle ear inflammation than the RWM in this AOM model.

In this study, histologic examination on the control and AOM ears indicates that microstructures of the TM, RWM, and SAL in the diseased ears varied from those of controls. The ear tissues' structural changes in later phase of AOM were more prominent than those in early phase of the disease, which suggests that the mechanical properties of those tissues may change over the course of the disease.

Future works are needed to increase numbers of TM and RWM specimens of control and two AOM groups for statistical analysis on their thickness. Histologic preparation for SAL needs to be improved to maintain an intact inner capsule.

## 2.4. Conclusion

AOM was produced in the chinchillas by transbullar injection of *H. influenzae*. Microstructures of the TM, RWM, and SAL were examined in normal, 4D AOM, and 8D AOM ears by histology. Thickness of the TM and RWM were quantified in the three experimental groups. In early phase of AOM, TM thickness was increased and cellular proliferation and infiltration in outer layer were primary contributors. RWM was also thickened by infiltration of neutrophils into the middle fibrous layer. Outer capsule of the SAL was thickened due to cell infiltration. In later infection phase, TM

was further thickened by edema and cell proliferation in the outer and inner layer. Middle fibrous layer of the RWM became swollen. Thickness of the SAL's outer capsule was further increased by edema. This study characterized the histopathologic changes of those middle ear tissues during the course of AOM and provides fundamental structural evidence to aid in understanding their mechanical properties.

# CHAPTER 3: AUDITORY BRAINSTEM RESPONSE OF CHINCHILLA AOM EARS

## 3.1 Introduction

In this chapter, hearing level changes of the chinchillas in early and later phases of AOM was evaluated by measuring the animals' auditory brainstem response (ABR). ABR is an auditory evoked potential generated along the path from the inner ear auditory nerves to the inferior colliculus in the midbrain. This electrical activity can be recorded via electrodes placed on the scalp.

ABR signal is characterized by a series of waves produced usually in the first 10 milliseconds after onset of an auditory stimulus. Figure 3.1 shows ABR of a chinchilla in response to sound stimulus at various intensities. The amplitude of each wave in the ABR is reduced as the sound level decreases. ABR cannot be identified when sound intensity declines to a certain level, which is usually considered as the threshold of ABR or hearing.

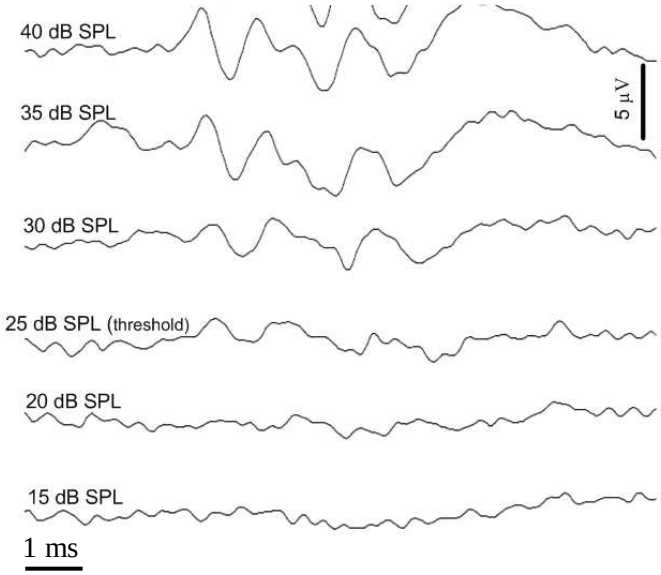


**Figure 3.1** ABR of a chinchilla ear in response to sound stimulus at various intensities.

ABR has been widely used to determine changes of hearing threshold or hearing loss in animals with OM. Petrova et al. (2006) investigated the effects of the middle ear fluid and pressure on the auditory threshold by measuring the ABR in live guinea pigs. Qin et al. (2010) investigated the hearing loss in mice ears with middle ear effusion by measuring the ABR threshold. Recently, we conducted ABR measurement in guinea pigs to investigate the hearing loss produced by middle ear fluid (Guan and Gan 2011).

This chapter describes the methods of ABR measurement and the results of hearing loss in the chinchillas represented by ABR threshold shifts at 4 days (4D) and 8 days (8D) post inoculation.

## 3.2 Methods

### 3.2.1 Animal preparation

Fifteen chinchillas (*Chinchilla lanigera*) weighing between 600-780 g were included in this study. The study protocol was approved by the Institutional Animal Care and Use Committee of the University of Oklahoma and met the guideline of the National Institutes of Health. All animals were free from middle ear disease (as evaluated by otoscopic examination) at the beginning of the study.

The chinchillas were divided into control and AOM groups. The control group included six animals, the group of 4D AOM included five animals, and the group of 8D AOM included four animals. AOM was produced by transbullar injection of HI 86-028NP suspension in both ears following the procedure described in Chapter 2. At the 4th or 8th day post-inoculation, animals were anesthetized as described above. Additional anesthesia was administered as needed to maintain areflexia.

The pinna and the skin covering the ear canal were removed surgically to expose the entrance of the ear canal. In each animal, the experiment was conducted bilaterally (N=12 for control; N=10 for 4D AOM; N=8 for 8D AOM). For both control and AOM groups, the body temperature of the animal was maintained throughout the experiment at approximately 38° C by placing the animal in a prone position on a thermoregulated surgical heating blanket.

### 3.2.2 ABR measurement

Pure-tone ABR thresholds of the AOM and control animals were recorded following the procedure reported in Guan and Gan (2011). Repeated tone burst stimuli with alternating polarity from TDT system III (Tucker-Davis Technologies, Alachua, FL) were delivered by the speaker (CF1, TDT, Alachua, FL) to the probe of a ER-10B+ microphone (Etymotic Research, Elk Grove Village, IL), which was inserted into the ear canal. The microphone and the sound delivery tube were integrated in the probe. The tip of the probe was approximately 3 to 5 mm away from the umbo.

Tone burst stimulus with duration of 4 ms (0.5 ms rise/fall, 3 ms plateau) at frequencies of 0.5, 1, 2, 4, and 8 kHz was applied in the ear canal at the rate of 13/s. Figure 3.2 displays the waveform of the stimulus to evoke ABR. The stimuli of tone burst started from 80 dB and down (or up) to the threshold in steps of 5 dB. The ABR threshold was defined as the lowest sound intensity at which clear ABR waves could be observed (Qin et al. 2010; Jeselsohn et al. 2005; Petrova et al. 2006). The ABR waveform at each level was measured in 10 ms recording window, averaged 200 times, and recorded on a computer. The input sound pressure levels were calibrated by using the microphone in every ear before the test.

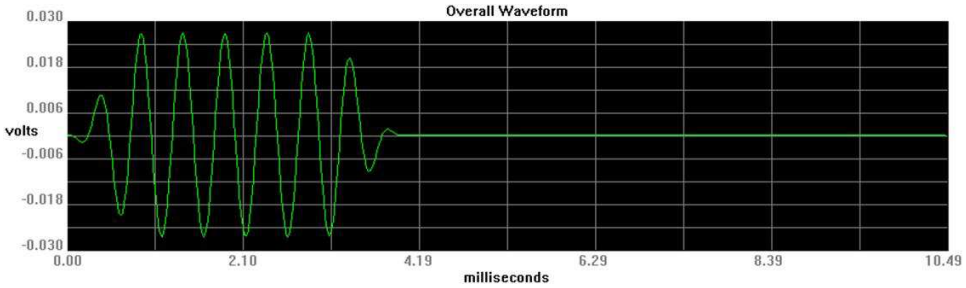


**Figure 3.2** Waveform of tone burst stimulus to evoke ABR.

The negative recording electrode (steel needle electrode) was inserted subcutaneously at the mastoid area and the positive recording electrode was placed at the vertex. The ground electrode was placed in the hind leg. ABR signals were amplified and averaged using TDT system III and Biosig software. The no-testing ear canal was sealed with dental cement during the ABR measurement.

### 3.3 Results

Figure 3.3 shows the individual and mean threshold of pure tone ABR over frequencies of 0.5-8 kHz in twelve control, ten 4D AOM, and eight 8D AOM ears. The gray area indicates ±1 standard deviation (SD) around mean.

ABR thresholds of control ears with mean and individual curves are displayed in Fig. 3.3A. The mean threshold was relatively high at low frequencies and gradually decreased as the frequency increased to 8 kHz. Published data from Hsu et al. (2001) were plotted in Fig. 3.3A for comparison. The difference between our results and their data was within 5 dB over 1-8 kHz except 4 kHz, where the threshold of normal chinchillas measured by Hsu et al. was 8 dB greater than that obtained in the current study. This may result from different methods of stimulus calibration between the two

studies. The stimulus was calibrated in a 1 $cm^3$ coupler in the study by Hsu et al. In our current study, the stimulus was calibrated in ear before the measurement.

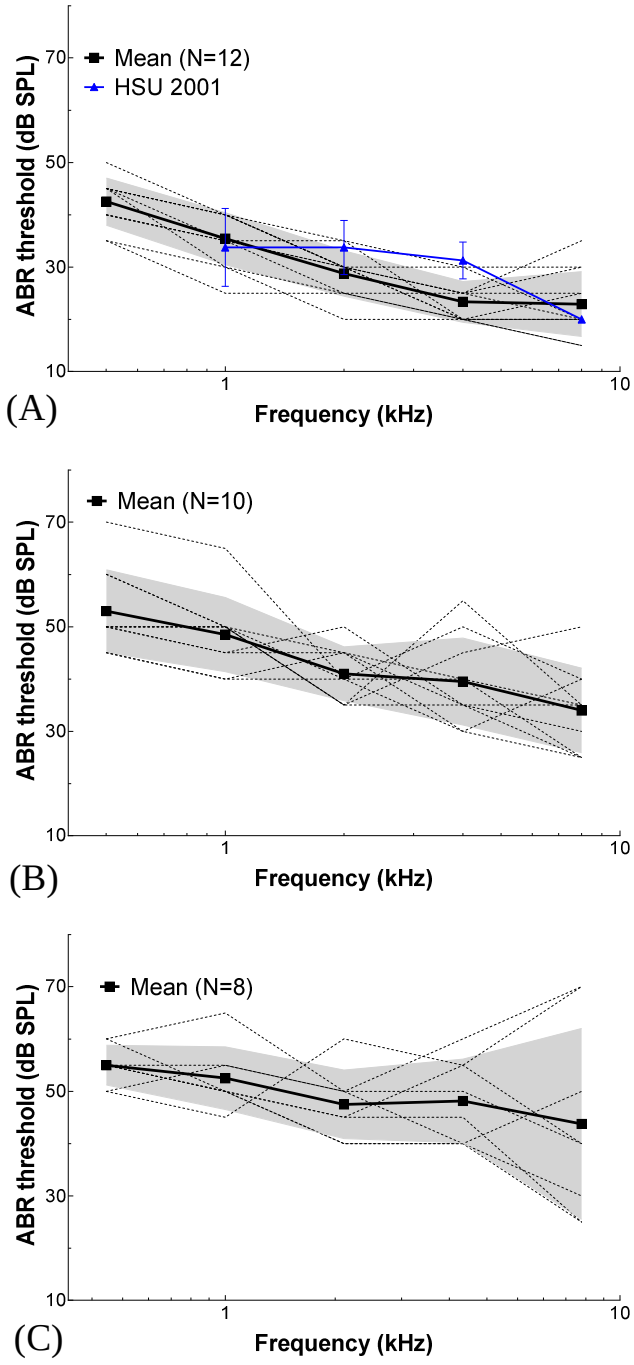


**Figure 3.3** Threshold of ABR over 0.5 to 8 kHz in (A) control, (B) 4D AOM, and (C) 8D AOM ears. Dotted lines represent the individual curves. Solid line represents the mean curve. Shaded area represents ± 1 SD around mean. Blue line represents the ABR threshold of normal chinchilla ears reported by Hsu et al. (2001).

The mean ABR threshold of 4D AOM ears elevated at all tested frequencies (Fig. 3.3B). Individual ABR curves show variations at low and high frequencies, which may be caused by different levels of middle ear pressure and effusion between ears.

Figure 3.3C shows the individual and mean ABR threshold of 8D AOM ears. The mean threshold at high frequencies further increased compared with 4D ears. The variation of individual threshold was large at 8 kHz.

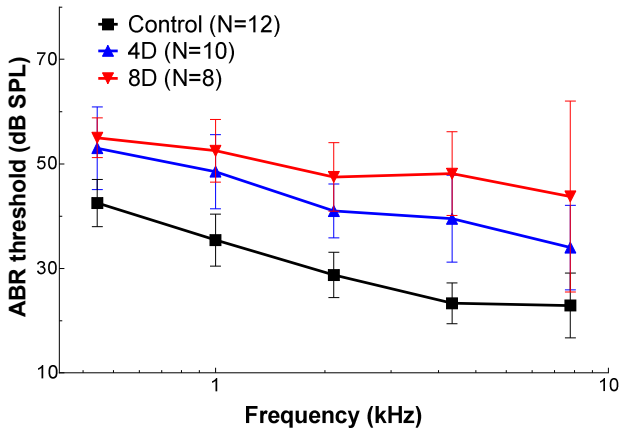


**Figure 3.4** Comparison of mean ABR threshold with SD between control (black line), 4D (blue line), and 8D ears (red line).

Figure 3.4 displays the comparison of the mean ABR data over the frequencies between three groups. Student t-tests were used to analyze the group difference at each frequency and the statistical results are listed in Table 3.1. The ABR threshold of both AOM groups is significantly greater than that of control ears at all tested frequencies. As shown in Fig. 3.4, the mean ABR threshold of 8D ears is higher than that of 4D ears over the frequencies, but the increase is significant only at 2 and 4 kHz (Table 3.1).

**Table 3.1** List of P values derived from unpaired t-test on the ABR threshold data between control, 4D, and 8D ears.

| | 0.5 kHz | 1 kHz | 2 kHz | 4 kHz | 8 kHz |
|---|---|---|---|---|---|
| Control vs 4D | 0.00 | 0.00 | 0.00 | 0.00 | 0.00 |
| Control vs 8D | 0.00 | 0.00 | 0.00 | 0.00 | 0.01 |
| 4D vs 8D | 0.49 | 0.21 | 0.04 | 0.04 | 0.19 |

### 3.4 Discussion

Elevation of ABR threshold in 4D and 8D ears indicates that the animals had conductive hearing loss in early and later phases of AOM. The hearing loss resulted from a combination of middle ear pressure, effusion, and structural changes induced by the middle ear infection. The 8D ears tend to have greater hearing loss than the 4D ears over all the frequencies and significant difference in hearing loss level occurred at certain frequencies between the two AOM phases. Our findings demonstrate that the hearing loss was more profound as the infection persisted in the middle ear.

Our previous study in guinea pig model indicated that when saline was injected into the middle ear the hearing loss strongly correlated with the loss of TM mobility at umbo (Guan and Gan 2011). Studying mechanisms of TM mobility loss would help in understanding the conductive hearing loss associated with AOM. In next chapter, we investigate the factors contributing to the loss of umbo mobility in the early and late phases of AOM.

### 3.5 Conclusion

The hearing loss of 4D and 8D AOM ears were evaluated by changes of ABR threshold. ABR threshold of chinchillas at 4D or 8D post inoculation significantly increased over 0.5-8 kHz. The threshold in 8D ears was greater than that in 4D ears at all the frequencies, but significant increase was observed only at 2 and 4 kHz.

# CHAPTER 4: FACTORS AFFECTING LOSS OF TYMPANIC MEMBRANE MOBILITY IN CHINCHILLA AOM MODEL

## 4.1 Introduction

The mechanisms of conductive hearing loss associated with AOM are not well understood. Recently we utilized a *Streptococcus pneumoniae* (SP) type 3 strain to produce a 3-day AOM model in guinea pigs (Guan and Gan, 2013). Data from that study unequivocally showed that changes in middle ear pressure, effusion volume, together with infection-induced structural changes each contributed to the loss of TM mobility (Guan and Gan, 2013). However, it is not clear how those factors vary along the course of the disease and whether those effects are reproducible in different species. The present study was designed to address these issues.

In this chapter, we focus on characterizing the roles of middle ear pressure (MEP), middle ear effusion (MEE), and middle ear structural changes such as ossicular adhesions and soft tissue property changes in sound transmission during the course of middle ear infection, we utilized the chinchilla AOM model initiated by transbullar injection of strain *Haemophilus influenzae* (HI) 86-028NP. The infected animals were divided into two groups: 4 days (early phase of AOM) and 8 days (later phase of AOM) post inoculation. In each group, the TM vibration at the umbo was measured using laser Doppler vibrometry (LDV) at three experimental stages: the unopened AOM ear with MEP and MEE, upon release of MEP, and after removal of MEE. We then quantified and compared the effects of middle ear pressure, effusion, and structural changes on TM mobility loss at these two phases of AOM.

## 4.2 Methods

### 4.2.1 Animal preparation

Eighteen chinchillas (Chinchilla lanigera) weighing between 600-780 g were included in this study. The study protocol was approved by the Institutional Animal Care and Use Committee of the University of Oklahoma and met the guideline of the National Institutes of Health. All animals were free from middle ear disease (as evaluated by otoscopic examination) at the beginning of the study.

The animals were divided into control and AOM groups. The control group included eight animals, and the AOM group of 10 animals was subdivided into two groups: the 4 days (4D) group of six animals and the 8 days (8D) group of four animals. AOM was produced by transbullar injection of HI 86-028NP suspension in both ears following the procedure described in Chapter 2. Under general anesthesia [ketamine (10 mg/kg) and xylazine (2 mg/kg)], 0.3 ml bacterial suspension containing 3000 CFU was injected into the superior bulla bilaterally using a 1 cc syringe with a 26 gauge needle. After the challenge dose was administrated, otoscopic examination was performed daily. The animals of control group were untreated.

At the 4th or 8th day post-inoculation, animals were anesthetized as described above. Additional anesthesia was administered as needed to maintain areflexia. The TM was examined microscopically, and then surgery was performed (see description below). In each animal, the experiment was conducted bilaterally (N=16 for control; N=12 for 4D AOM; N=8 for 8D AOM). For both control and AOM groups, the body temperature of the animal was maintained throughout the experiment at approximately

38° C by placing the animal in a prone position on a thermoregulated surgical heating blanket.

### 4.2.2 Experimental protocol

To expose the entrance of the ear canal, the pinna and the skin covering the ear canal were removed surgically. The TM was examined under a microscope to identify signs of AOM. Then the middle ear pressure and energy absorbance were measured by using a wideband tympanometer (Model AT235h, Interacoustic, MN).

Upon the completion of tympanometry, a 3 mm diameter hole was drilled in the lateral wall of the ear canal to expose the umbo. Then a laser reflective tape (0.2 x 0.2 $mm^2$, < 0.01 mg, 3M, St. Paul, MN) was passed through the hole and placed on the center of the lateral surface of the TM (umbo) to establish the laser target for measuring TM vibration (Fig. 4.1).

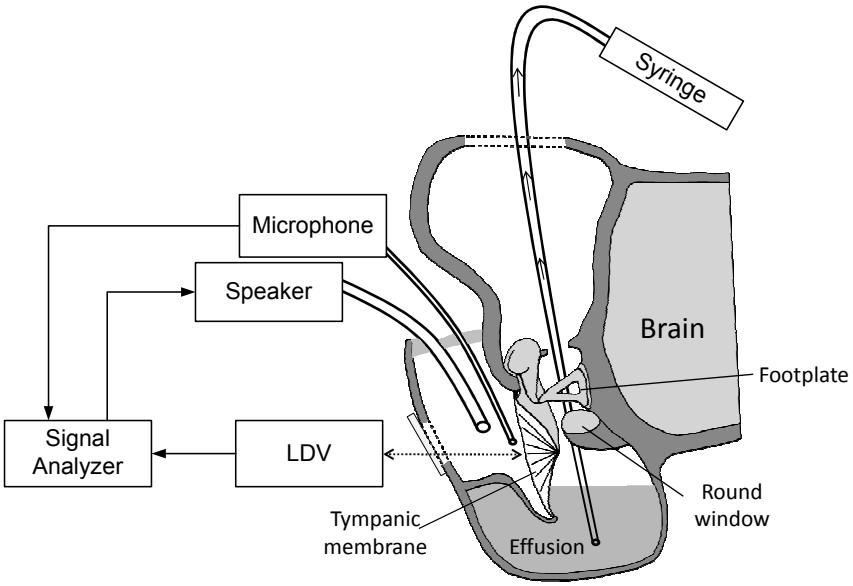


**Figure 4.1** Schematic diagram of the experimental setup with laser vibrometry at the umbo in the tympanic membrane in chinchillas and the methods for aspiration of the middle ear effusion.

The TM vibration measurement in AOM ears was performed in three experimental stages: OM-1, undisturbed bulla had intrinsic middle ear pressure and effusion; OM-2, the pressure was released from the middle ear; and OM-3, the effusion was drained from the middle ear. A sound delivery tube and a probe microphone were placed in the ear canal and the movement of the TM at umbo was measured. At each experimental stage, the TM measurement was conducted bilaterally using LDV.

After completion of the vibration measurement in stage OM-1, the skin of the superior temporal bone was partly removed to expose the middle ear bony wall on top of the temporal bone. A hole of 1 mm diameter was drilled into the roof of the middle ear to release the middle ear pressure. After sealing the hole with dental cement (PD-135, Pac-Dent, CA), the OM-2 evaluation was performed.

Upon the completion of LDV measurements for stage OM-2, the hole on top of the temporal bone was opened and enlarged to 3-4 mm in diameter using a drill (Fig. 1). Under microscopic visualization a silicone tube was inserted to the bottom of the middle ear cavity through this hole. The middle ear effusion was then aspirated manually from the cavity with a 1 ml syringe. The aspiration process was repeated as necessary until no additional fluid could be drained from the tympanic cavity. The total effusion volume obtained from each ear was then recorded.

Adhesions were frequently found on the malleus head and between the manubrium and the cochlear promontory when the top cavity was opened for stage OM-3. These ossicular adhesions were not disturbed during the aspiration of the effusion. The opening on top of the temporal bone was then covered by a thin glass sheet, and sealed with dental cement. Then, LDV was performed for stage OM-3. After

measurements were completed at all 3 OM stages, the bulla was harvested. Then another hole (diameter of ~4 mm) was opened on the posterior area from the medial side to allow a microscopic examination of the middle ear. The ossicles were examined from the superior view to assess the malleus-incus complex and from the posterior-medial view to evaluate the manubrium and the area adjacent to the round window.

Control ears were prepared and analyzed in the same manner as described above for ears with AOM. To exclude the effect of middle ear pressure in anesthetized animals (Guinan and Peake 1967), a hole of 1 mm diameter was drilled on the top of the middle ear cavity to release any pre-existing pressure. A reflective tape was placed on the umbo and the small opening on the roof of the temporal bone was sealed by dental cement. TM vibration was then measured by LDV as described in the next section. Note that the pressure was not measured in the control ears since any unbalanced pressure had been released in the preparation.

### 4.2.3 Laser Doppler vibrometry measurement

Figure 4.1 shows a schematic of the experimental setup for measuring TM vibration at the umbo with LDV. The methods of stimulus generation and umbo vibration measurement closely resembled those used in our previous guinea pig study (Guan and Gan, 2013). Briefly, pure tones at 80 dB SPL were presented into the ear canal sequentially from 100 Hz to 10 kHz for 50 cycles at each tone through a sound delivery tube. A probe microphone (Model ER-7C, Etymotic Research, IL) was inserted in the ear canal and the tip of the probe was placed approximately 2 mm from the umbo to monitor the input SPL. After the sound delivery tube and the probe microphone were placed, the entrance of the ear canal was sealed with dental cement. As shown in Fig.

4.1, the opening in the lateral surface of the ear canal wall was covered by a transparent glass sheet, and the gap between the glass sheet and the bony wall was sealed with dental cement. Vibrations of the TM were measured by the laser vibrometer (Polytec CLV 2534, Tustin, CA). The direction of the laser beam was approximately normal to the lateral surface of the umbo. The peak-to-peak displacements (dp-p in unit of μm) of the TM at the umbo were calculated from the voltage output of the laser vibrometer velocity decoder by $d_{p-p}= 2A_{volt}/\pi f$, where $A_{volt}$ is the amplitude of vibrometer output (velocity) in Volts and f is the frequency of pure tone in kHz. To obtain the TM displacement phase, the measured velocity phase was shifted by $-90^{o}$ at all tested frequencies.

Surgical preparation of each animal (inclusion of both ears) required 15-20 minutes. Tympanometry was completed within 2 minutes, and the LDV measurement at each experimental stage usually took about 10 minutes. The TM vibration data for the unopened bulla (OM-1) were collected about 30 minutes after the anesthesia. For other OM stages, the TM vibration data were obtained within 5 minutes after re-sealing the opening on the bulla to avoid any pressure variations that might occur with a longer interval.

## 4.3 Results

### 4.3.1 Microscopic observation and MEP of AOM ears

After removing the pinna, the TM was examined microscopically to identify signs of AOM. The thin, translucent TM typical of normal (uninfected control) chinchillas is shown in Fig. 4.2A. The changes typical for the TM of an AOM ear at 4D

are shown in Fig. 4.2B. After this short time post infection, the TM appeared opaque and a middle ear effusion (yellow in color) was evident. However, at this low magnification such TMs exhibited no observable structural changes compared to control TMs. As shown in Fig. 4.2B, an air-fluid interface behind the TM was usually visible and associated with AOM in 4D ears. The volume of MEE in 4D AOM ears ranged from 0.3-0.6 ml and had a mean value of 0.42 ml (± 0.11 ml standard deviation, SD) when the MEE was aspirated for experimental stage OM-2. In two of the ears exhibiting AOM at 4D, the volume of effusion was sufficiently large (~0.6 ml) to fill the middle ear over the umbo. The effusion level in the other ears from the 4D group filled the middle ear cavity to a level below the umbo.

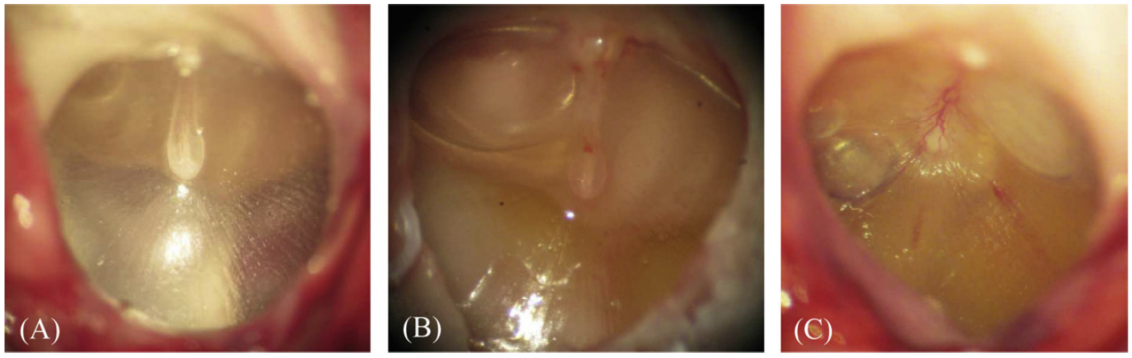


**Figure 4.2** Microscopic photographs of (A) control eardrum, (B) 4 days AOM eardrum, and (C) 8 days AOM eardrum.

A view of the TM in an 8D AOM ear is shown in Fig. 4.2C. TMs from this time period were hyperemic and opaque. A yellow-colored MEE was observed in each ear. In these ears, the effusion almost filled the entire middle ear space. MEE volume ranged from 0.7-0.9 ml with an average value of 0.82 ml (± 0.09 ml, SD). The observed mean fluid volume was significantly greater than that found in AOM ears after infection for four days (student t-test, $p < 0.05$). MEEs from both 4D and 8D ears were clearly purulent. The appearance of MEEs obtained at these two times following bacterial

challenge could not be distinguished from one another by the unaided eye or under low power light microscopy.

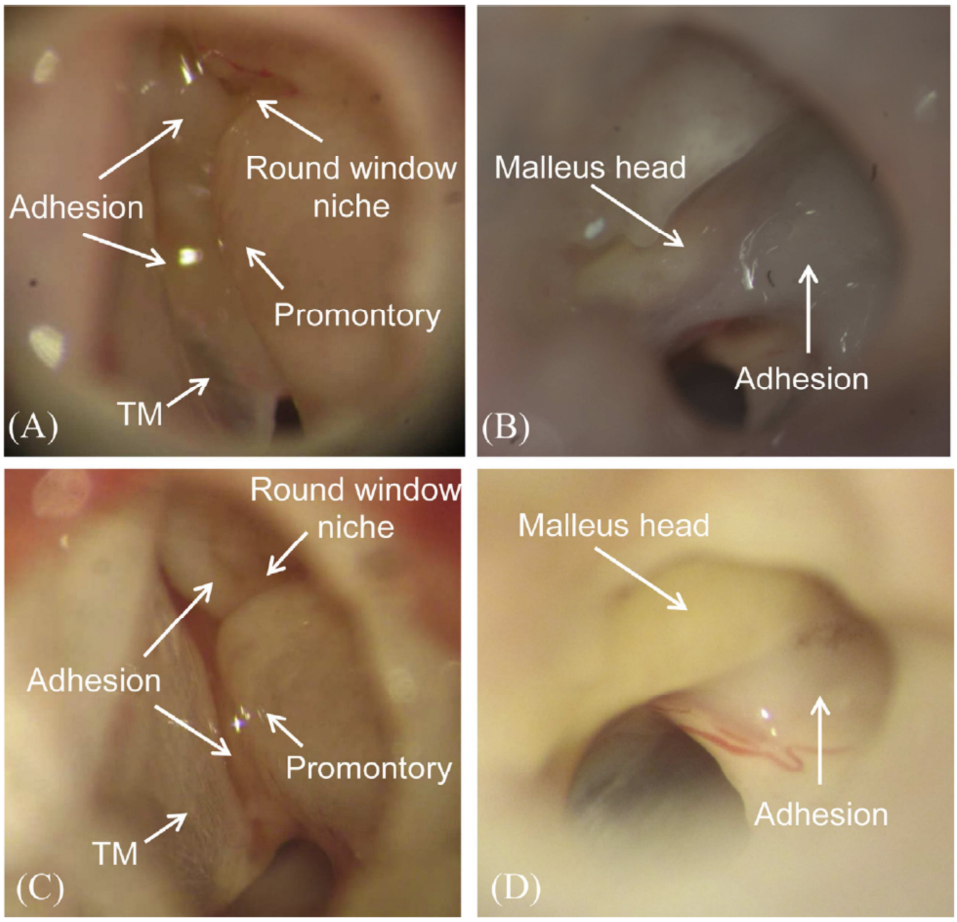


**Figure 4.3** Microscopic photographs of (A) middle ear cavity and ossicles in 4 days AOM ear, (B) malleus head in 4 days AOM ear, (C) middle ear cavity and ossicles in 8 days AOM ear, and (D) malleus head in 8 days AOM ear.

Next we evaluated the occurrence of changes in ossicular appearance and structure at 4D and 8D post challenge (Fig. 4.3). Prior to these assessments, MEEs were removed to better visualize the changes which occurred. Adhesions were formed between the TM and the cochlear promontory as well as around the round window niche by Day 4 (Fig. 4.3A). The manubrium, stapes, and long process of the incus were

covered with adhesions. As shown in Fig. 4.3B, adhesions were also observed on the malleus head.

The typical appearance of the ossicles in ears of chinchillas experiencing AOM for 8 days is shown in Figs. 4.3C and 4.3D. Modest adhesions were observed in the round window niche and between the manubrium and promontory (Fig. 4.3C). Figure 4.3D illustrates the adhesions formed on the malleus head. Adhesions also were observed between the ossicles and the adjacent middle ear walls in both 4D and 8D AOM animals. These AOM-associated ossicular changes in the chinchilla closely resemble those previously described in the guinea pig (Guan and Gan, 2013) and the gerbil AOM models (von Unge et al., 1997). Adhesions between the manubrium and cochlear promontory in 4D ears appeared to be thicker than those observed in 8D ears. In contrast, adhesions around the malleus head in 4D ears did not appear to differ from those occurring at 8D. In Fig. 4.3D, we also observed dilated capillaries in the mucosa near the malleus head. The changes of capillaries suggest a possible thickening of the mucosa layer.

The MEP in stage OM-1 was measured by wideband tympanometry before the measurement of TM vibration. The MEP of all 4D AOM ears was negative and had a mean value of -176 ± 54 daPa. In the 8D AOM group, four ears exhibited a flat tympanogram, and the MEP was could not be identified. We believe that this observation probably reflects large amount of effusion present in the middle ear cavity (Jerger 1970; Paradise et al., 1976). The MEP of the remaining 8D ears with AOM were all negative (mean value -145 ± 65 daPa).

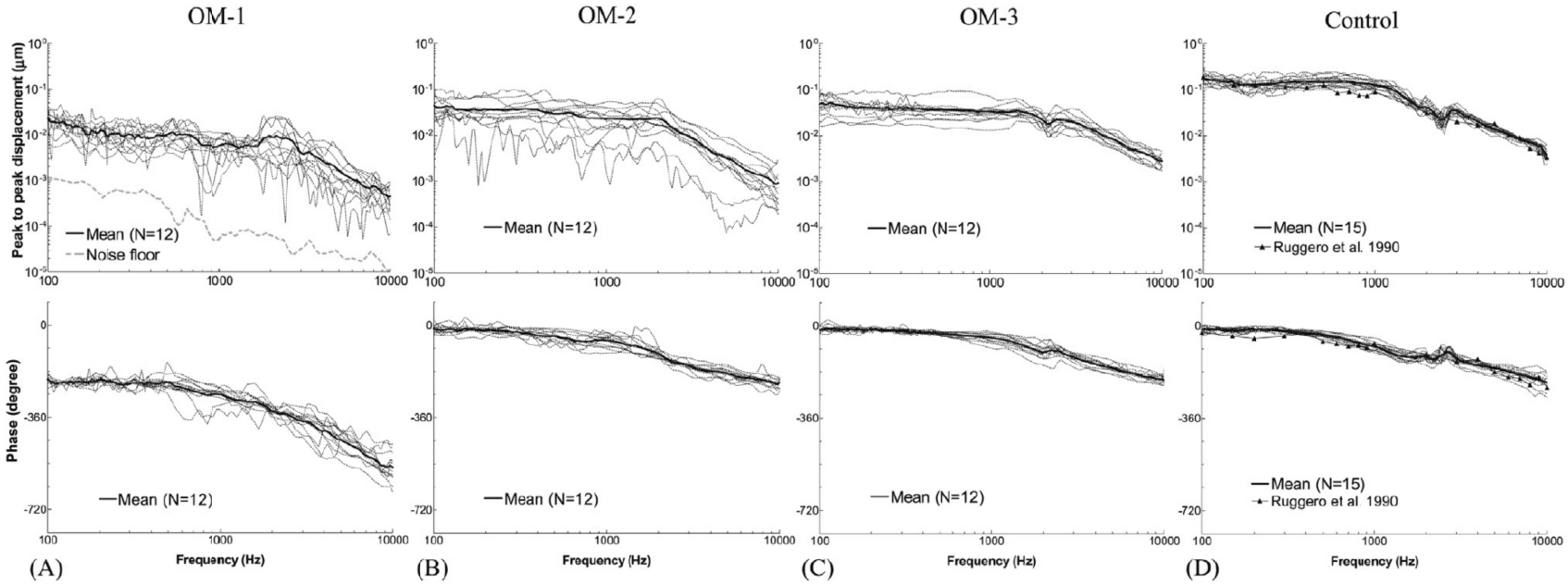


**Figure 4.4** Peak to peak displacement magnitude (upper panel) and phase angle (lower panel) of the TM at umbo in response to 80 dB SPL sound input at the ear canal in 4 days (A) OM-1, (B) OM-2, (C) OM-3, and (D) control ears. The solid lines represent the mean curves; the dotted lines represent the individual curves; the black line with triangles represents the TM displacement of normal chinchilla ears reported by Ruggero et al. (1990).

### 4.3.2 TM mobility change in 4D AOM ears

Figure 4.4 shows the individual and mean curves for TM displacement at the umbo in response to 80 dB SPL pure tones over frequencies of 0.1-10 kHz measured in twelve 4D AOM and 15 control ears. In each AOM ear, TM vibration was recorded at three experimental stages: OM-1, OM-2, and OM-3. The upper panels display the frequency response curves of the peak-to-peak displacement magnitude. The displacement phase curves are shown in the lower panels.

TM displacement at the umbo measured in OM-1 with mean and individual curves is shown in Fig. 4.4A. At stage OM-1, the middle ear was unopened, and TM movement was affected by the MEP, MEE, and structural changes in the middle ear. The mean displacement magnitude gradually decreased from 0.023 μm to 0.009 μm over 0.1-2 kHz, and a continued reduction to 0.44 nm at 10 kHz was observed. The mean phase of OM-1 was flat for frequencies between 0.1-0.5 kHz with a value of -212$^{o}$ to -230$^{o}$, and decreased at higher frequencies. The noise level for LDV measurement is plotted in the upper panel of Fig. 4.4A. It shows that the TM displacement magnitude in OM-1 was at least 10 dB greater than the noise level for most tested frequencies. Considering that TM mobility in OM-1 should be the lowest when compared to the other OM stages in this study, the LDV measurement is expected to be reliable.

At stage OM-2 (Fig. 4.4B), the mean TM displacement curve was flat at 0.1-2 kHz with a value of 0.022-0.045 μm and decreased after 2 kHz as frequency increased when the MEP was released. The mean phase decreased slowly from -14$^{o}$ to -230$^{o}$ over 0.1-10 kHz. We noted that individual TM displacement values exhibited relatively large variations compared to the curves obtained in stage OM-1. The two lowest

displacement curves were obtained from the ears with 0.6 ml of MEE, the largest amount observed in the 4D ears.

The magnitude and phase of TM displacement after the MEE was removed (stage OM-3) are shown in Fig. 4.4C. The variation of the individual displacement curves in OM-3 was smaller than that in OM-1 and OM-2. The mean displacement was flat between 0.1-1.5 kHz with a value of 0.034-0.052 μm, and decreased continually as frequency increased. The mean phase angle of OM-3 gradually decreased from $-11^{o}$ to $-210^{o}$ over 0.1-10 kHz. It is important to note that the purulent adhesions still remained on the ossicles at this stage, a finding different from control ears.

The TM displacement magnitude and phase determined from 15 control ears without AOM are displayed in Fig. 4.4D (16 control ears were initially involved in this study, but one TM was damaged during preparation and was excluded from our study for this reason). Mean TM displacement was flat between 0.1-1.2 kHz with a value of 0.11-0.18 μm, then decreased to 0.004 μm as the frequency increased to 10 kHz. The mean phase curve slowly decreased from $-11^{o}$ to $-210^{o}$ over the tested frequencies. Published data from Ruggero et al. (1990) describing pressure-released normal chinchilla ears were included in Fig. 4.4D for comparison with our newly obtained data. The displacement magnitude and phase curves obtained in our current study closely resemble those based on Ruggero's data.

The mean TM displacement curves at control and 3 OM stages in Fig. 4.4 are extracted and displayed with SD bars in Fig. 4.5. The statistical results (p-values) for Fig. 4.5A displacement data are listed in Table 4.1. Repeated-Measures ANOVA and Tukey post-hoc tests were used to compare the three OM stages since the displacements

were measured from the same population. An unpaired t-test was used to compare OM-3 to uninfected control ears because these two middle ear conditions were from different populations. Statistical analysis was performed using Prism software (Graphpad, La Jolla, CA). The p-values of post-hoc test were reported as inequalities in the software.

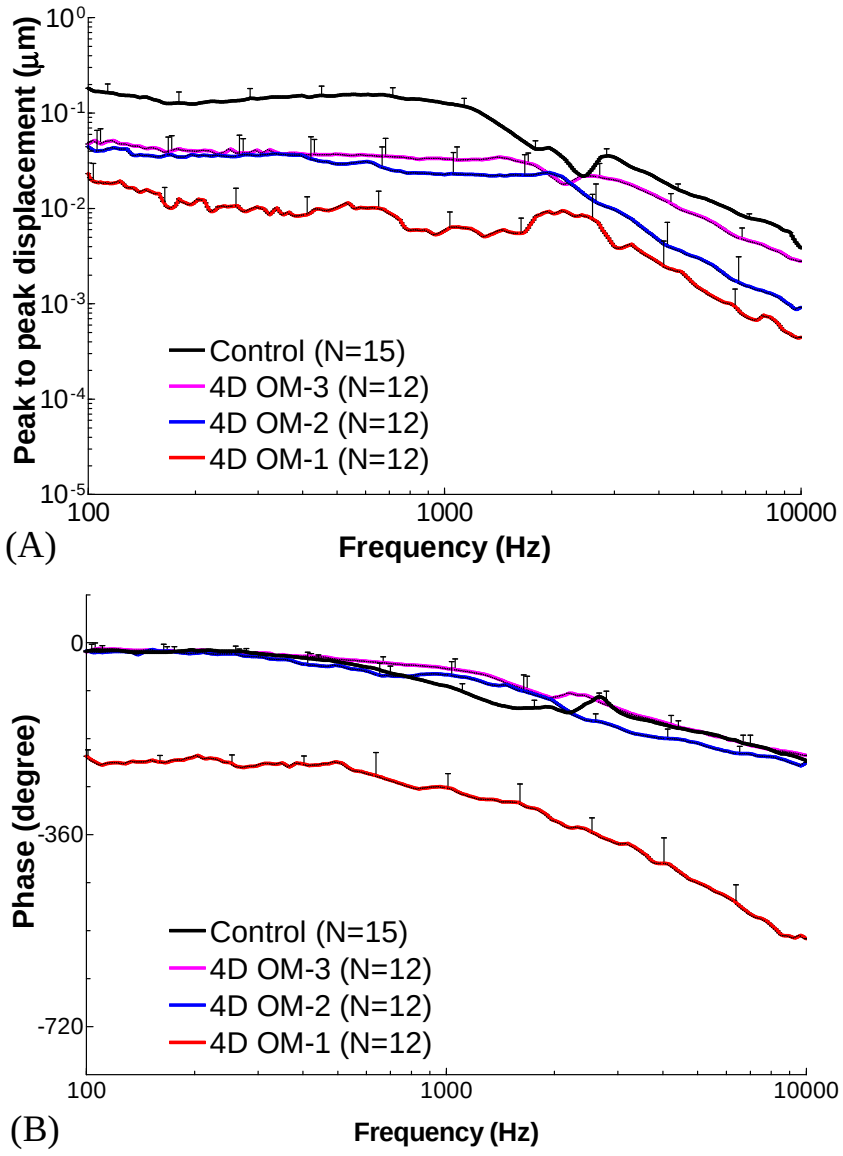


**Figure 4.5** Mean peak to peak displacement magnitude (A) and phase angle (B) of the TM at umbo with SD in response to 80 dB SPL sound input at the ear canal in 4 days OM-1 (red line), OM-2 (blue line), OM-3 (purple line), and control ears (black line).

**Table 4.1** List of P values derived from: (1) One way Repeated-Measures ANOVA test and Tukey post-hoc test on the TM displacement magnitude data between three 4D OM stages; (2) Unpaired Student t-test on the TM magnitude data between OM-3 and control.

| Frequency (kHz) | ANOVA P value | Tukey P value OM-1 vs OM-3 | Tukey P value OM-1 vs OM-2 | Tukey P value OM-2 vs OM-3 | Unpaired t-test P value OM-3 vs Control |
|---|---|---|---|---|---|
| 0.25 | 0.0014 | < 0.01 | < 0.05 | > 0.05 | 0.0000 |
| 0.5 | 0.0016 | < 0.01 | < 0.05 | > 0.05 | 0.0000 |
| 0.75 | 0.0009 | < 0.001 | < 0.05 | > 0.05 | 0.0000 |
| 1 | 0.0001 | < 0.001 | < 0.05 | > 0.05 | 0.0001 |
| 2 | 0.0110 | < 0.05 | < 0.05 | > 0.05 | 0.0000 |
| 4 | 0.0001 | < 0.001 | > 0.05 | < 0.001 | 0.0000 |
| 6 | 0.0001 | < 0.001 | > 0.05 | < 0.001 | 0.0000 |
| 8 | 0.0001 | < 0.001 | > 0.05 | < 0.001 | 0.0000 |
| 10 | 0.0001 | < 0.001 | > 0.05 | < 0.001 | 0.0160 |

Note: The P values with grey background represent significant difference between groups ($P < 0.05$). The P values of Tukey post-hoc test are shown as inequalities since no exact value is reported by the software.

Significant changes in TM displacement occurred among the three OM stages (Table 4.1, column 2). As shown in Fig. 4.5A and Table 4.1, the TM displacement of OM-3 was significantly greater than that of OM-1 over frequencies of 0.1-10 kHz (column 3 of Table 4.1). After pressure in the middle ear was released (OM-2), the TM displacement increased significantly at low frequencies (0.1-2 kHz, see column 4 of Table 4.1). As the effusion was drained from the cavity (OM-3), TM displacement was significantly increased compared to OM-2 at 4-10 kHz (column 5 of Table 4.1). When the OM-3 values were compared with those of control ears, there was a significant difference at all tested frequencies (column 6 of Table 4.1). It should be noted that at frequencies > 2 kHz, the TM displacement of OM-3 was slightly, but significantly, lower than that of controls (Fig. 4.5A).

Figure 4.5B shows the mean ± SD of the TM displacement phase curves measured in control ears and three experimental stages of 4D AOM ears. The mean phase in undisturbed AOM ears (OM-1) was much lower than that in control and other stages by $190^{o}$ (roughly a half-cycle) over 0.1-10 kHz. After middle ear pressure was released (OM-2), the TM phase generally overlapped with the control at frequencies below 800 Hz and was greater at 0.8-2 kHz and lower at f > 2 kHz compared with the control curve. After the effusion was removed (OM-3), the TM phase was almost the same as that of controls at all tested frequencies except 0.6-2.4 kHz, where the phase was greater than control.

### 4.3.3 TM mobility change in 8D AOM ears

Figure 4.6 shows the individual and mean curves of the TM displacement at the umbo in response to 80 dB SPL pure tones over frequencies of 0.1-10 kHz measured

from eight 8D AOM ears at the three experimental stages. The control curves shown in Fig. 4.6D are the same as those in Fig. 4.4D for comparison purposes. The upper panels display the frequency response curves of the displacement magnitude and the lower panels show the displacement phase curves.

The TM displacement curves measured from unopened ears (OM-1) are shown in Fig. 4.6A. The mean displacement continually decreased from 0.03 µm to 0.22 nm over 0.1-10 kHz. The mean phase curve was flat at 100-300 Hz with a value of -215$^{o}$ to -240$^{o}$, and decreased at higher frequencies.

Figure 4.6B shows the TM displacement curves after the MEP was released (OM-2). The individual variation of displacement magnitude at OM-2 was large, similar to the 4D OM-2 ears. This variation may relate to the different levels of middle ear effusion and the degree of middle ear ossicular and soft tissue changes between individual ears. The mean displacement decreased from 0.04 µm to 0.3 nm over 0.1-10 kHz. The mean phase was -77$^{o}$ at 100 Hz, increased to -40o at 200 Hz, then gradually decreased to -280$^{o}$ at 10 kHz.

Figure 4.6C displays the TM displacement curves at stage OM-3, in which the effusion was removed but the adhesions on the ossicles remained unaltered. Inter-individual variation in TM displacement was smaller than that in OM-2 and occurred mainly at frequencies below 2 kHz. The individual difference in 8D ears was greater than that in 4D ears (Fig. 4.4C) at stage OM-3. The mean displacement curve of OM-3 in 8D was flat with a value of 0.06-0.08 µm at 0.1-1 kHz, and decreased to 2 nm at 10 kHz. The mean phase slowly decreased from -10$^{o}$ to -230$^{o}$ over 0.1-10 kHz.

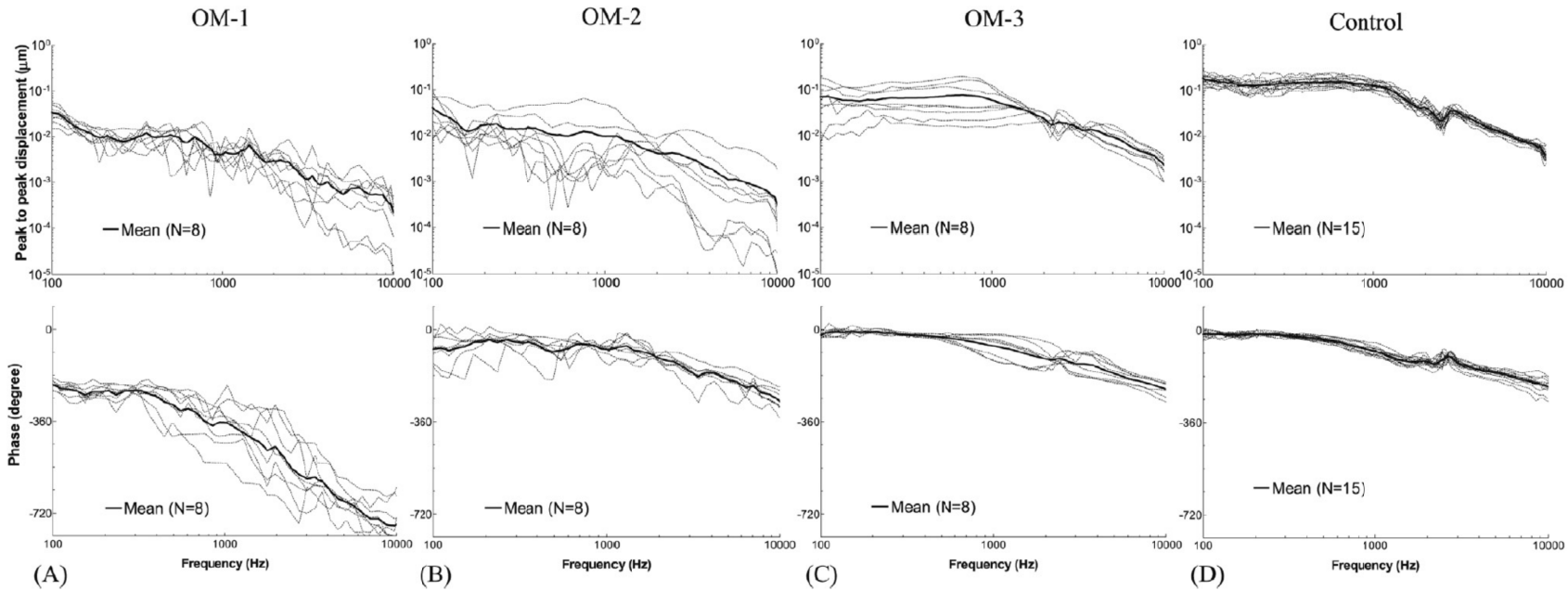


**Figure 4.6** Peak to peak displacement magnitude (upper panel) and phase angle (lower panel) of the TM at umbo in response to 80 dB SPL sound input at the ear canal in 8 days (A) OM-1, (B) OM-2, (C) OM-3, and (D) control ears. The solid lines represent the mean curves; the dotted lines represent the individual curves.

**Table 4.2** List of P values derived from: (1) One way Repeated-Measures ANOVA test and Tukey post-hoc test on the TM displacement magnitude data between three 8D OM stages; (2) Unpaired Student t-test on the TM magnitude data between OM-3 and control.

| Frequency (kHz) | ANOVA P value | Tukey P value OM-1 vs OM-3 | Tukey P value OM-1 vs OM-2 | Tukey P value OM-2 vs OM-3 | Unpaired t-test P value OM-3 vs Control |
|---|---|---|---|---|---|
| 0.25 | 0.0019 | < 0.01 | > 0.05 | < 0.01 | 0.0031 |
| 0.5 | 0.0055 | < 0.05 | > 0.05 | < 0.05 | 0.0043 |
| 0.75 | 0.0106 | < 0.05 | > 0.05 | < 0.05 | 0.0210 |
| 1 | 0.0014 | < 0.01 | > 0.05 | < 0.01 | 0.0014 |
| 2 | 0.0001 | < 0.001 | > 0.05 | < 0.001 | 0.0001 |
| 4 | 0.0001 | < 0.001 | > 0.05 | < 0.001 | 0.0012 |
| 6 | 0.0001 | < 0.001 | > 0.05 | < 0.001 | 0.0042 |
| 8 | 0.0001 | < 0.001 | > 0.05 | < 0.001 | 0.0002 |
| 10 | 0.0001 | < 0.001 | > 0.05 | < 0.001 | 0.0037 |

Note: The P values with grey background represent significant difference between groups ($P < 0.05$). The P values of Tukey post-hoc test are shown as inequalities since no exact value is reported by the software.

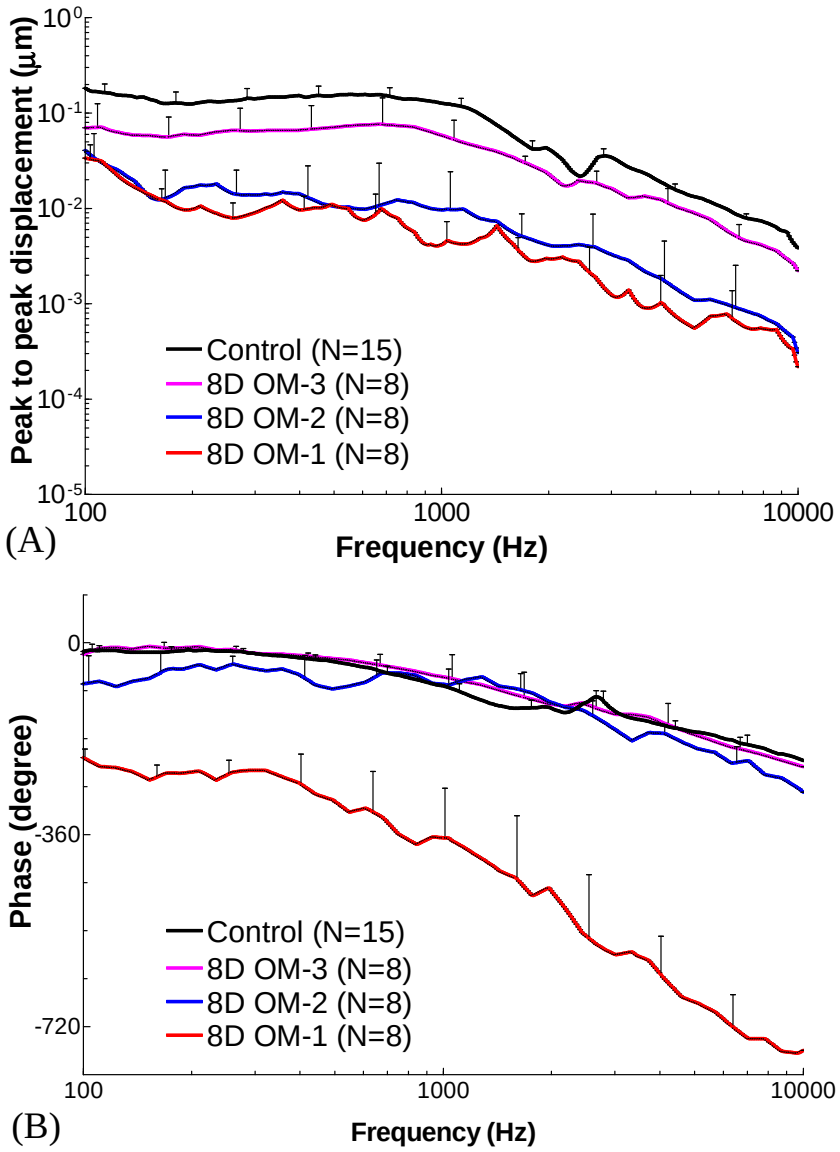


**Figure 4.7** Mean peak to peak displacement magnitude (A) and phase angle (B) of the TM at umbo with SD in response to 80 dB SPL sound input at the ear canal in 8 days OM-1 (red line), OM-2 (blue line), OM-3 (purple line), and control ears (black line).

The mean TM displacement curves from control ears and three OM stages in Fig. 4.6 were collected and displayed in Fig. 4.7. Figure 4.7A shows that the TM vibration slightly increased upon the release of pressure in 8D ears and the increase was smaller than that observed in 4D ears (Fig. 4.5A). The difference of TM displacement between OM-2 and controls in 8D ears (blue line versus black line) was larger than the

difference between OM-2 and controls in 4D ears (blue line versus black line) shown in Fig. 4.5A. After removal of the effusion, the TM displacement increased substantially and the difference between OM-3 and control in 8D ears (pink line versus black line) was smaller than that in 4D ears. This observation indicates that MEE is a primary factor contributing to the loss of TM mobility in 8D ears.

The statistical analyses for the data in Fig. 4.7A are tabulated in Table 4.2 using the same methods as those for 4D ears. Comparing Table 4.2 with Table 4.1, we observed that the TM displacement in 8D ears did not change significantly at all tested frequencies after pressure was released (OM-1 versus OM-2). In contrast, releasing MEP significantly increased the TM mobility in 4D ears at low frequencies. After effusion was removed, the TM mobility in 8D ears increased significantly over the entire frequencies (OM-2 versus OM-3), but in 4D ears significant changes were observed only at high frequencies. In both 4D and 8D ears, the TM mobility at OM-3 was significantly different from controls.

For a quantitative comparison of TM mobility changes in two infection periods, Table 4.3 summarizes the mean values for TM displacement magnitude in 4D, 8D, and control ears. Six frequencies were selected to represent low, middle, and high frequency ranges.

**Table 4.3** List of mean peak-to-peak TM displacement magnitude of control, 4D, and 8D ears at the three experimental stages (μm).

| Frequency (kHz) | 4D | | | 8D | | | Control |
|---|---|---|---|---|---|---|---|
| | OM-1 | OM-2 | OM-3 | OM-1 | OM-2 | OM-3 | |
| 0.25 | 0.0105 | 0.0350 | 0.0421 | 0.0081 | 0.0152 | 0.0651 | 0.1338 |
| 0.5 | 0.0102 | 0.0294 | 0.0370 | 0.0108 | 0.0105 | 0.0711 | 0.1530 |
| 1 | 0.0058 | 0.0227 | 0.0331 | 0.0042 | 0.0097 | 0.0587 | 0.1269 |
| 4 | 0.0027 | 0.0045 | 0.0128 | 0.0010 | 0.0019 | 0.0126 | 0.0198 |
| 8 | 0.0007 | 0.0013 | 0.0040 | 0.0005 | 0.0007 | 0.0040 | 0.0072 |
| 10 | 0.0004 | 0.0009 | 0.0028 | 0.0002 | 0.0003 | 0.0022 | 0.0039 |

The TM phase data measured in control and three OM stages in 8D ears are shown in Fig. 4.7B. The mean phase in unopened AOM ears (OM-1) was much lower than that in control and other OM stages by $190^{o}$, and these differences increased with increasing frequency. After release of MEP, the mean phase curve in stage OM-2 was greater than control at 0.8-2 kHz but lower at other frequencies. After the removal of MEP and MEE, the phase of OM-3 stage generally overlapped with the control curve but was slightly greater than control at 0.9-2 kHz. The large phase lag of the umbo movement observed in stage OM-1 of 8D ears is similar to that of 4D ears (Fig. 5B).

## 4.4 Discussion

### 4.4.1 Factors affecting TM mobility loss in AOM ears

In this study, the TM mobility of chinchilla AOM ears was investigated at 4 days and 8 days post transbullar inoculation with H. influenzae. These time points represent relatively early and later stages of AOM. Comparing the TM displacement curves obtained in the unopened 4D and 8D ears (stage OM-1) with that of control ears (Fig. 4.8A), the TM mobility at 8D did not differ significantly from that of infected ears at 4D at $f < 1.5$ kHz (also see columns of "OM-1" under 4D and 8D in Table 4.3). However, the results in Tables 4.1 and 4.2 suggest that the middle ear pressure (OM-1 versus OM-2), effusion (OM-2 versus OM-3), and ossicular structure change (OM-3 versus Control) at early infection contributed to the loss of TM mobility in a different manner from those at the later infection period. To quantify the effects of three factors (MEP, MEE, and structural change) on the loss of TM mobility at two infection periods, the results in Figs. 4.5A and 4.7A were calculated as the increase of TM mobility

(displacement in dB) at an OM stage with respect to the previous stage as shown in Figs. 4.8B-D. The effects of MEP, MEE, and middle ear structural changes on TM mobility over frequencies from 100 Hz to 10 kHz are shown in these figures and described in following sections.

#### 4.4.1.1 Effect of MEP on TM mobility along the course of AOM

Figure 4.8B displays the increase of TM displacement caused by release of MEP after 4 days or 8 days of infection. In 4D ears (red line), an average 5-12 dB increase at frequencies below 3 kHz and a smaller increase (about 5 dB) at frequencies above 3 kHz were observed after the release of MEP. However, in 8D ears the TM displacement increase due to pressure release was under 4 dB or even negative at some frequencies (blue line).

Pressure in the middle ear increases the stiffness of the TM and thus decreases the TM movement as reported by Dai et al. (2008). Lee and Rosowski (2002) reported the reduction of the umbo mobility with controlled MEP in gerbil ears. Release of the MEP would reduce the tension in the TM and increase the TM mobility. In our present study, the increase of TM displacement upon releasing MEP in 4D is larger than that in 8D ears. The effect of MEP on TM mobility may relate to the residual air space in the middle ear in these two inflammatory phases. In 4D ears the air-fluid interface was at or below the umbo and about half of the tympanic cavity was air-filled. In contrast, the effusion almost filled the entire space behind the TM (i.e., tympanic cavity) in 8D ears and only the superior cavity of the chinchilla middle ear remained air filled. The air space behind the TM is critical to its mobility and Ravicz et al. (2004) reported that even a small amount of air would be sufficient to facilitate umbo's motion. However,

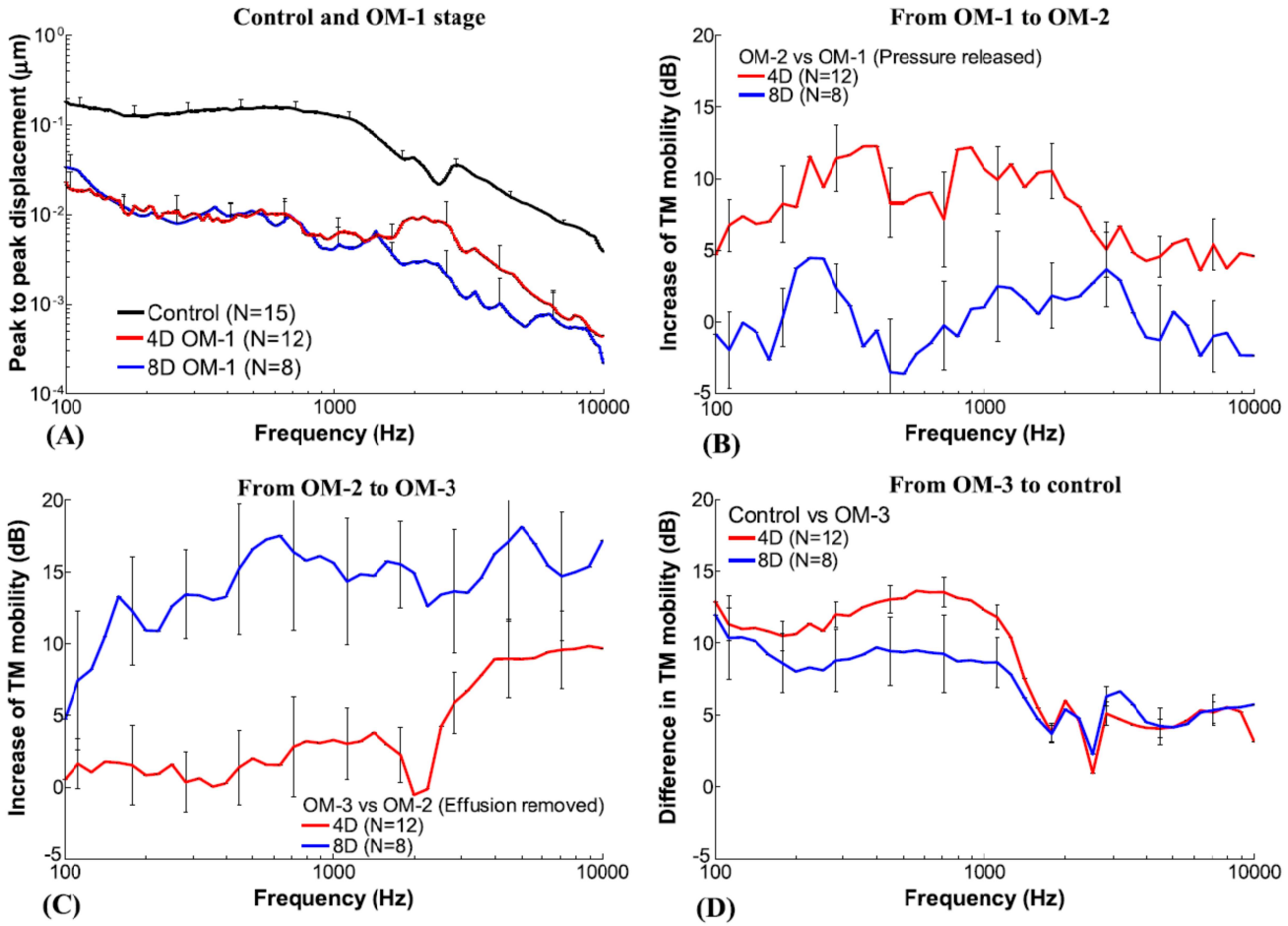


**Figure 4.8** (A) Mean TM displacement of control, 4D and 8D AOM ears at OM-1 from Fig. 4.5A and Fig. 4.7A. (B) Mean increase (with SD) of TM displacement at umbo after release of middle ear pressure in 4 days and 8 days AOM ears (OM-2 vs OM-1). (C) Mean increase of TM displacement after removal of middle ear effusion in 4 days and 8 days AOM ears (OM-3 vs OM-2). (D) Mean difference of TM displacement between control and OM-3 of 4 days and 8 days AOM ears (Control vs OM-3). Red lines and blue lines represent the TM displacement increase in 4 days and 8 days group, respectively.

there was little air space behind the TM in 8D ears compared with 4D ears. After the air pressure was released in 8D ears, the increase of TM motion was very limited because the tympanic cavity was almost filled by fluid as observed just before the aspiration of MEE. In 4D ears the TM displacement significantly increased upon the release of MEP due to sufficient air space behind the TM. Therefore, the MEP was a dominant factor on TM mobility loss in the early infection of AOM ears. In the extended (8D) AOM infection, MEP had little effect on TM movement because MEE filled the tympanic cavity.

MEP in 4D and 8D ears substantially changed the phase of the umbo movement. In gerbil ears it has been reported that a small negative MEP stiffened the middle ear and led to a flat extension into the high frequencies in the phase curve (Lee and Rosowski 2001; Rosowski and Lee 2002). However, when the negative MEP became large, e.g. -250 to -300 daPa in gerbil ears, a half-cycle phase lag in the umbo vibration was observed (Fig. 7 in Lee and Rosowski 2001; Fig. 5 in Rosowski and Lee 2002). In the streptococcal AOM model recently reported by Guan and Gan (2013) in guinea pigs, one ear at stage OM-1 showed the half-cycle phase change. The large phase lag observed in the present study is probably related to large negative MEP or tissue infection in AOM. The mechanisms behind these observations are not clear and need further study.

#### 4.4.1.2 Effect of MEE on TM mobility along the course of AOM

As can be seen in Fig. 4.8C, TM mobility increased by an average of 10-18 dB over 140 Hz to 10 kHz after the effusion was removed in 8D ears (blue line). In 4D ears, removal of the effusion resulted in an average of 5-10 dB increase of TM

movement at frequencies greater than 3 kHz but had not much effect at low frequencies (red line). There was a huge difference of the MEE's effect on TM mobility loss between 8D and 4D ears over the frequency range. The principal reason for this TM mobility change during the disease course is the increase of MEE amount in the middle ear (on average from 0.42 to 0.84 ml) and the decrease of middle ear air space from 4D to 8D infection. The MEE in 4D ears neither covered the entire TM nor filled the tympanic cavity as shown in Fig. 4.2. There might be a possible viscosity change in MEE from 4D to 8D, but we did not measure the viscosity of the MEE in the present study.

Middle ear fluid decreases TM mobility by two mechanisms: stiffening of the middle ear by reducing air space, and increasing effective mass of the TM (Ravicz et al. 2004). The loss of middle ear air space and the increase of TM mass together reduce the umbo's mobility at low and high frequencies, respectively. An increase in MEE contacting the TM would lead to an increase of TM mass and more reduction of displacement at high frequencies as determined in human temporal bones by Ravicz et al. (2004) and Gan et al. (2006). The increase of TM displacement at high frequencies after the removal of the MEE in 8D ears was greater than that in 4D ears. This new observation in our present study is in agreement with the findings of the Ravicz et al. and Gan et al. studies.

The TM mobility at low frequencies was decreased by reduction of the air space in the middle ear cavity and this effect became notable only when the middle ear was almost filled with fluid (Ravicz et al., 2004; Gan et al., 2006; Guan and Gan, 2011). In the present study, the volume of air space in the tympanic cavity of chinchilla ears is

0.9-1.0 ml. In 4D ears, the MEE occupied less than half of the tympanic cavity (Fig. 4.2) and the restoration of air space had little effect on TM movement at low frequencies. In 8D ears, the effusion occupied almost the entire middle ear air space, which not only increased the mass of the TM but also substantially decreased the middle ear air volume. Therefore, removal of the effusion significantly increased TM mobility over all tested frequencies in 8D ears. Thus, the MEE was the primary contributor to decreased TM mobility in the late stage of OM.

Thornton et al. (2013) reported changes of the umbo velocity and cochlear microphonic threshold in chinchillas when the middle ear was filled with different volumes of silicone oil. Their results demonstrated that a reduction of the umbo mobility and an elevation of cochlear microphonic threshold both increased as middle ear fluid volume increased from 0.5 ml to 1.25 ml (Fig. 2A and Fig. 5A in their paper). Their study also demonstrated that the decrease of TM mobility at umbo was related to frequency. A small decrease in umbo velocity at low frequencies was observed when a small amount of fluid was instilled into the middle ear. As more fluid was added, the reduction of umbo velocity extended to high frequencies and a large value of reduction was observed (Fig. 5A in their paper). The effect of MEE on TM movement reported in the present study is in general agreement with the findings of Thornton et al.

It should be noted that the volume of MEE and the area of TM covered by the effusion in our study was different from the study by Thornton et al. (2013). From our observation, the entire TM was covered by MEE with 0.8-0.9 ml in the infected ears. Thornton et al. (2013) used 1.25 ml of silicone oil and the TM was 100% covered by the fluid, simulating a MEE in a normal ear. In our AOM model, we found a small

amount of pus remained in the small crevices of the middle ear cavity during the post experiment examination. This purulent material could not be aspirated with the MEE in the OM-3 stage. In addition, the middle ear mucosa was thickened in our infected chinchilla ears. It is possible that the space for the fluid in the more severely infected middle ear was smaller than that in the healthy ear, and thus required a smaller fluid volume to cover the TM in our infected ears.

#### 4.4.1.3 Effect of middle ear structural changes on TM mobility along the course of AOM

As shown in Fig. 4.8D, the TM mobility of control ears was higher than that of OM-3 (MEP released and MEE removed) in both 4D and 8D ears. The residual reduction of TM mobility after release of pressure and removal of effusion suggested that infection-induced middle ear structural changes, including the ossicular adhesions and the possible micro-structural changes of middle ear soft tissues, contributed to the TM mobility loss. The residual TM mobility loss was frequency dependent as displayed in Fig. 8D. The middle ear structural changes in early and late stages of AOM resulted in about 5 dB loss of TM mobility at $f > 1$ kHz. The reduction of TM mobility was enhanced to 8 dB for 8D ears and 13 dB for 4D ears at $f < 1$ kHz. In addition, the phase at OM-3 in both 4D and 8D ears was slightly higher than control at frequencies around 1 kHz (pink line vs black line in Figs. 5B and 7B). These changes show that the middle ear was stiffer than controls in both 4D and 8D situations at stage of OM-3. Similar results were observed in our previous study of guinea pig AOM ears (Guan and Gan, 2013). The AOM-induced structural changes in chinchillas may increase middle ear

stiffness and caused TM mobility loss mainly at low frequencies, similar to the AOM ear of guinea pigs.

Ossicular adhesions have been observed in AOM models of gerbils (von Unge et al., 1997), rats (Caye-Thomasen et al., 1996; Caye-Thomasen and Tos, 2000), and guinea pigs (Guan and Gan, 2013). In the gerbil AOM model, von Unge et al. (1997) reported that TM stiffness was increased in ears with ossicular adhesions compared with normal ears. In this study it is possible that the adhesions in AOM ears (Fig. 4.3) could have fixed the manubrium, malleus head, incus, and stapes and increase the overall stiffness of the middle ear.

Rosowski et al. (2008) reported the umbo vibration in patients with malleus and stapes fixation and their results indicated that significant loss of umbo mobility occurred at $f < 3$ kHz in both stapes-fixed and malleus-fixed groups (Fig. 9 in their paper). In a study of human temporal bones by Dai et al. (2007), fixation of the malleus caused a reduction of 15 dB at the umbo or stapes at low frequencies. Nakajima et al. (2005A; 2005B) reported the vibration patterns of the umbo and stapes when adhesives were applied to the ossicles in human temporal bones and their results suggested that ossicular fixation increased the stiffness of the middle ear, reduced the umbo's mobility mainly at $f < 1.5$ kHz, and increased the phase near 1 kHz (see Figs. 5-7 in Nakajima et al. 2005A).

The residual TM mobility loss observed in the chinchilla AOM ears seems to be consistent with those published data measured from ears with ossicular fixation. If we assume that the adhesions fixed the ossicles in 4D and 8D ears, TM mobility at the umbo would be decreased. In addition, the mass of the adhesions might also affect the

TM mobility at high frequencies. Therefore, ossicular adhesions are likely to contribute to the residual mobility loss of the TM in our model. Figure 8D also suggests that the effect of ossicular changes in 4D ears was greater than that in 8D ears at f < 1 kHz, which may relate to the fact that the adhesions in 4D ears were generally thicker or denser compared with 8D ears as observed in Fig. 4.3. A possible explanation is that the inflammatory process has changed by the 8th day of AOM.

Infection in the middle ear also commonly causes structural changes of middle ear soft tissues such as the TM (Larsson et al., 2003; von Unge et al., 1993; von Unge et al., 1997) and round window membrane (Gan et al., 2013). The mechanical properties of the TM in diseased ears are different from those of normal ears as reported by Luo et al. (2009); this also could affect middle ear vibration. Gan et al. (2013) reported soft tissue property changes of the round window membrane in a guinea pig AOM model; this might alter the cochlear load or cochlear input impedance to the middle ear. Pathological changes of the ossicular joints and stapedial annular ligament may also occur during middle ear infection. Therefore, in addition to the ossicular adhesions, the mechanical property changes of the TM, round window membrane, and other middle ear soft tissues may also contribute to the difference in TM mobility between OM-3 and uninfected control ears. However, it is difficult to differentiate the effects between ossicular adhesions and middle ear tissue structural changes in live animals. Future studies are needed to quantify whether and how such soft tissue changes contribute to the middle ear mobility change during the course of AOM.

### 4.4.2 Comparison of chinchilla and guinea pig AOM models

In our previous study of the guinea pig AOM model (Guan and Gan 2013), AOM was created by injection of *Streptococcus pneumoniae* into the middle ear and the change in TM mobility was measured after 3 days of inoculation. In the current study, *Haemophilus influenzae* was used to induce the middle ear infection and produce this AOM model in chinchillas. SP and HI are two leading bacterial pathogens commonly used for creating AOM in animals. To our knowledge, the middle ear biomechanics during AOM was reported only in SP-induced models (von Unge et al., 1997; Larsson et al., 2003; Guan and Gan, 2013). The current study is the first to evaluate the middle ear mechanics in a HI-induced AOM model.

Comparing the loss in TM mobility at the early phase of the disease in these two species with different bacterial pathogens, we found that the factors causing TM mobility loss at the early phase of the disease (3 days for guinea pig and 4 days for chinchilla) were similar for these two species although the bacterial pathogens used for creating AOM were different. In both AOM models, negative pressure was generated in the middle ear and resulted in about 10 dB reduction in TM (umbo) vibration at $f < 2$ kHz. At higher frequencies, the effect of MEP on TM motion was not significant. Purulent effusion was found in both chinchilla and guinea pig models. The effusion filled about half of the tympanic cavity in guinea pigs and slightly less than half of the tympanic cavity in chinchillas. MEE led to the loss of TM mobility mainly at frequencies greater than 2 kHz at early phase of infection in both models (9-15 dB for guinea pig and 5-10 dB for chinchilla). In both species, ossicular adhesions were present and commonly located between the manubrium and cochlear promontory and around the round window niche. After the MEP and MEE were removed from the

middle ear, TM mobility at the umbo was lower than in control ears, mainly at low frequencies (< 2 kHz) for both species, which corresponds to the effect of ossicular adhesions and other middle ear structural changes on middle ear mechanics. Therefore, the middle ear pressure, effusion, and middle ear structural changes are the main factors leading to TM mobility loss in guinea pig and chinchilla AOM models in the early phase of the disease.

The chinchilla AOM model reported in this study showed a slow development of middle ear infection compared with other AOM models such as the AOM model in guinea pigs reported in our previous study (Guan and Gan 2013). The type of bacteria and infective dosage in the middle ear affects the time scale of infectious process and thus can potentially influence the biomechanical changes of the middle ear for sound transmission. In our future studies on AOM induced by HI, the histological changes of the middle ear and mechanical properties of the middle ear soft tissues such as the TM, ossicular joints, and round window membrane will be included.

### 4.5 Conclusion

The roles of middle ear pressure, effusion, and structural changes in TM vibration loss in chinchilla AOM ears were quantified over the course of the disease (4 days and 8 days post inoculation). The effects of those three factors on TM mobility loss vary with the course of AOM. The middle ear pressure was the dominant factor on reduction of the TM mobility in 4D AOM ears, but showed little effect in 8D ears when MEE filled the tympanic cavity. The middle ear effusion was the primary factor on TM mobility loss for 8D ears, but affected the 4D ears only at high frequencies. After

release of MEP and removal of MEE, there was residual TM mobility loss mainly at low frequencies in both 4D and 8D ears, which was associated with middle ear structural changes. More residual reduction of TM movement occurred in the early phase of the disease. This study establishes that the factors contributing to TM mobility loss in chinchilla middle ears infected with *H. influenzae* closely resemble those we previously reported in guinea pig middle ears infected with *S. pneumoniae*.

# CHAPTER 5: WIDEBAND ENERGY ABSORBANCE MEASUREMENT IN AOM MODEL OF CHINCHILLAS

## 5.1 Introduction

Wideband energy absorbance (EA) describes the sound power transmitted into the middle ear over a broad range of frequency (Feeney et al. 2003). Several clinical studies reported that EA or energy reflectance (ER=1-EA) was affected by various middle ear disorders including tympanosclerosis (Rosowski et al. 2012), ossicular discontinuity (Feeney et al. 2003; 2009; Nakajima et al. 2012; Voss et al. 2012), otosclerosis (Allen et al. 2005; Shahnaz 2009A; 2009B; Sanford et al. 2012; Nakajima et al. 2012; Voss et al. 2012), and otitis media with effusion (Hunter et al. 2008; Beers et al. 2010; Ellison et al. 2012; Feeney et al .2003; Prikoyski et al. 1999; Voss et al. 2012; Allen et al. 2005; Keefe et al. 2012; Hunter and Margolis 1997). EA is sensitive to middle ear pathologies and the measurement over the frequency range can assist diagnosis of middle ear diseases.

Acute otitis media (AOM) is a rapid infection of the middle ear and the most frequently diagnosed disease in pediatric population in the United States (Gould et al. 2010; Hoberman et al. 2011). In Chapter 4, we identified that the middle ear pressure (MEP), middle ear effusion (MEE), and together with infection-induced structural changes each contributed to the loss of TM mobility during the course of the chinchilla AOM model produced by *H. influenzae*. Results show that the effect of each factor is frequency dependent and varies at early and later infection period (The contents in Chapter 4 have been published in Guan et al. 2014). A series studies reported EA changes in otitis media with effusion (OME). However, there is a lack of EA

measurement in AOM ears and particularly, it is unclear how the EA measurement can differentiate the effects of MEP, MEE, and the tissue structural changes in AOM ear.

As an extension of the previous study of chinchilla AOM ears, in this chapter, we report the effects of those middle ear changes on ambient EA along the course of infection. The arrangement of the experiment is similar to that in the previous study. EA as function of ear-canal pressure and frequency was measured in normal, 4 days (4D), and 8 days (8D) AOM ears by using a wideband tympanometer. In each disease group, EA was measured at three experimental stages: the unopened AOM ear with MEP and MEE, upon release of MEP, and after removal of MEE. Threshold of auditory brainstem response (ABR) was recorded in all unopened AOM ears. EA at ambient ear-canal pressure was extracted from the joint data. We then identified the effects of middle ear pressure, effusion, and structural changes on ambient EA at these two AOM periods.

## 5.2 Methods

### 5.2.1 Animal preparation

Fifteen chinchillas (*Chinchilla lanigera*) weighing between 600-780 g were included in this study. The study protocol was approved by the Institutional Animal Care and Use Committee of the University of Oklahoma and met the guideline of the National Institutes of Health. All animals were free from middle ear disease (as evaluated by otoscopic examination) at the beginning of the study.

The animals were divided into control and two AOM groups. The control group included six animals, and the AOM group had nine animals divided based on disease time course: the 4 days (4D) post-inoculation AOM group of five animals and the 8

days (8D) post-inoculation group of four animals. AOM was produced by transbullar injection of *H. influenzae* 86-028NP suspension in both ears following the procedure described in Chapter 2. The animals of control group were untreated.

At the 4th or 8th day post-inoculation, animals were anesthetized with mixture of ketamine (10 mg/kg) and xylazine (2 mg/kg). Additional anesthesia was administered as needed to maintain areflexia. To expose the entrance of the ear canal, the pinna and the skin covering the ear canal were removed surgically. The TM was examined under a microscope to identify signs of AOM. In each animal, the experiment was conducted bilaterally (N=12 for control; N=10 for 4D AOM; N=8 for 8D AOM). For both control and AOM groups, the body temperature of the animal was maintained throughout the experiment at approximately 38° C by placing the animal in a prone position on a thermoregulated surgical heating blanket.

### 5.2.2 EA measurement

The EA was measured by using a wideband tympanometer (Model AT235h, Interacoustic, MN) with Reflwin software on a PC. The measurement probe with commercial tips (outer diameter of 8 mm) was pressed to the bony rim of the entrance of the ear canal and held by hand to achieve a pressure seal. Using click stimuli, the EA was measured at 60 frequencies between 0.25 and 8 kHz while air pressure in the ear canal swept between -300 and 200 daPa in descending direction. The surface area of the probe in the ear canal was used for calculation of EA (Keefe et al. 1993). In this study, the diameter at the entrance of the bony part of chinchilla ear canal was measured as 4-6 mm. The system was calibrated in a set of two rigidly terminated tubes with an inner diameter of 4.5 mm.

The EA measurement in AOM ears was performed in three experimental stages: OM-1, unopened bulla had the MEP and MEE; OM-2, the pressure was released from the middle ear; and OM-3, the effusion was removed from the middle ear. At each experimental stage, the EA measurement was conducted bilaterally.

After completion of the EA measurements in stage OM-1, further surgery was performed following the procedure by Guan et al. (2014). Briefly, the skin of the superior temporal bone was partly removed to expose the middle ear bony wall on top of the temporal bone. A hole of 1 mm diameter was drilled into the roof of the middle ear to release the middle ear pressure. After sealing the hole with dental cement (PD-135, Pac-Dent, CA), the OM-2 test was performed.

Upon the completion of EA measurements for stage OM-2, the hole on top of the temporal bone was opened and enlarged to 3-4 mm in diameter using a drill (Fig. 4.1 in Chapter 4). Under microscopic visualization a silicone tube was inserted to the bottom of the middle ear cavity through this hole. The middle ear effusion was then aspirated manually from the cavity with a 1 ml syringe. The aspiration process was repeated as necessary until no additional fluid could be drained from the tympanic cavity. The total effusion volume obtained from each ear was then recorded. Ossicular adhesions were frequently found on malleus head and between the manubrium and the cochlear promontory when the top cavity was opened for stage OM-3. These ossicular adhesions were not disturbed during the aspiration of the effusion. The opening on top of the temporal bone was then covered by a thin glass sheet, and sealed with dental cement. Then, EA measurement was performed for stage OM-3.

Control ears were prepared in the same manner as described above for ears with AOM. To exclude the effect of middle ear pressure in anesthetized animals (Guinan and Peake 1967), a hole of 1 mm diameter was drilled on the top of the middle ear cavity to release any pre-existing pressure. Measurement of EA was then performed.

## 5.3 Results

### 5.3.1 Wideband EA tympanogram

Wideband EA tympanogram is represented by plotting EA as a function of ear-canal pressure (-300 to 200 daPa) and frequency (0.25 to 8 kHz). Because the goal of this study is to assess the effects of AOM on EA-frequency data at ambient pressure, we only show representative 3D EA tympanograms and 2D EA-pressure curves measured from control and unopened AOM ears (stage OM-1) in Figure 1 and 2, respectively. Analysis of 3D EA tympanograms measured in AOM at stage OM-2 or OM-3 will be included in future study.

Figure 5.1A shows typical EA tympanogram from a control chinchilla ear. EA peaked at ambient pressure (p=0) with a value of 0.3 at 250 Hz. The value and width of the peak gradually increased as frequency increases to 2 kHz. A “ridge” was observed near ambient pressure in low-mid frequency range. At higher frequencies, EA showed a shape of “M” and the valley of the “M” was near 50 daPa. With increasing frequency, EA increased in the regions of -300 to -100 daPa and 100 to 200 daPa.

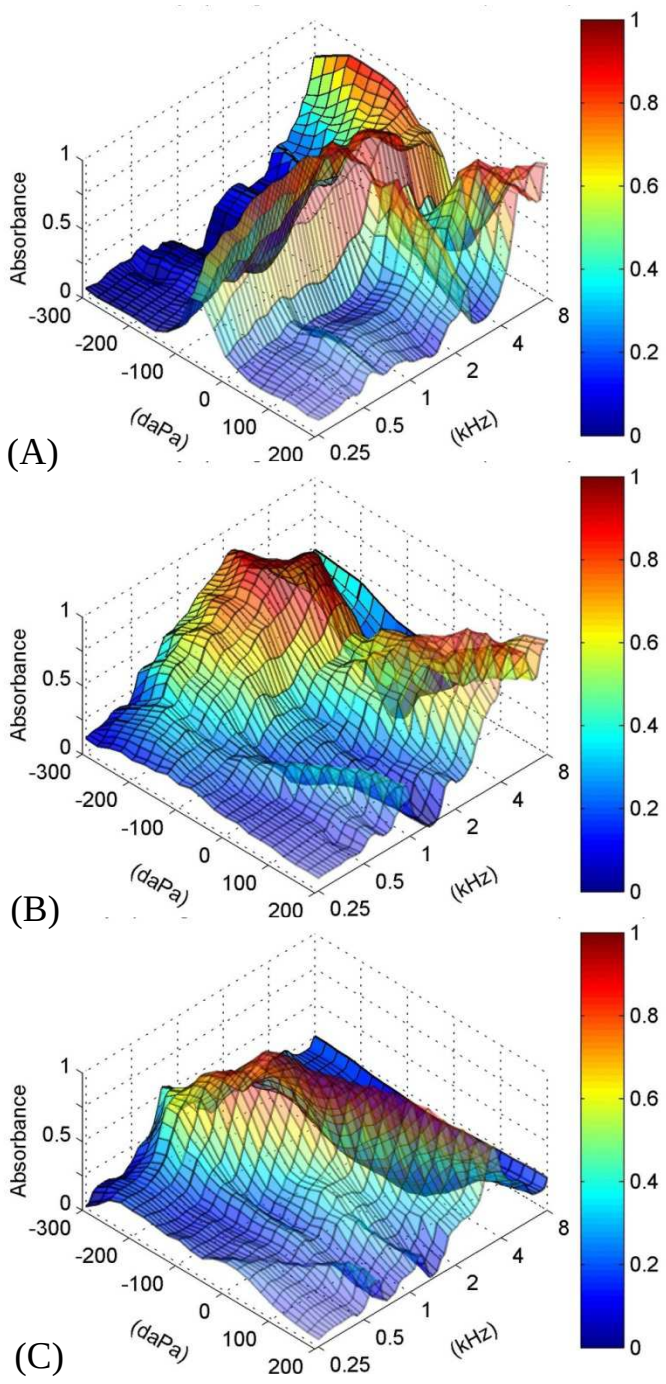


**Figure 5.1** Energy absorbance tympanogram (as a function of ear-canal pressure and frequencies) in (A) control, (B) unopened 4D, and (C) unopened 8D AOM ear.

Figure 5.1B displays typical EA tympanogram from a 4D AOM ear with 0.4 ml MEE. EA maximizes near -200 daPa at low-mid frequencies and the peak is more rounded than that in control ear. EA in the region of positive pressure starts to increase

at 1 kHz. At higher frequencies (f > 2 kHz), EA peaks at two locations: -200 and +200 daPa.

Figure 5.1C shows typical EA tympanogram from an 8D ear with 0.9 ml effusion. A small rounded peak is observed near -200 daPa at low frequencies (f < 0.5 kHz). EA at -200 daPa maximizes at 1 kHz, and the frequency at which maximum EA is observed gradually shifts from 1 to 3 kHz as ear canal pressure increases to 200 daPa. The overall EA in the 8D ear is lower than that in 4D ear.

### 5.3.2 EA-pressure curve

To better describe the EA variation with the ear-canal pressure from -300 to 200 daPa at the low, mid, and high frequency, the EA-pressure curves were extracted from the control, 4D, and 8D tympanograms shown in Fig. 5.1 at 0.5, 1, and 4 kHz. Figure 5.2A shows the EA-pressure curve at three frequencies of the control ear. Single sharp peak is observed near 0 daPa at both 0.5 and 1 kHz similar to conventional tympanogram at 226 Hz and 1 kHz. The peak EA reached at zero MEP or ambient pressure. At 4 kHz EA-pressure curve shows two peaks at 0 and 170 daPa, respectively.

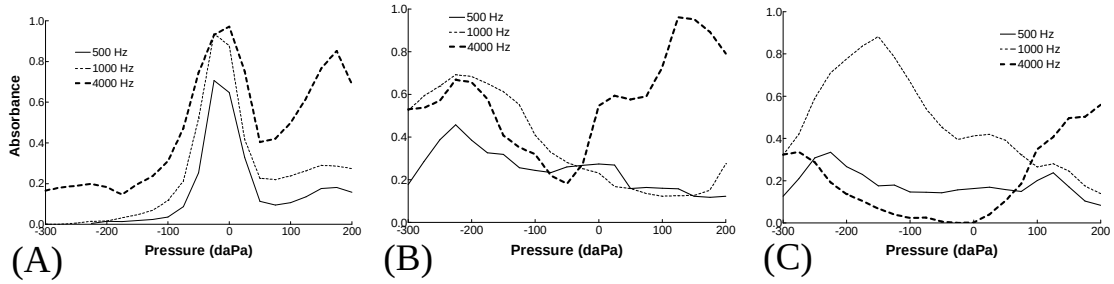


**Figure 5.2** EA-pressure curve at 0.5 (solid line), 1 (thin dashed line), and 4 kHz (thick dashed line) in (A) control, (B) unopened 4D, and (C) unopened 8D AOM ear.

Figure 5.2B displays the EA-pressure curves of the 4D ear in stage OM-1. In both 0.5 and 1 kHz curves, a rounded peak is observed at -220 daPa and EA is generally flat at positive pressure. The value of the absorbance in the region of pressure >100

daPa and pressure < -200 daPa is greater than that near ambient pressure in the 4 kHz curve.

Figure 5.2C shows the EA-pressure curves of the unopened 8D ear. The EA curve of 500 Hz is almost flat over the pressure range and a small rounded peak can be seen between -250 and -200 daPa. Absorbance at 1 kHz is greater than that at low frequency in the 8D ear and a large peak is observed at -150 daPa. The EA curve of 4 kHz shows an "U" shape and the absorbance between -150 to 50 daPa is less than 0.1.

### 5.3.4 MEP and MEE in AOM ears

The MEP in stage OM-1 was quantified by reading the location of the peak in EA-pressure curve at 500 Hz. The MEP of all 4D AOM ears was negative and had a mean value of -184 (± 40 daPa, standard deviation, SD). In the 8D AOM group, three ears exhibited a flat EA-pressure curve, and the MEP was could not be identified. The MEP of the remaining 8D ears with AOM were all negative (mean value -145 ± 65 daPa).

The volume of MEE in 4D AOM ears ranged from 0.3-0.6 ml and had a mean value of 0.4 ml (± 0.13 ml, SD) when the MEE was aspirated for experimental stage OM-2. The MEE volume in 8D ears ranged from 0.7-0.95 ml with an average value of 0.8 ml (± 0.14 ml). The amount of MEP and volume of MEE in 4D and 8D ears are not significantly different from those in our previous study (Guan et al. 2014).

### 5.3.5 Ambient EA-frequency in 4D AOM ears

Figure 5.3 shows the individual curves (dashed lines) of the ambient EA over frequencies of 0.25-8 kHz measured from ten 4D AOM ears and twelve control ears. Shaded area represents ±1 SD around mean. In each AOM ear, absorbance was

measured at three experimental stages: OM-1, OM-2, and OM-3 as shown in Fig. 3A, B, and C, respectively.

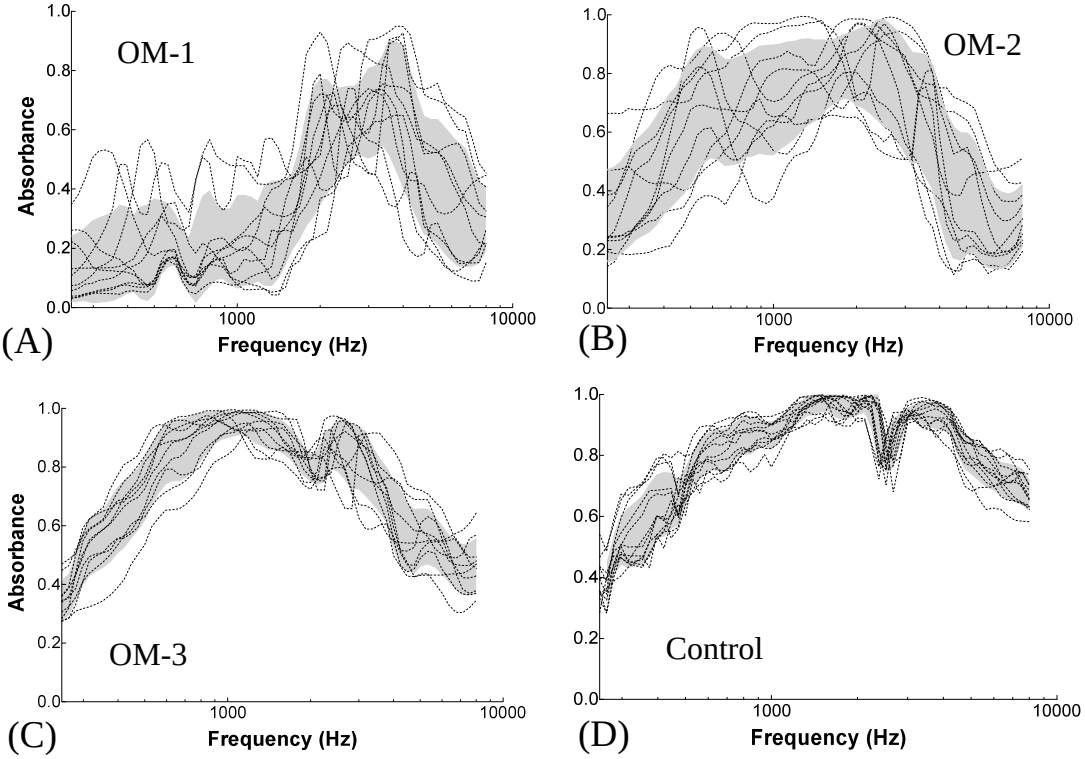


**Figure 5.3** Ambient EA-frequency curve in 4 days (A) OM-1, (B) OM-2, (C) OM-3, and (D) control ears. The dotted lines represent the individual curves. The shaded area represents ± 1 SD around mean.

In stage OM-1 (Fig. 5.3A), the middle ear was unopened, and EA was affected by combination of the MEP, MEE, and structural changes in the middle ear. The EA was generally flat with fluctuation at low frequencies, maximized between 2 to 4 kHz, and decreased at higher frequencies.

In stage OM-2 (Fig. 5.3B), EA increased over 0.25-2 kHz and then decreased at higher frequencies. Large individual variation in EA curves is observed at low frequencies due to the local EA peak between 500 to 800 Hz occurred in four. This

variation may relate to the different amount of middle ear fluid and structural changes between individual ears.

In stage OM-3 (Fig. 5.3C), the effusion was removed but the ossicular adhesions remained unaltered. Inter-individual variation of EA curves was reduced compared with in OM-2. EA increased at low frequencies, maintained maximum value at 1-3 kHz with a small decrease near 2.2 kHz, and decreased at frequencies greater than 3 kHz. As can be seen in Fig. 5.3C, there is no local peaks at low frequencies after the effusion was removed.

Figure 5.3D displays the ambient EA curves measured from 12 control ears. The absorbance continually increased from 250 Hz to 1 kHz, was flat between 1.5 to 4 kHz with a notch at 2.5 kHz, and then decreased at higher frequencies.

The mean EA-frequency curves from control ears and three OM stages in Fig. 5.3 were extracted and displayed in Fig. 5.4 with error bars. The statistical results (p-values) for the EA data in Fig. 5.4 are listed in Table 5.1. Repeated-Measures ANOVA and Tukey post-hoc tests were used to compare three OM stages since EA were measured from the same population. An unpaired t-test was used to compare OM-3 to control ears because the middle ear condition in these two groups was from different populations. Statistical analysis was performed using Prism software (Graphpad, La Jolla, CA). The p-values of post-hoc test were reported as inequalities in the software.

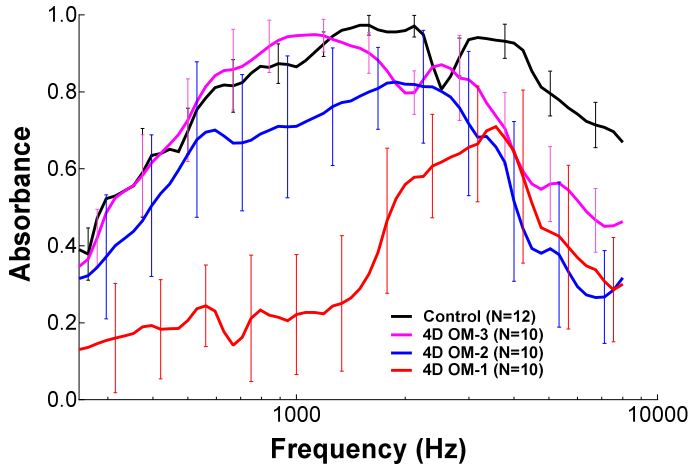


**Figure 5.4** Mean ambient EA-frequency curve with SD in 4 days OM-1 (red line), OM-2 (blue line), OM-3 (purple line), and control ears (black line).

As shown in Fig. 5.4 and Table 5.1, significant changes in absorbance occurred among the three OM stages (Table 5.1, column 2). The EA of OM-3 was significantly greater than that of OM-1 over frequencies of 250 Hz to 8 kHz except 4-6 kHz (column 3 of Table 5.1). After pressure in the middle ear was released (OM-2), the absorbance increased significantly at low frequencies (0.25-2 kHz, see column 4 of Table 5.1). As the effusion was removed from the cavity (OM-3), EA was significantly increased compared to OM-2 near 1 kHz and high frequencies (6-8 kHz, column 5 of Table 5.1). When the OM-3 values were compared with those of control ears, there was a significant difference at frequencies greater than 1 kHz (column 6 of Table 5.1).

**Table 5.1** List of P values derived from: (1) One way Repeated-Measures ANOVA test and Tukey post-hoc test on the ambient EA data between three 4D OM stages; (2) Unpaired Student t-test on the TM magnitude data between OM-3 and control.

| Frequency (kHz) | ANOVA P value | Tukey P value OM-1 vs OM-3 | Tukey P value OM-1 vs OM-2 | Tukey P value OM-2 vs OM-3 | Unpaired t-test P value OM-3 vs Control |
|---|---|---|---|---|---|
| 0.25 | 0.0014 | < 0.01 | < 0.01 | > 0.05 | 0.2812 |
| 0.5 | 0.0001 | < 0.001 | < 0.001 | > 0.05 | 0.4658 |
| 0.75 | 0.0001 | < 0.001 | < 0.001 | < 0.05 | 0.3548 |
| 1 | 0.0001 | < 0.001 | < 0.001 | < 0.01 | 0.0005 |
| 2 | 0.0026 | < 0.01 | < 0.01 | > 0.05 | 0.0000 |
| 4 | 0.1084 | > 0.05 | > 0.05 | > 0.05 | 0.0000 |
| 6 | 0.0115 | > 0.05 | > 0.05 | < 0.01 | 0.0000 |
| 8 | 0.0027 | < 0.01 | > 0.05 | < 0.01 | 0.0000 |

Note: The P values with grey background represent significant difference between groups ($P < 0.05$). The P values of Tukey post-hoc test are shown as inequalities since no exact value is reported by the software.

### 5.3.6 Ambient EA-frequency in 8D AOM ears

Figures 5.5A-C show the individual curves (dashed lines) of the ambient EA over frequencies of 0.25-8 kHz measured from eight 8D AOM ears at three experimental stages. The control curves are also displayed in Fig. 5.5D which are the same as those in Fig. 5.3D.

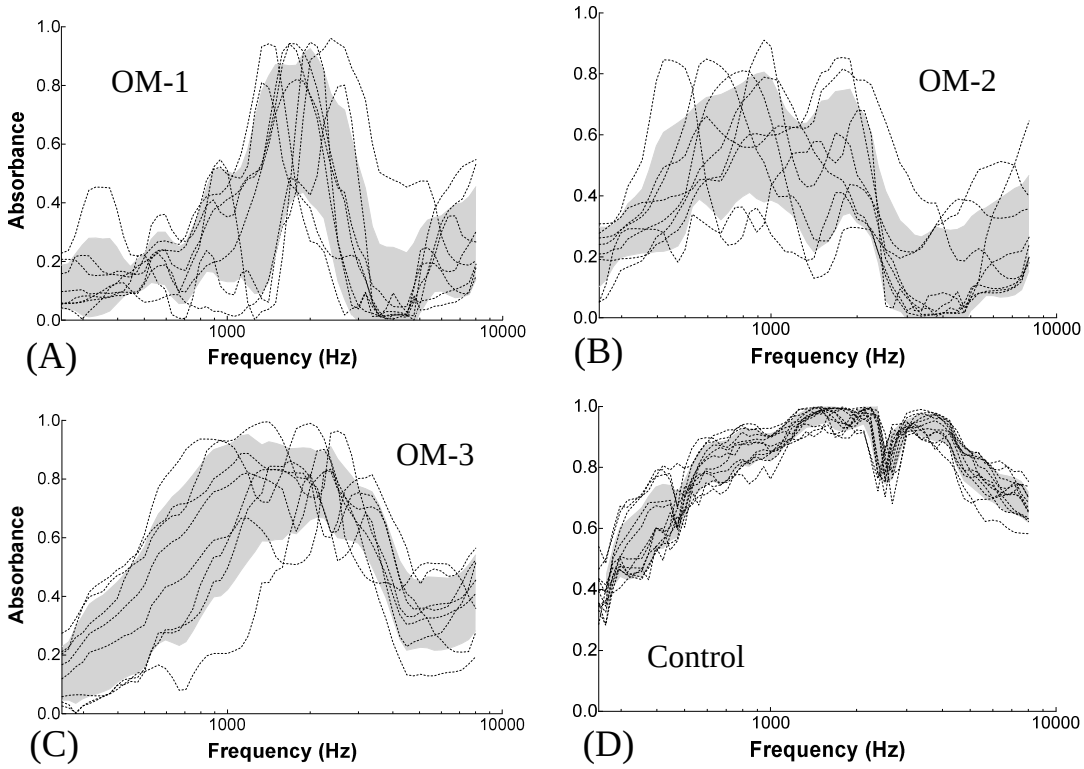


**Figure 5.5** Ambient EA-frequency curve in 8 days (A) OM-1, (B) OM-2, (C) OM-3, and (D) control ears. The dotted lines represent the individual curves. The shaded area represents ± 1 SD around mean.

In stage OM-1 (Fig. 5.5A), the absorbance was generally below 0.2 at frequencies less than 700 Hz, had peak at frequencies of 1-3 kHz, quickly dropped to the lowest value at 4-5 kHz, and increased at higher frequencies. All individual curves exhibited a narrow peak between 1 and 3 kHz. The location of the peak varied between ears, therefore, the inter-individual variation of EA was large in this frequency range.

In stage OM-2, large variation of EA between individuals was observed at low-mid frequencies in Fig. 5.5B. Six out of eight ears exhibited single low-frequency peak at 0.25-1 kHz. The location of the peak varied between individuals. The width of the peak was broader compared with that at stage OM-1. In most 8D ears, the EA declined to a minimum at 3-4 kHz and increased slightly at higher frequencies.

In stage OM-3 (Fig. 5.5C), the individual variation was observed at low frequencies and the curves showed the same pattern over the frequency range. EA increased at low frequencies, maximized between 1 to 2 kHz, and decreased at higher frequencies. The individual difference may relate to the different levels of ossicular adhesions and tissue changes between the ears after inoculation.

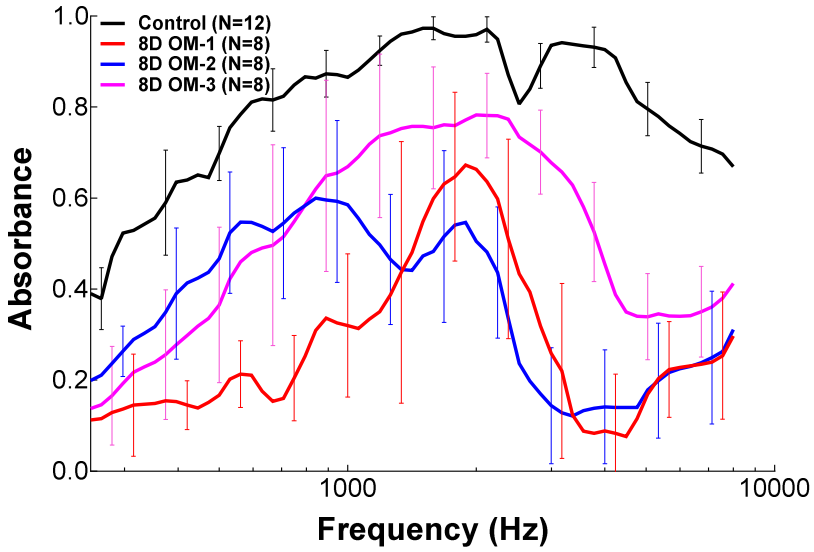


**Figure 5.6** Mean ambient EA-frequency curve with SD in 8 days OM-1 (red line), OM-2 (blue line), OM-3 (purple line), and control ears (black line).

**Table 5.2** List of P values derived from: (1) One way Repeated-Measures ANOVA test and Tukey post-hoc test on the ambient EA data between three 8D OM stages; (2) Unpaired Student t-test on the TM magnitude data between OM-3 and control.

| Frequency (kHz) | ANOVA P value | Tukey P value OM-1 vs OM-3 | Tukey P value OM-1 vs OM-2 | Tukey P value OM-2 vs OM-3 | Unpaired t-test P value OM-3 vs Control |
|---|---|---|---|---|---|
| 0.25 | 0.0906 | > 0.05 | > 0.05 | > 0.05 | 0.0000 |
| 0.5 | 0.0013 | < 0.05 | < 0.01 | > 0.05 | 0.0022 |
| 0.75 | 0.0008 | < 0.01 | < 0.01 | > 0.05 | 0.0150 |
| 1 | 0.0137 | < 0.05 | > 0.05 | > 0.05 | 0.0604 |
| 2 | 0.0223 | > 0.05 | > 0.05 | < 0.05 | 0.0044 |
| 4 | 0.0002 | < 0.001 | > 0.05 | < 0.01 | 0.0000 |
| 6 | 0.0313 | > 0.05 | > 0.05 | < 0.05 | 0.0000 |
| 8 | 0.0318 | > 0.05 | > 0.05 | < 0.05 | 0.0000 |

Note: The P values with grey background represent significant difference between groups ($P < 0.05$). The P values of Tukey post-hoc test are shown as inequalities since no exact value is reported by the software.

The mean EA curves from control and three OM stages in Fig. 5.5 were displayed in Fig. 5.6. The statistical analyses for the data in this figure are listed in Table 5.2 using the same methods as those for 4D ears. As can be seen in Fig. 5.6 and Table 5.2, EA in 8D ears increased statistically in a narrow range of low frequencies after pressure was released (column 4 of Table 5.2). In contrast, releasing MEP significantly increased the TM mobility in 4D ears over 0.25 to 2 kHz. After effusion was removed, the EA in 8D ears increased significantly at frequencies greater than 1 kHz (column 5 of Table 5.2), but in 4D ears significant changes were observed near 1 and 8 kHz. In 8D ears, the EA at OM-3 was significantly different from controls over the frequencies except 1 kHz (column 6 of Table 5.2).

## 5.4 Discussion

### 5.4.1 Comparison with published data

Margolis et al. (2001) reported reflectance tympanogram (reflectance versus ear canal pressure and frequency) and ambient reflectance (reflectance versus frequency) of normal and chinchillas with Eustachian tube obstruction. Hsu et al. (2001) reported ER of neonatal and adult chinchillas. Our EA tympanogram of control ear (Fig. 1A) shows an inverted “V” shape at low frequencies (< 2 kHz) and a “M” shape at higher frequencies. The pattern of the control EA tympanogram is consistent with that of the normal ER tympanogram reported by Margolis et al. (2001) and Hsu et al. (2001). However, in these two earlier studies the value of the ambient ER from normal chinchillas was close to 1 (zero for EA) at frequencies below 1 kHz (Fig. 11 A in Margolis et al.; Fig. 4 in Hsu et al.). In the present study, the ambient EA of control ears

was much greater than zero at low frequencies. One possible reason for the discrepancy is that the cross-sectional area of the ear canal used to calculate EA or ER in this tudy was different from the previous studies. The calculation of EA depends on the cross-sectional area of the ear canal. The ear-canal area at the measurement location should be used in calculation (Keefe et al. 1993) and larger ear-canal area decreases EA at low frequencies (Voss et al. 2008). In this study, EA was measured at the entrance of the osseous portion of the ear canal, where the ear-canal diameter was 4 to 6 mm. A constant area with a diameter of 4.5 mm was used to calculate the EA in wideband tympanometry. The measurement location in the earlier studies seems the same as ours, but a constant area with diameter 8 mm was used in Margolis et al. (2001), and acoustically estimated ear-canal area was used in Hsu et al. (2001). In human temporal bones, Voss et al. (2008) reported that the acoustically measured ear-canal area was greater than the physical measured ear-canal area in most cases. The relatively large area used for the calculation in the earlier studies probably resulted in smaller EA at low frequencies.

For chinchilla ears with zero MEP, the peak of EA curves centers at ambient pressure at low frequencies and EA is low and flat at other pressure levels (Fig. 1A). When MEP is present, the EA peak at low frequencies would shift away from zero pressure, which results in a low EA at ambient pressure. In the present study, any pre-existing MEP in control ears was eliminated before the measurement because the MEP can build up due to anesthesia effect (Guinan and Peake 1967). The admittance tympanograms of normal chinchillas reported by Margolis et al. (Fig. 14 in their paper) and Hsu et al. (Fig. 2 in their paper) suggest that MEP existed in some animals in their

studies. Thus, anesthesia-induced MEP might occur and contribute to the high ambient ER (low EA) at low frequencies in these chinchilla ears.

### 5.4.2 Factors affecting ambient EA in AOM ears

In this study, EA at ambient pressure in the chinchilla AOM ears was investigated at early (4D) and later (8D) phases of AOM. The effects of middle ear pressure, effusion, and structural changes on EA at each AOM period were investigated by comparing the EA-frequency curves at an OM stage with respect to the previous stage (Figs. 5.3 and 5.5) together with the statistical analysis (Tables 5.1 and 5.2). The results demonstrated that three factors, the MEP (OM-1 versus OM-2), MEE (OM-2 versus OM-3), and middle ear tissue structural changes (OM-3 versus Control) at early infection affected the ambient EA in a different manner from those at the later infection period. The effects of these three factors on EA during the AOM time-course are discussed with TM mobility change in the following sections.

#### 5.4.2.1 Effect of MEP on ambient EA

In unopened AOM ears (OM-1), EA at ambient pressure was affected by combination of MEP, MEE, and structural changes. The EA of 4D and 8D ears at stage OM-1 was generally flat at low frequencies and reached maximum value abruptly in mid-high frequency range. This pattern is consistent with the ER results observed in patients with otitis media with effusion (OME) by Beers et al. (2010) and Feeney et al. (2003), although the major pathologic changes in the OME ears were pressure and effusion. The narrow peak at mid-high frequencies might be related to resonant vibration of the TM, which was produced by combination of the MEP and MEE.

After the MEP was released (OM-2), EA substantially increased at low frequencies in both 4D and 8D ears. Stiffness of the middle ear dominates the TM mobility at low frequencies (Ravicz. et al. 2004; Gan et al. 2006). Voss et al. (2012) reported that the ER was increased at frequencies below 2 kHz when positive or negative pressure was introduced to the middle ear of cadaveric bones. In our current study, release of the MEP reduced the stiffness of the TM and increased the low-frequency EA. The changes of EA due to release of the pressure agree with the effect of MEP on the reflectance observed by Voss et al. (2012).

The increase of ambient EA upon releasing MEP in 4D was greater than that in 8D ears (see blue line vs red line in Figs. 5.4 and 5.6). Our previous study of umbo mobility in this chinchilla AOM model showed that the increase of umbo displacement in 4D ears was also more prominent than that in 8D ears after releasing the pressure (Guan and Gan 2014). It has been reported that the air space in the middle ear cavity is critical to TM mobility (Ravicz et al. 2004) and EA (Voss et al. 2008). The effect of MEP on EA is dependent on the residual air space in the middle ear. The tympanic cavity of 4D ears was nearly half-filled with MEE and the cavity of 8D was almost fully filled with effusion. The increase of EA after release of the pressure was limited because a relatively large amount of effusion remained in the tympanic cavity. In 4D ears the EA significantly increased upon the release of MEP due to sufficient air space behind the TM. Thus, the effect of the MEP on EA in the early phase of AOM was greater than that in the later phase. MEP was the primary contributor to reduction of EA at low frequencies in 4D AOM ears.

#### 5.4.2.2 Effect of MEE on ambient EA

After the MEE was removed from the middle ear (OM-3), two changes were observed in the ambient EA-frequency curves for both AOM phases: (1) EA was significantly increased at high frequencies; (2) the peaks at low frequencies observed at stage OM-2 no longer existed and the EA tended to simply increase as a function of frequency at $f < 1$ kHz.

MEE affects the middle ear mechanics by reducing the middle ear air space and adding mass to the TM (Ravicz et al. 2004). Upon removal of effusion EA was increased at high frequencies in both 4D and 8D ears due to a reduction of TM mass. However, the effect of fluid on EA at low frequencies is not as simple. Our results demonstrate that MEE resulted in a single EA peak at low frequencies in some 4D ears and in most 8D ears. There was no such explicit peak at low frequencies in the umbo displacement curves (Guan and Gan 2014). Voss et al. (2012) reported that when over half of the cavity was filled with fluid ER increased substantially at high frequencies and meanwhile there was a low-frequency notch in the ER curve (Fig. 6 in their paper). They proposed that the rapid changes of ER at low frequencies might result from air bubbles in the middle ear fluid (Voss et al. 2012). In our current study, air bubbles were observed only occasionally behind the TMs in 4D and 8D ears. The low-frequency peak may be caused by resonant vibration of the whole TM when large amount of fluid were present in the middle ear. It is possible that when TM stiffness was reduced by release of the pressure the resonance frequency of TM vibration decreased, therefore, the narrow EA peak at mid-high frequencies in stage OM-1 shifted to low frequencies in OM-2. After the effusion was removed, the low-frequency peak disappeared in 4D and

8D ears. In summary, MEE contributed to reduction of EA at high frequencies and resulted in narrow EA peak at low frequencies in some 4D and most 8D ears.

#### 5.4.2.3 Effect of structural changes on ambient EA

After the pressure and effusion were removed from the middle ear (OM-3), residual reduction of ambient EA was observed at high frequencies in 4D ears and over all the frequencies in 8D ears (pink line vs black line in Figs. 5.4 and 5.6). The residual reduction of EA suggested that the infection-induced structural changes also contributed to EA changes. The structural changes include ossicular adhesions and mechanical property changes of middle ear soft tissues.

As shown in our previous study, ossicular adhesions were found on the malleus head, between the manubrium and the cochlear promontory, and around the stapes in the round window niche for both 4D and 8D ears. Those adhesions fixed ossicles and reduced umbo mobility mainly at low frequencies (Guan and Gan 2014). Effect of ossicular adhesions on EA has not been reported in the current literature. Margolis et al. (2001) reported the results of multi-frequency tympanograms obtained from one chinchilla ear with stapes adhesion, but the EA or ER of that ear was not shown in their paper. Otosclerosis is considered to have a similar effect on the movement of ossicular chain as the adhesions. Shahnaz et al. (2009) showed that there is an increase of ER (decrease of EA) below 1 kHz in patients with confirmed otosclerosis. However, there is a considerable overlap between the range of ER for the patients and that for normal ears. Voss et al. (2012) reported the ER in five cadaveric ears with stapes fixed with dental cement. Their results show that in three of five ears the fixation of stapes led to small increases of ER at low frequencies, and in the other two ears the ER was not

affected much by stapes fixation (Fig. 7 in their paper). Based on those published data, the effect of ossicular fixation on EA or ER seems to be relatively small compared with its effect on umbo movement (Rosowski et al. 2008; Nakajima et al. 2005).

If we assume that the EA was minimally affected by the adhesions in chinchilla AOM ears, the residual reduction of EA in OM-3 was caused by changes of ear tissues, particularly changes of TM. The mechanical properties of the TM are believed to be crucial to EA because EA measures the mechanoacoustic response of the whole TM. The TM properties are dependent on the micro-structure of the membrane. Our ongoing histologic study indicated that the TM of 4D AOM was thicker than control and the thickening occurred mainly in the outer epithelial layer. As middle ear infection persisted to 8D, the thickening of TM was more prominent due to the edema and infiltration of inflammatory cells in the outer epithelium and inner mucosa (results not included in this study). Those histopathological changes suggest that the stiffness and mass of TM may differ between control, 4D, and 8D ears. The residual reduction of EA in 8D was observed over the tested frequencies, while the residual loss of EA in 4D ears occurred at frequencies above 3 kHz. This difference may relate to different degrees of TM structural changes between the early and later phases of AOM. The TM changes might be the primary contributor to the residual loss of EA in AOM ears.

### 5.4.3 Relation between changes of EA, umbo displacement, and ABR threshold

In order to test if EA or umbo mobility can reflect the hearing loss in AOM, we compared the changes between EA, umbo displacement, and ABR threshold in unopened AOM ears of the chinchillas.

Figure 5.7 displays the mean ambient EA of control (black line), unopened 4D (blue line), and unopened 8D ears (pink line) extracted from Figs. 5.4 and 5.6. As can be seen, the EA in both AOM groups was lower than control over the entire frequencies. The reduction of 4D EA at 2 to 4 kHz was smaller than that at other frequencies. The minimal loss of EA in 8D ears was observed near 2 kHz.

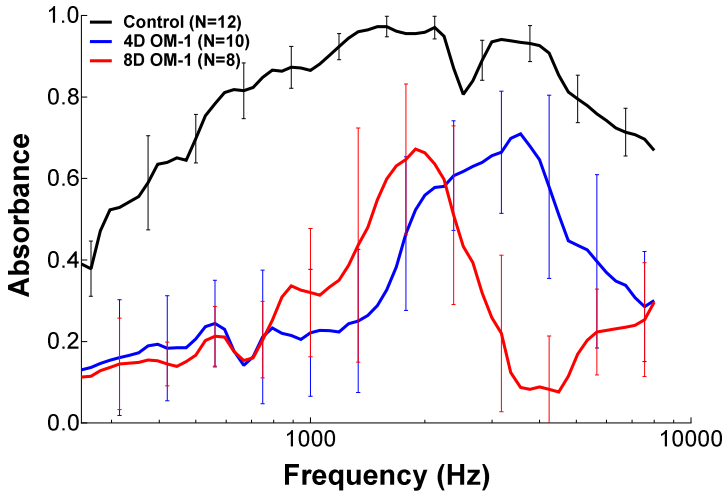


**Figure 5.7** Comparison of mean ambient EA-frequency curve with SD between control (black line), unopened 4D (blue line), and unopened 8D ears (red line).

The ABR threshold in both 4D and 8D ears was elevated over the tested frequencies (Fig. 3.4 in Chapter 3), which agrees with the reduction of EA. However, in both AOM groups the elevation of ABR did not decrease at frequencies where the reduction of EA decreased.

The ABR changes correlated stronger with the changes of umbo displacement (Fig. 4.8A in Chapter 4) in 4D and 8D ears. Particularly, the umbo mobility at 2-6 kHz in 8D ears was substantially lower than that in 4D ears, which is consistent with statistical results of ABR data.

EA describes the total energy absorbed by the middle ear. Some of the energy was transmitted to the cochlea through ossicular chain, and some was dissipated in the middle ear cavity. Our findings suggest that the relation between the reduction of EA and the loss of the energy transmitted to the cochlea in AOM is not simple. Loss of umbo displacement reflected the changes of ABR threshold between 4D and 8D ears.

## 5.5 Conclusion

The effects of MEP, effusion, and structural changes on ambient EA in chinchilla AOM ears were examined over the course of the disease (4 days and 8 days post inoculation). Results show that the MEP was the primary contributor to reduction of EA in 4D AOM ears and had a smaller effect in 8D ears. MEE contributed to reduction of EA at high frequencies in both 4D and 8D ears and resulted in narrow EA peak at low frequencies in some 4D and most 8D ears. After release of MEP and removal of MEE, there was residual EA loss over all the frequencies in 8D ears and at high frequencies in 4D ears, which was probably associated with TM morphological changes. The ABR threshold elevated in both 4D and 8D AOM ears and the elevation of ABR did not decrease at the frequency where the reduction of EA decreased. This study characterizes the roles of MEP, MEE, and structural changes in reduction of EA in chinchilla AOM ears.

## CHAPTER 6: SUMMARY AND FUTURE WORKS

To understand middle ear biomechanics in AOM ears, a chinchilla AOM model was produced by transbullar injection of *H. influenzae*. We identified that middle ear pressure, effusion, together with structural changes such as ossicular adhesion and ear tissue microstructural changes each contributed to reduction of sound transmission in the chinchilla AOM ears. Our findings demonstrated that these factors changed from early to later phase of AOM and their contributions to loss of TM mobility varied during the course of the disease. This study established the structure-function relation of the middle ear in the AOM model. The major findings are summarized below.

Microstructures of the TM, RWM, and SAL in early and later phases of AOM in chinchillas were characterized by histologic analysis. The results show that the structures of those ear tissues underwent substantial changes in 4D AOM and the changes were more prominent in 8D ears. Thickness of the TM and RWM in normal and diseased ears was obtained to aid in deriving their mechanical properties in future studies.

Conductive hearing loss of 4D and 8D AOM ears were evaluated by ABR measurement. The results demonstrate that the chinchillas in both 4D and 8D groups had significant hearing loss over the frequencies and the hearing loss in 8D ears tends to be greater than that in 4D ears.

Effects of MEP, MEE, and structural changes on TM mobility loss were quantified and compared between early and later phases of AOM. The results show that MEP was the dominant contributor to reduction of TM mobility in 4D AOM ears. MEE was the primary factor affecting TM mobility loss in 8D ears. After removal of MEP

and MEE, there was residual loss of TM mobility at low frequencies in both 4D and 8D ears, which was associated with middle ear structural changes. The factors contributing to TM mobility loss in the chinchilla ear were similar to those we reported previously for the guinea pig AOM ears induced by *S. pneumoniae*.

Effects of the middle ear pathologic changes on EA were examined in 4D and 8D ears. The results illustrated that EA was sensitive to MEP, MEE, and middle ear structural changes.

All the research objectives listed in Chapter 1 are fulfilled. Our findings characterize the roles of middle ear pressure, effusion, and structural changes in middle ear biomechanics in early and later phases of the AOM model. The contribution of this study is to provide useful data for understanding the mechanism of conductive hearing loss in AOM.

Following the current works on ear mechanics of the chinchilla AOM model, future works needed to extend our understanding on the mechanoacoustic response of the middle ear in AOM are discussed below.

Mechanical properties of the ear tissues are crucial to sound transmission. Our histologic study showed the microstructural changes of the TM, RWM, and SAL in AOM ears. Their mechanical properties are still unclear. In order to understand the impact of AOM on tissue property changes, the following works needs to be done: (1) increase the numbers of TM, RWM, and SAL specimens in histologic study for statistical analysis on their morphologic changes, (2) improve the preparation of SAL sample to maintain its intrinsic structure, and (3) couple the structural changes obtained from histology with modeling to derive mechanical properties of those ear tissues.

The current study provided experimental data of TM mobility and EA changes in AOM ears. A finite-element (FE) model of the chinchilla ear would give additional insight into sound transmission in AOM ear. Effects of MEP, MEE, ossicular adhesion, and ear tissue mechanical property changes on middle ear vibration can be further investigated in the FE model.

## REFERENCES


1. Ahmed, S., Shapiro, N.L., and Bhattacharyya, N. (2014) Incremental health care utilization and costs for acute otitis media in children. Laryngoscope, 124(1): p. 301-5.

2. Allen, J.B. (1986) Measurement of eardrum acoustic impedance in Peripheral Auditory Mechanisms., J.B. Allen, et al., Editors. Springer: Berlin. p. 44-51.

3. Allen, J.B., Jeng, P.S., and Levitt, H. (2005) Evaluation of human middle ear function via an acoustic power assessment. J Rehabil Res Dev, 42(4 Suppl 2): p. 63-78.

4. Bakaletz, L.O. (2009) Chinchilla as a robust, reproducible and polymicrobial model of otitis media and its prevention. Expert review of vaccines, 8(8): p. 1063-82.

5. Bakaletz, L.O., Kennedy, B.J., Novotny, L.A., Duquesne, G., Cohen, J., et al. (1999) Protection against development of otitis media induced by nontypeable Haemophilus influenzae by both active and passive immunization in a chinchilla model of virus-bacterium superinfection. Infection and immunity, 67(6): p. 2746-62.

6. Beers, A.N., Shahnaz, N., Westerberg, B.D., and Kozak, F.K. (2010) Wideband reflectance in normal Caucasian and Chinese school-aged children and in children with otitis media with effusion. Ear Hear, 31(2): p. 221-33.

7. Békésy, v., Experiments in Hearing1960: American Institute of Physics.

8. Berger, G., Sachs, Z., and Sade, J. (1996) Histopathologic changes of the tympanic membrane in acute and secretory otitis media. Ann Otol Rhinol Laryngol, 105(6): p. 458-62.

9. Bluestone, C.D. and Klein, J.O., Otitis media with effusion, atelectasis, and eustachian tube dysfuncion, in Pediatric Otolaryngology, C.D. Bluestone and S.E. Stool, Editors. 1983A, W. B. Saunders Company: Philadelphia, PA. p. 419-432.

10. Bluestone, C.D. and Klein, J.O., Intratemporal complications and sequelae of otitis media., in Pediatric Otolaryngology, C.D. Bluestone and S.E. Stool, Editors. 1983B, W. B. Saunders Company: Philadelphia, PA. p. 513-515.

11. Bluestone, C.D., Stephenson, J.S., and Martin, L.M. (1992) Ten-year review of otitis media pathogens. The Pediatric infectious disease journal, 11(8 Suppl): p. S7-11.

12. Bolz, E.A. and Lim, D.J. (1972) Morphology of the stapediovestibular joint. Acta Otolaryngol, 73(1): p. 10-7.

13. Browning, G.C. and Granich, M.S. (1978) Surgical anatomy of the temporal bone in the chinchilla. The Annals of otology, rhinology, and laryngology, 87(6 Pt 1): p. 875-82.

14. Caye-Thomasen, P., Hermansson, A., Tos, M., and Prellner, K. (1996) Pathogenesis of middle ear adhesions. Laryngoscope, 106(4): p. 463-9.

15. Caye-Thomasen, P. and Tos, M. (2000) Polyp and fibrous adhesion formation in acute otitis media caused by non-typeable or type b Haemophilus influenzae or Moraxella catarrhalis. Acta Otolaryngol, 120(7): p. 810-4.

16. Cheng, J.T., Aarnisalo, A.A., Harrington, E., Hernandez-Montes Mdel, S., Furlong, C., et al. (2010) Motion of the surface of the human tympanic membrane measured with stroboscopic holography. Hear Res, 263(1-2): p. 66-77.

17. Cheng, J.T., Hamade, M., Merchant, S.N., Rosowski, J.J., Harrington, E., et al. (2013) Wave motion on the surface of the human tympanic membrane: holographic measurement and modeling analysis. J Acoust Soc Am, 133(2): p. 918-37.

18. Cheng, T., Dai, C., and Gan, R.Z. (2007) Viscoelastic properties of human tympanic membrane. Ann Biomed Eng, 35(2): p. 305-14.

19. Chien, W., Ravicz, M.E., Merchant, S.N., and Rosowski, J.J. (2006) The effect of methodological differences in the measurement of stapes motion in live and cadaver ears. Audiol Neurootol, 11(3): p. 183-97.

20. Dai, C., Cheng, T., Wood, M.W., and Gan, R.Z. (2007) Fixation and detachment of superior and anterior malleolar ligaments in human middle ear: experiment and modeling. Hearing Research, 230(1-2): p. 24-33.

21. Dai, C., Wood, M.W., and Gan, R.Z. (2007) Tympanometry and laser Doppler interferometry measurements on otitis media with effusion model in human temporal bones. Otology & Neurotology, 28(4): p. 551-8.

22. Dai, C., Wood, M.W., and Gan, R.Z. (2008) Combined effect of fluid and pressure on middle ear function. Hear Res, 236(1-2): p. 22-32.

23. Dankbaar, W.A. (1970) The pattern of stapedial vibration. J Acoust Soc Am, 48(4): p. 1021-2.

24. Daphalapurkar, N.P., Dai, C., Gan, R.Z., and Lu, H. (2009) Characterization of the linearly viscoelastic behavior of human tympanic membrane by nanoindentation. J Mech Behav Biomed Mater, 2(1): p. 82-92.

25. Decraemer, W.F., Maes, M.A., and Vanhuyse, V.J. (1980) An elastic stress-strain relation for soft biological tissues based on a structural model. J Biomech, 13(6): p. 463-8.

26. Decraemer, W.F., Maes, M.A., Vanhuyse, V.J., and Vanpeperstraete, P. (1980) A non-linear viscoelastic constitutive equation for soft biological tissues, based upon a structural model. J Biomech, 13(7): p. 559-64.

27. Ehrlich, G.D., Veeh, R., Wang, X., Costerton, J.W., Hayes, J.D., et al. (2002) Mucosal biofilm formation on middle-ear mucosa in the chinchilla model of otitis media. JAMA, 287(13): p. 1710-5.

28. Fay, J., Puria, S., Decraemer, W.F., and Steele, C. (2005) Three approaches for estimating the elastic modulus of the tympanic membrane. J Biomech, 38(9): p. 1807-15.

29. Feeney, M.P., Grant, I.L., and Marryott, L.P. (2003) Wideband energy reflectance measurements in adults with middle-ear disorders. J Speech Lang Hear Res, 46(4): p. 901-11.

30. Feldman, A.S. (1963) Impedance Measurements at the Eardrum as an Aid to Diagnosis. Journal of Speech & Hearing Research, 13: p. 315-27.

31. Forbes, M.L., Horsey, E., Hiller, N.L., Buchinsky, F.J., Hayes, J.D., et al. (2008) Strain-specific virulence phenotypes of Streptococcus pneumoniae assessed using the Chinchilla laniger model of otitis media. PLoS One, 3(4): p. e1969.

32. Fulghum, R.S., Brinn, J.E., Smith, A.M., Daniel, H.J., 3rd, and Loesche, P.J. (1982) Experimental otitis media in gerbils and chinchillas with Streptococcus pneumoniae, Haemophilus influenzae, and other aerobic and anaerobic bacteria. Infect Immun, 36(2): p. 802-10.

33. Gan, R.Z., Dai, C., and Wood, M.W. (2006) Laser interferometry measurements of middle ear fluid and pressure effects on sound transmission. J Acoust Soc Am, 120(6): p. 3799-810.

34. Gan, R.Z., Nakmali, D., and Zhang, X. (2013) Dynamic properties of round window membrane in guinea pig otitis media model measured with electromagnetic stimulation. Hearing Research, 301: p. 125-36.

35. Gan, R.Z., Wood, M.W., and Dormer, K.J. (2004) Human middle ear transfer function measured by double laser interferometry system. Otol Neurotol, 25(4): p. 423-35.

36. Gan, R.Z., Yang, F., Zhang, X., and Nakmali, D. (2011) Mechanical properties of stapedial annular ligament. Medical engineering & physics, 33(3): p. 330-9.

37. Giebink, G.S. (1999) Otitis media: the chinchilla model. Microbial drug resistance, 5(1): p. 57-72.

38. Goksu, N., Haziroglu, R., Kemaloglu, Y., Karademir, N., Bayramoglu, I., et al. (1992) Anatomy of the guinea pig temporal bone. Ann Otol Rhinol Laryngol, 101(8): p. 699-704.

39. Goode, R.L., Ball, G., and Nishihara, S. (1993) Measurement of umbo vibration in human subjects--method and possible clinical applications. Am J Otol, 14(3): p. 247-51.

40. Gould, J.M. and Matz, P.S. (2010) Otitis media. Pediatrics in review / American Academy of Pediatrics, 31(3): p. 102-16.

41. Goycoolea, M.V. and Lundman, L. (1997) Round window membrane. Structure function and permeability: a review. Microsc Res Tech, 36(3): p. 201-11.

42. Green, B.A., Vazquez, M.E., Zlotnick, G.W., Quigley-Reape, G., Swarts, J.D., et al. (1993) Evaluation of mixtures of purified Haemophilus influenzae outer

membrane proteins in protection against challenge with nontypeable H. influenzae in the chinchilla otitis media model. Infection and immunity, 61(5): p. 1950-7.

43. Guan, X., Chen, Y., and Gan, R.Z. (2014) Factors affecting loss of tympanic membrane mobility in acute otitis media model of chinchilla. Hear Res, 309: p. 136-46.

44. Guan, X. and Gan, R.Z. (2011) Effect of middle ear fluid on sound transmission and auditory brainstem response in guinea pigs. Hear Res, 277(1-2): p. 96-106.

45. Guan, X. and Gan, R.Z. (2013) Mechanisms of tympanic membrane and incus mobility loss in acute otitis media model of guinea pig. J Assoc Res Otolaryngol, 14(3): p. 295-307.

46. Guan, X., Li, W., and Gan, R.Z. (2013) Comparison of eardrum mobility in acute otitis media and otitis media with effusion models. Otol Neurotol, 34(7): p. 1316-20.

47. Guinan, J.J., Jr. and Peake, W.T. (1967) Middle-ear characteristics of anesthetized cats. J Acoust Soc Am, 41(5): p. 1237-61.

48. Gyo, K., Aritomo, H., and Goode, R.L. (1987) Measurement of the ossicular vibration ratio in human temporal bones by use of a video measuring system. Acta Otolaryngol, 103(1-2): p. 87-95.

49. Hanamure, Y. and Lim, D.J. (1987) Anatomy of the chinchilla bulla and eustachian tube: I. Gross and microscopic study. American journal of otolaryngology, 8(3): p. 127-43.

50. Heiland, K.E., Goode, R.L., Asai, M., and Huber, A.M. (1999) A human temporal bone study of stapes footplate movement. Am J Otol, 20(1): p. 81-6.

51. Hendley, J.O. (2002) Clinical practice. Otitis media. N Engl J Med, 347(15): p. 1169-74.

52. Hoa, M., Syamal, M., Sachdeva, L., Berk, R., and Coticchia, J. (2009) Demonstration of nasopharyngeal and middle ear mucosal biofilms in an animal model of acute otitis media. Ann Otol Rhinol Laryngol, 118(4): p. 292-8.

53. Hoberman, A., Paradise, J.L., Rockette, H.E., Shaikh, N., Wald, E.R., et al. (2011) Treatment of acute otitis media in children under 2 years of age. N Engl J Med, 364(2): p. 105-15.

54. Hong, W., Mason, K., Jurcisek, J., Novotny, L., Bakaletz, L.O., et al. (2007) Phosphorylcholine decreases early inflammation and promotes the establishment of stable biofilm communities of nontypeable Haemophilus influenzae strain 86-028NP in a chinchilla model of otitis media. Infection and immunity, 75(2): p. 958-65.

55. Hsu, G.S., Margolis, R.H., and Schachern, P.A. (2000) Development of the middle ear in neonatal chinchillas. I. Birth to 14 days. Acta Otolaryngol, 120(8): p. 922-32.

56. Hsu, R.W., Margolis, R.H., Schachern, P.A., and Javel, E. (2001) The development of the middle ear in neonatal chinchillas II. Two weeks to adulthood. Acta Otolaryngol, 121(6): p. 679-88.

57. Huang, G., Daphalapurkar, N.P., Gan, R.Z., and Lu, H. (2008) A method for measuring linearly viscoelastic properties of human tympanic membrane using nanoindentation. J Biomech Eng, 130(1): p. 014501.

58. Huang, G.T., Rosowski, J.J., Flandermeyer, D.T., Lynch, T.J., 3rd, and Peake, W.T. (1997) The middle ear of a lion: comparison of structure and function to domestic cat. Journal of the Acoustical Society of America, 101(3): p. 1532-49.

59. Jerger, J. (1970) Clinical experience with impedance audiometry. Archives of Otolaryngology, 92(4): p. 311-24.

60. Jurcisek, J., Greiner, L., Watanabe, H., Zaleski, A., Apicella, M.A., et al. (2005) Role of sialic acid and complex carbohydrate biosynthesis in biofilm formation by nontypeable Haemophilus influenzae in the chinchilla middle ear. Infect Immun, 73(6): p. 3210-8.

61. Keefe, D.H., Bulen, J.C., Arehart, K.H., and Burns, E.M. (1993) Ear-canal impedance and reflection coefficient in human infants and adults. J Acoust Soc Am, 94(5): p. 2617-38.

62. Kirikae, I., The structure and function of the middle ear.1960, Tokyo: the University of Tokyo Press. 419-432.

63. Larsson, C., Dirckx, J.J., Decraemer, W.F., Bagger-Sjoback, D., and von Unge, M. (2003) Pars flaccida displacement pattern in purulent otitis media in the gerbil. Otology & Neurotology, 24(3): p. 358-64.

64. Lee, C.Y. and Rosowski, J.J. (2001) Effects of middle-ear static pressure on pars tensa and pars flaccida of gerbil ears. Hearing Research, 153(1-2): p. 146-63.

65. Lin, J., Tsuboi, Y., Pan, W., Giebink, G.S., Adams, G.L., et al. (2002) Analysis by cDNA microarrays of altered gene expression in middle ears of rats following pneumococcal infection. International journal of pediatric otorhinolaryngology, 65(3): p. 203-11.

66. Long, J.P., Tong, H.H., Shannon, P.A., and DeMaria, T.F. (2003) Differential expression of cytokine genes and inducible nitric oxide synthase induced by opacity phenotype variants of Streptococcus pneumoniae during acute otitis media in the rat. Infection and immunity, 71(10): p. 5531-40.

67. Luo, H., Lu, H., Dai, C., and Gan, R.Z. (2009) A comparison of Young's modulus for normal and diseased human eardrums at high strain rates. Experimental and Computational Biomechanics, 1(1): p. 1-22.

68. Luotonen, J., Herva, E., Karma, P., Timonen, M., Leinonen, M., et al. (1981) The bacteriology of acute otitis media in children with special reference to Streptococcus pneumoniae as studied by bacteriological and antigen detection methods. Scandinavian journal of infectious diseases, 13(3): p. 177-83.

69. MacArthur, C.J., Hefeneider, S.H., Kempton, J.B., Parrish, S.K., McCoy, S.L., et al. (2006) Evaluation of the mouse model for acute otitis media. Hear Res, 219(1-2): p. 12-23.

70. MacArthur, C.J. and Trune, D.R. (2006) Mouse models of otitis media. Current opinion in otolaryngology & head and neck surgery, 14(5): p. 341-6.

71. Manley, G.A. and Johnstone, B.M. (1974) Middle-ear function in the guinea pig. The Journal of the Acoustical Society of America, 56(2): p. 571-6.

72. Margolis, R.H., Paul, S., Saly, G.L., Schachern, P.A., and Keefe, D.H. (2001) Wideband reflectance tympanometry in chinchillas and human. J Acoust Soc Am, 110(3 Pt 1): p. 1453-64.

73. Mason, K.M., Munson, R.S., Jr., and Bakaletz, L.O. (2003) Nontypeable Haemophilus influenzae gene expression induced in vivo in a chinchilla model of otitis media. Infection and immunity, 71(6): p. 3454-62.

74. Melhus, A. and Ryan, A.F. (2000) Expression of cytokine genes during pneumococcal and nontypeable Haemophilus influenzae acute otitis media in the rat. Infection and immunity, 68(7): p. 4024-31.

75. Melhus, A. and Ryan, A.F. (2003) A mouse model for acute otitis media. APMIS : acta pathologica, microbiologica, et immunologica Scandinavica, 111(10): p. 989-94.

76. Merchant, S.N., Ravicz, M.E., Puria, S., Voss, S.E., Whittemore, K.R., Jr., et al. (1997) Analysis of middle ear mechanics and application to diseased and reconstructed ears. American Journal of Otology, 18(2): p. 139-54.

77. Merchant, S.N., Ravicz, M.E., Voss, S.E., Peake, W.T., and Rosowski, J.J. (1998) Toynbee Memorial Lecture 1997. Middle ear mechanics in normal, diseased and reconstructed ears. J Laryngol Otol, 112(8): p. 715-31.

78. Møller, A.R. (1965) An Experimental Study of the Acoustic Impedance of the Middle Ear and Its Transmission Properties. Acta Oto-Laryngologica, 60: p. 129-49.

79. Møller, A.R., Physiology of the ear, in Pediatric Otolaryngology, C.D. Bluestone and S.E. Stool, Editors. 1983, W. B. Saunders Company: Philadelphia, PA. p. 112-138.

80. Morton, D.J., Bakaletz, L.O., Jurcisek, J.A., VanWagoner, T.M., Seale, T.W., et al. (2004) Reduced severity of middle ear infection caused by nontypeable Haemophilus

influenzae lacking the hemoglobin/hemoglobin-haptoglobin binding proteins (Hgp) in a chinchilla model of otitis media. Microbial pathogenesis, 36(1): p. 25-33.

81. Morton, D.J., Hempel, R.J., Seale, T.W., Whitby, P.W., and Stull, T.L. (2012) A functional tonB gene is required for both virulence and competitive fitness in a chinchilla model of Haemophilus influenzae otitis media. BMC research notes, 5: p. 327.

82. Murakami, S., Gyo, K., and Goode, R.L. (1997) Effect of middle ear pressure change on middle ear mechanics. Acta Otolaryngol, 117(3): p. 390-5.

83. Naguib, M.B., Hunter, R.E., and Henley, C.M. (1994) Cochlear polyamines: markers of otitis media-induced cochlear damage. Laryngoscope, 104(8 Pt 1): p. 1003-7.

84. Nakajima, H.H., Ravicz, M.E., Merchant, S.N., Peake, W.T., and Rosowski, J.J. (2005) Experimental ossicular fixations and the middle ear's response to sound: evidence for a flexible ossicular chain. Hearing Research, 204(1-2): p. 60-77.

85. Nakajima, H.H., Ravicz, M.E., Rosowski, J.J., Peake, W.T., and Merchant, S.N. (2005) Experimental and clinical studies of malleus fixation. The Laryngoscope, 115(1): p. 147-54.

86. Nakajima, H.H., Rosowski, J.J., Shahnaz, N., and Voss, S.E. (2013) Assessment of ear disorders using power reflectance. Ear Hear, 34 Suppl 1: p. 48S-53S.

87. Novotny, L.A., Mason, K.M., and Bakaletz, L.O. (2005) Development of a chinchilla model to allow direct, continuous, biophotonic imaging of bioluminescent nontypeable Haemophilus influenzae during experimental otitis media. Infection and immunity, 73(1): p. 609-11.

88. Ohashi, M., Ide, S., Kimitsuki, T., Komune, S., and Suganuma, T. (2006) Three-dimensional regular arrangement of the annular ligament of the rat stapediovestibular joint. Hear Res, 213(1-2): p. 11-6.

89. Paradise, J.L., Smith, C.G., and Bluestone, C.D. (1976) Tympanometric detection of middle ear effusion in infants and young children. Pediatrics, 58(2): p. 198-210.

90. Parekh, A., Mantle, B., Banks, J., Swarts, J.D., Badylak, S.F., et al. (2009) Repair of the tympanic membrane with urinary bladder matrix. Laryngoscope, 119(6): p. 1206-13.

91. Petrova, P., Freeman, S., and Sohmer, H. (2006) The effects of positive and negative middle ear pressures on auditory threshold. Otology & Neurotology, 27(5): p. 734-8.

92. Prieve, B.A., Vander Werff, K.R., Preston, J.L., and Georgantas, L. (2013) Identification of conductive hearing loss in young infants using tympanometry and wideband reflectance. Ear Hear, 34(2): p. 168-78.

93. Qin, Z., Wood, M., and Rosowski, J.J. (2010) Measurement of conductive hearing loss in mice. Hear Res, 263(1-2): p. 93-103.

94. Rabinowitz, W.M. (1981) Measurement of the acoustic input immittance of the human ear. J Acoust Soc Am, 70(4): p. 1025-35.

95. Ravicz, M.E., Rosowski, J.J., and Merchant, S.N. (2004) Mechanisms of hearing loss resulting from middle-ear fluid. Hear Res, 195(1-2): p. 103-30.

96. Ravicz, M.E., Rosowski, J.J., and Voigt, H.F. (1992) Sound-power collection by the auditory periphery of the Mongolian gerbil Meriones unguiculatus. I: Middle-ear input impedance. Journal of the Acoustical Society of America, 92(1): p. 157-77.

97. Reid, S.D., Hong, W., Dew, K.E., Winn, D.R., Pang, B., et al. (2009) Streptococcus pneumoniae forms surface-attached communities in the middle ear of experimentally infected chinchillas. The Journal of infectious diseases, 199(6): p. 786-94.

98. Rosowski, J.J., Davis, P.J., Merchant, S.N., Donahue, K.M., and Coltrera, M.D. (1990) Cadaver middle ears as models for living ears: comparisons of middle ear input immittance. Annals of Otology, Rhinology & Laryngology, 99(5 Pt 1): p. 403-12.

99. Rosowski, J.J., Dobrev, I., Khaleghi, M., Lu, W., Cheng, J.T., et al. (2013) Measurements of three-dimensional shape and sound-induced motion of the chinchilla tympanic membrane. Hear Res, 301: p. 44-52.

100. Rosowski, J.J. and Lee, C.Y. (2002) The effect of immobilizing the gerbil's pars flaccida on the middle-ear's response to static pressure. Hear Res, 174(1-2): p. 183-95.

101. Rosowski, J.J., Nakajima, H.H., and Merchant, S.N. (2008) Clinical utility of laser-Doppler vibrometer measurements in live normal and pathologic human ears. Ear Hear, 29(1): p. 3-19.

102. Rosowski, J.J., Stenfelt, S., and Lilly, D. (2013) An overview of wideband immittance measurements techniques and terminology: you say absorbance, I say reflectance. Ear Hear, 34 Suppl 1: p. 9S-16S.

103. Ruggero, M.A., Rich, N.C., Robles, L., and Shivapuja, B.G. (1990) Middle-ear response in the chinchilla and its relationship to mechanics at the base of the cochlea. Journal of the Acoustical Society of America, 87(4): p. 1612-29.

104. Sato, K., Kawana, M., Nonomura, N., and Nakano, Y. (1999) Course of IL-1beta, IL-6, IL-8, and TNF-alpha in the middle ear fluid of the guinea pig otitis media model induced by nonviable Haemophilus influenzae. Ann Otol Rhinol Laryngol, 108(6): p. 559-63.

105. Schachern, P., Tsuprun, V., Cureoglu, S., Ferrieri, P., Briles, D., et al. (2008) The round window membrane in otitis media: effect of pneumococcal proteins. Archives of otolaryngology--head & neck surgery, 134(6): p. 658-62.

106. Schachern, P.A., Paparella, M.M., and Duvall, A.J., 3rd (1982) The normal chinchilla round window membrane. Arch Otolaryngol, 108(9): p. 550-4.

107. Schachern, P.A., Paparella, M.M., Goycoolea, M., Goldberg, B., and Schlievert, P. (1981) The round window membrane following application of staphylococcal exotoxin: an electron microscopic study. The Laryngoscope, 91(12): p. 2007-17.

108. Shaikh, N., Hoberman, A., Kaleida, P.H., Rockette, H.E., Kurs-Lasky, M., et al. (2011) Otoscopic signs of otitis media. Pediatr Infect Dis J, 30(10): p. 822-6.

109. Soriano, F., Parra, A., Cenjor, C., Nieto, E., Garcia-Calvo, G., et al. (2000) Role of Streptococcus pneumoniae and Haemophilus influenzae in the development of acute otitis media and otitis media with effusion in a gerbil model. J Infect Dis, 181(2): p. 646-52.

110. Suzuki, K. and Bakaletz, L.O. (1994) Synergistic effect of adenovirus type 1 and nontypeable Haemophilus influenzae in a chinchilla model of experimental otitis media. Infection and immunity, 62(5): p. 1710-8.

111. Takanashi, Y., Shibata, S., Katori, Y., Murakami, G., Abe, S., et al. (2013) Fetal development of the elastic-fiber-mediated enthesis in the human middle ear. Ann Anat, 195(5): p. 441-8.

112. Thornton, J.L., Chevallier, K.M., Koka, K., Gabbard, S.A., and Tollin, D.J. (2013) Conductive hearing loss induced by experimental middle-ear effusion in a chinchilla model reveals impaired tympanic membrane-coupled ossicular chain movement. Journal of the Association for Research in Otolaryngology : JARO, 14(4): p. 451-64.

113. Turcanu, D., Dalhoff, E., Muller, M., Zenner, H.P., and Gummer, A.W. (2009) Accuracy of velocity distortion product otoacoustic emissions for estimating mechanically based hearing loss. Hear Res, 251(1-2): p. 17-28.

114. von Unge, M., Decraemer, W.F., Bagger-Sjoback, D., and Dirckx, J.J. (1993) Displacement of the gerbil tympanic membrane under static pressure variations measured with a real-time differential moire interferometer. Hear Res, 70(2): p. 229-42.

115. von Unge, M., Decraemer, W.F., Bagger-Sjoback, D., and Van den Berghe, D. (1997) Tympanic membrane changes in experimental purulent otitis media. Hear Res, 106(1-2): p. 123-36.

116. von Unge, M., Decraemer, W.F., Dirckx, J.J., and Bagger-Sjoback, D. (1999) Tympanic membrane displacement patterns in experimental cholesteatoma. Hear Res, 128(1-2): p. 1-15.

117. Voss, S.E. and Allen, J.B. (1994) Measurement of acoustic impedance and reflectance in the human ear canal. J Acoust Soc Am, 95(1): p. 372-84.

118. Voss, S.E., Horton, N.J., Woodbury, R.R., and Sheffield, K.N. (2008) Sources of variability in reflectance measurements on normal cadaver ears. Ear Hear, 29(4): p. 651-65.

119. Voss, S.E., Merchant, G.R., and Horton, N.J. (2012) Effects of middle-ear disorders on power reflectance measured in cadaveric ear canals. Ear Hear, 33(2): p. 195-208.

120. Voss, S.E., Rosowski, J.J., Merchant, S.N., and Peake, W.T. (2000) Acoustic responses of the human middle ear. Hear Res, 150(1-2): p. 43-69.

121. Vrettakos, P.A., Dear, S.P., and Saunders, J.C. (1988) Middle ear structure in the chinchilla: a quantitative study. American journal of otolaryngology, 9(2): p. 58-67.

122. Wysocki, J. and Sharifi, M. (2005) Measurements of selected parameters of the guinea pig temporal bone. Folia Morphol (Warsz), 64(3): p. 145-50.

123. Zhang, X. and Gan, R. (2010) Dynamic properties of human tympanic membrane. International Journal of Experimental and Computational Biomechanics, 1(3): p. 252-270.

124. Zhang, X. and Gan, R.Z. (2011) Experimental measurement and modeling analysis on mechanical properties of incudostapedial joint. Biomechanics and modeling in mechanobiology, 10(5): p. 713-26.

125. Zhang, X. and Gan, R.Z. (2013) Dynamic properties of human round window membrane in auditory frequencies running head: dynamic properties of round window membrane. Med Eng Phys, 35(3): p. 310-8.

126. Zhang, X., Guan, X., and Gan, R. (Under review) Imaging the human tympanic membrane motion using scanning laser doppler vibrometer and finite element model. Jaro.

127. Zwislocki, J. (1957) Some measurements of the impedance at the eardrum. J Acoust Soc Am, 29: p. 349-356.

128. Zwislocki, J. (1962) Analysis of the middle-ear function, part I: input impedance. J Acoust Soc Am, 34: p. 1514-1523.

129. Zwislocki, J. (1963) An Acoustic Method for Clinical Examination of the Ear. J Speech Hear Res, 6: p. 303-14.